

TECTONIC EVOLUTION OF THE AEFJORD-SITAS AREA, NORWAY-SWEDEN

by

Kip Vernon Hodges

B.S., University of North Carolina
(1978)

SUBMITTED TO THE DEPARTMENT OF
EARTH AND PLANETARY SCIENCES
IN PARTIAL FULFILLMENT OF
THE REQUIREMENTS FOR THE
DEGREE OF

DOCTOR OF PHILOSOPHY

at the

MASSACHUSETTS INSTITUTE OF TECHNOLOGY

June 1982

© Kip Vernon Hodges

The author hereby grants to M.I.T. permission to reproduce and to
distribute copies of this thesis document in whole or in part.

Signature of Author

Department of Earth and Planetary Sciences
May 24, 1982

Certified by

B.C. Burchfiel
Thesis Supervisor

Accepted by

Theodore R. Madden
Chairman, Departmental Graduate Committee

Uindgren

MASSACHUSETTS INSTITUTE
OF TECHNOLOGY

JUL 1 1982

TECTONIC EVOLUTION OF THE AEFJORD-SITAS AREA, NORWAY-SWEDEN

by

KIP VERNON HODGES

Submitted to the Department of Earth and Planetary Sciences on May 24, 1982 in partial fulfillment of the requirements for the Degree of Doctor of Philosophy in Geology

Abstract

The Aefjord-Sitas area (approximately 68°15'N;16°45'E) includes three of the principal tectonic elements of the northern Scandinavian Caledonides: a) a nappe complex, representing the main Caledonian allochthon and consisting of metasedimentary and metaigneous rock sequences that are probably in part of oceanic provenance; b) the Rombak window, a fenster through the nappe complex revealing Baltic Shield basement gneisses below; and c) the Aefjord culmination, part of the Archean-Proterozoic "Western Gneiss Region" of Scandinavia. Similarities in mineralogy and age between principal rock types in the Aefjord and Rombak gneissic terrains suggests that the Aefjord culmination represents the westward extension of the Baltic Shield to the Norwegian coast. Emplacement of the nappe complex onto the Aefjord and Rombak terrains is considered to have occurred during underthrusting of the Baltic craton beneath the Greenland craton in late Ordovician to Silurian time.

The rock sequences in the area have been subdivided into ten lithotectonic units. This tectonic stratigraphy enables the recognition of six deformational events. D₁ represents stacking of individual nappes within the allochthon. D₂ resulted in emplacement of the main Caledonian allochthon onto the Aefjord basement terrain along the Forsa thrust, and in large-scale recumbent folding of the nappe pile. D₃ and D₄ led to the development of N-S (?) recumbent and E-W upright folds, respectively. D₅ resulted in imbrication of the Aefjord-Rombak basement terrain and further cratonward translation of the main Caledonian allochthon along the Frostisen-Mereftasfjell thrust complex. D₆ is represented by N-S trending, west vergent back-folds.

The minimum age of synmetamorphic D₂ deformation is constrained by K-Ar hornblende cooling ages which average 449±19 my. Through the use of discordant hornblende and biotite K-Ar ages and currently available experimental data for Ar diffusion in these minerals, closure temperatures for the two mineral-isotopic systems and the average cooling rate over the discordancy interval can be independently determined. The calculated closure temperature for Aefjord hornblendes is 473(+11/-7)°C, that for biotite is 263(+10/-5)°C, and the cooling rate is estimated as 3.0(+2.9/-1.0)°C/my.

Rocks of the main Caledonian allochthon and subjacent Aefjord basement terrain were metamorphosed at uniform kyanite-grade conditions. The D₅ Mereftasfjell thrust, which forms the eastern margin of the nappe complex, marks a metamorphic discontinuity separating amphibolite facies nappe terrain rocks in the upper plate from greenschist facies lower plate rocks which constitute a D₅ schuppenzone (the Storriten complex). Low variance mineral assemblages are common in certain pelitic horizons within the nappe complex, and these permit the use of mineral equilibria geothermometers and geobarometers to constrain metamorphic conditions. Samples which show textural evidence of retrogradation yield a linear array on a pressure-temperature diagram. This array is thought to represent a portion of the P-T trajectory of the Aefjord area during uplift and cooling.

Thesis Supervisor: Dr. B.C. Burchfiel
Title: Professor of Geology

TABLE OF CONTENTS

I. TECTONIC STRATIGRAPHY AND STRUCTURAL EVOLUTION OF THE AEFJORD-SITASJAURE AREA, NORTHERN SCANDINAVIAN CALEDONIDES.....	10
ABSTRACT.....	11
INTRODUCTION.....	13
TECTONIC STRATIGRAPHY.....	14
Western Sector -- Autochthon and Parautochthon.....	15
Western Sector -- Allochthon.....	16
Eastern Sector -- Autochthon/Parautochthon.....	20
STRUCTURAL DEVELOPMENT OF THE AEFJORD SITASJAURE AREA.....	22
D1 -- Thrusts within the Main Caledonian Allochthon.....	22
D2 -- Isoclinal folding and development of the Forsa thrust.....	23
D3 -- Tight to isoclinal folding.....	25
D4 -- Cross-folding.....	26
D5 -- Basement-involved thrusting.....	26
D6 -- Back-folding.....	30
KINEMATIC ANALYSIS.....	30
IMPLICATIONS AND DISCUSSION.....	34
Timing of deformational events.....	34
Regional nappe correlations.....	37
Structural style.....	39
CONCLUSIONS.....	41
REFERENCES.....	43
II. THE USE OF DISCORDANT APPARENT MINERAL AGES IN DETERMINING CLOSURE TEMPERATURES AND COOLING RATES IN GEOLOGIC ENVIRONMENTS..	59
ABSTRACT.....	60
INTRODUCTION.....	61
METHOD.....	62
APPLICATION.....	64
Evaluation of parameters.....	64
The Aefjord area, northern Norway - a regional metamorphic example.....	66
Analytical technique.....	68
Analytical results.....	68
DISCUSSION.....	69
Comparison of calculated T_c and \bar{T} with other estimates.....	69
Effects of errors in choice of diffusion parameters and other assumptions.....	70
CONCLUSIONS.....	71
REFERENCES.....	73
III. GEOTHERMOMETRY AND GEOBAROMETRY OF RETROGRADED METAMORPHIC ROCKS: AN INDICATION OF THE UPLIFT TRAJECTORY OF A PORTION OF THE NORTHERN SCANDINAVIAN CALEDONIDES.....	86
Abstract.....	87
Introduction.....	88
Geologic setting.....	89

TABLE OF CONTENTS (continued)

Sample selection and analytical technique.....	90
Descriptive mineralogy.....	92
Petrographic evidence for retrogression.....	94
Primary mineral compositions and phase equilibria.....	96
Variations in distribution coefficients.....	99
Garnet zonation evidence for retrogression.....	100
Geothermometry and geobarometry.....	101
Interpretation.....	105
The closure temperature concept.....	107
Conclusions.....	109
References.....	111
 IV. STRUCTURAL EVOLUTION OF AN A-TYPE SUBDUCTION ZONE, LOFOTEN - ROMBAK AREA, NORTHERN SCANDINAVIAN CALEDONIDES.....	 144
ABSTRACT.....	145
INTRODUCTION.....	146
GEOLOGIC SETTING OF THE LOFOTEN-ROMBAKEN TRANSECT.....	148
BASEMENT-COVER RELATIONSHIPS.....	152
Eastern Hinnoy.....	152
The Aefjord culmination.....	156
Western edge of the Rombak window.....	157
Relationships between the Rombak and Aefjord basement-cover contacts.....	162
POSITION OF THE LOFOTEN-ROMBAK AREA WITHIN THE OROGEN.....	164
STRUCTURAL EVOLUTION OF AN A-TYPE SUBDUCTION ZONE - AN INTERPRETIVE MODEL.....	166
GENERAL APPLICABILITY OF THE MODEL.....	169
A-TYPE SUBDUCTION AND THE NATURE OF THE LOWER LITHOSPHERE.....	172
CONCLUSIONS.....	173
REFERENCES.....	174

INTRODUCTION

The Caledonian orogen, stretching from northern Scandinavia to the southeastern United States, is the oldest orogenic belt for which the plate tectonic setting of orogenesis can be deduced with some degree of certainty. In the North Atlantic region, the climactic phase of mountain building involved collision between the Baltic and Greenland cratons during late Ordovician-Silurian time (Dewey, 1969; Gee, 1975). Since that time, the Scandinavian Caledonides have not been substantially modified by plate interactions. This lack of post-Caledonian complications, coupled with a deep erosional level brought about by the age of the orogen, make the Scandinavian Caledonides one of the finest places to study collisional orogenesis at relatively deep crustal levels.

This is a report on a small portion of the Scandinavian Caledonides --the Aefjord-Sitasjaure area (approximately 68°15'N). Here, the classic far-traveled nappes of Scandinavia and their Archean to Proterozoic gneissic structural basement outcrop in subequal amounts, indicating an erosional level near the base of the Caledonian allochthon. This is an important and uncommonly exposed structural level in collisional orogens. It is the optimum level at which to study the phenomenon of continental crustal subduction, a process for which there is clear indirect evidence in many collisional orogens but for which there is very little real field data.

This thesis is divided into four autonomous sections. All four deal, in one way or another, with the tectonic evolution of the area. The first concerns the "nuts and bolts" of structural geology -- the recognition and description of a tectonic stratigraphy, and evaluation of

the nature and developmental sequence of major and minor structural features. The second paper illustrates the use of discordant mineral ages to determine the rate of post-metamorphic cooling during a portion of the uplift history of the area. The third paper deals with our capability to constrain the P-T path of this late-tectonic uplift. Finally, the fourth paper explores the tectonic ramifications of the structures observed at this latitude in the Caledonian orogen.

The autonomy of these papers, written in essentially publication-ready form, necessitates a certain amount of repetition of basic material, and for this I apologize.

ACKNOWLEDGMENTS

No one deserves all the credit for their thesis; in my case, I've had more than my share of helpful friends. B.C. Burchfiel, my advisor, deserves top-billing in this list of gratitudes for molding me into something of a structural geologist, and for showing me that unraveling orogenic belts depends largely on asking the right questions and looking for the answers in the right places. Frank Spear made me realize that there is more to tectonics than structural geology, and if I can call myself even a dabbler in metamorphic petrology, it's all Frank's fault. Stan Hart gave me carte blanche in his isotope laboratory, and I want him to know that I appreciate it even though none of the data I obtained there is sufficiently interpretable to make it into my thesis (sic semper cum geochronology...). Stan helped in another way, too. Once I heard someone ask J.B. Thompson about chemical disequilibrium in metamorphic petrology. "Without equilibrium," Thompson said, "we might

as well be selling insurance". No sooner had these fateful words sunk into my youthful psyche than Stan introduced me to that terrible dragon: kinetics. Soon I began seeing the tracks of this evil specter running through my microprobe data, and it became all too clear that I had better start finding a way to use geochemical kinetics to my advantage or get a job with Mutual of Omaha. So thanks, Stan, for causing me no end of mental anguish, and proving once again that nothing is as simple as you thought it would be when you started.

If the papers in this thesis ever get accepted by anyone, I'll have co-authors on all but the first. I'd like to take this opportunity to thank John Bartley, Clark Burchfiel, Larky Hodges, Hal Krueger, and Wiki Royden for the opportunity to collaborate with such fine people.

Thanks should also go to friends at M.I.T., too numerous to mention, who made these four years more than tolerable. Among others, Gary Axen, John Bartley, Bill Brace, Tim Byrne, Scott Cameron, Peter Guth, Dave Klepacki, John Sharry, Doug Walker, Brian Wernicke. and Jim Willemin kept my structural thinking from getting too fuzzy. Peter Crowley, Julie Morris, Mary Roden, Mike Roden, Tom Sando, and Jane Selverstone kept me from making an idiot of myself geochemically. Peter Molnar and Wiki Royden helped make geophysics understandable. John Bartley, Mike Roden, Tom Sando, Doug Walker, and Brian Wernicke helped me keep my sanity through the electronic wonder of video games. John Bartley and Doug Walker deserve special thanks; John for "showing me the ropes" in Norway and providing help, information and general companionship; Doug for keeping me on an even keel through the last few years of my stay here. These two guys give new dimensions to the word "friend".

I also want to express my gratitude to those who helped me through the logistics of thesis preparation. Margaret Sano and Jim Willemin read the final drafts and pointed out many glaring errors. Dorothy Frank helped out with the typing when things got rough.

An extra special award goes to Mal Hill for agreeing to be on yet another MIT thesis committee. I think battle pay is in order....

I would like to thank the National Science Foundation for funding part of my stay here at M.I.T. through a graduate fellowship, and for funding my work in Norway through grants to B.C. Burchfiel and Frank Spear. Funding for my first summer in Norway was provided by Bill Brace from one of his magic piggy-banks; without that grub-stake, I might never have gotten out of Cambridge. Arild Andresen, Bill Griffin, Mark Steltenpohl, Ulrich Sovegjarro, Jim Tull, and the Geological Survey of Norway provided invaluable aid and accomodation in Norway. I consider meeting and striking up a friendship with Ron Boyd of the Norwegian Survey one of my finest accomplishments in Norway. I was ably assisted in the field by Peter Vrolijk during the second summer, and Peter Crowley and Simon Peacock helped me keep my sense of humor through my unusually water-logged third field season .

And finally I come to the impossible task of adequately thanking Larky, my wife, for everything she has done. Between nursemaiding my psyche, being a friend, controlling my temper, making me laugh, drying the tears, field assisting for two summers in Norway, drafting the figures, typing the papers, and generally making the world a better place for me to live, I don't see how she has any time for her own life. I can never repay the debt I owe to Larky, and I'll never understand why she puts up with me - unless it's love. The feeling's mutual....

PART I

TECTONIC STRATIGRAPHY AND STRUCTURAL EVOLUTION OF THE AEFJORD-SITASJAURE
AREA, NORTHERN SCANDINAVIAN CALEDONIDES

TECTONIC STRATIGRAPHY AND STRUCTURAL EVOLUTION OF THE AEFJORD-SITASJAURE
AREA, NORTHERN SCANDINAVIAN CALEDONIDES

Abstract

The Aefjord-Sitasjaure area (~68°15'N) provides excellent exposures of the basal portions of the Caledonian nappe complex at this latitude in the Scandinavian Caledonides. The nappe complex has been subdivided into seven tectonostratigraphic units, and is considered broadly correlative with the Rodingsfjall Nappe. Structural basement for this allochthon consists of the Proterozoic (?) Tysfjord granite gneiss and its parautochthonous Storvann Group stratigraphic cover in the western part of the area. In the eastern part of the area, a major schuppenzone including large mylonitized slices of granitic basement gneisses, the Storriten complex, is interposed between the main Caledonian allochthon and the Proterozoic Rombak granite gneiss basement. This schuppenzone is considered broadly correlative with the Akkajaure complex of Kautsky (1953).

Four phases of folding and three thrusting events have been identified. Early folds are generally recumbent and reflect eastward tectonic transport. Late-stage features include cross-folds and back-folds. The earliest, premetamorphic thrusts were responsible for stacking units within the nappe complex. Synmetamorphic T₂ thrusts were east directed and placed the nappe complex onto the Tysfjord basement. The final, postmetamorphic thrusting event was southeast-directed and was characterized by large-scale basement involvement and development of the Storriten complex.

The age of T₂ thrusting, and thus initial emplacement of the nappe complex onto the Baltic craton, is constrained to be late Ordovician or older based on K-Ar cooling ages for metamorphic hornblendes.

INTRODUCTION

The Scandinavian Caledonides apparently record the early to middle Paleozoic closure of the Iapetus Ocean and subsequent continent-continent collision between the Baltic and Greenland cratons (Dewey, 1969; Gee, 1975). The most conspicuous result of Caledonian orogenesis was the emplacement of large-scale thrust nappes onto the Baltic Shield, as the passive Baltic margin was being subducted beneath an "Andean-type" Greenland margin during collision (Hodges et al., in preparation, a). Estimates for large transport distances (in excess of 500 km.) for the main Caledonian allochthon stem from the appearance of Baltic basement and stratigraphic cover sequences: a) in a series of windows through the nappe sequence which approximately parallels the Norwegian-Swedish international border, and b) in a more continuous belt along the west coast of Norway - the Western Gneiss Terrain (Tornebohm, 1896; Hogbom, 1909; Gee, 1975, 1978). Figure 1 shows the distribution of this structural basement, which appears to form a more or less continuous substrate beneath the Caledonian allochthon. The plethora of basement windows and half-windows in the western portions of the orogen suggest that the erosional level in those areas is ideal for studying the structural development of the basal portions of the nappe complex in Scandinavia.

The Aefjord-Sitasjaure area, Norway-Sweden ($\sim 68^{\circ}15'N$; Figure 2), spans an approximately 20 kilometer-wide synclorium of the Caledonian nappe terrain which occurs between a transverse basement culmination of the Western Gneiss Terrain on the west (the Aefjord culmination) and the Rombak basement window on the east. Late-stage folding associated with

development of the Aefjord culmination upended earlier structures associated with nappe emplacement such that a geologic map actually represents a cross-section through the nappe sequence, much as the Aar and Aiguilles Rouge culminations provide a cross-section through the western Helvetic Nappes in the Alps (Ramsay, 1981). My field work in the Aefjord-Sitasjaure area was aimed at: 1) a critical reevaluation of the nappe stratigraphy in this portion of the Caledonides; and 2) determination of the structural history of the area. In a larger context, the information gained through this study has important implications concerning the timing of deformational events in Scandinavia, and the extent of basement involvement in those events.

TECTONIC STRATIGRAPHY

Foslie (1941) generated the first geologic map of the Aefjord-Sitasjaure area and subdivided the nappe complex (which he considered to be a continuous stratigraphic succession) into a variety of subordinate units (Figure 3). Drawing heavily from the work of Vogt (1950) near Narvik, northeast of the Aefjord-Sitasjaure area, Gustavson (1966, 1972) subdivided the structural cover sequences in the Ofoten region into the tectonic stratigraphy shown in Figure 3. Gustavson suggested that his Narvik Group was correlative with the Reppi schist and overlying mica schists mapped by Foslie, and that his Rombak Group was represented by the mica schists, marbles, and metaigneous rocks underlying the Reppi schist. Detailed mapping in the Aefjord-Sitasjaure area shows

that the Reppi schist occupies the core of a major, early isoclinal fold (see below), such that Gustavson's extension of the thrust at the base of his Narvik Group to "beneath" the Reppi schist must be invalid.

Correlations drawn in Figure 3 between the tectonic stratigraphy described below and those of Foslie and Gustavson reflect this conclusion. For convenience, the tectonic stratigraphy of the Aefjord-Sitasjaure area will be described in terms of a western sector encompassing units exposed along the Aefjord culmination, and an eastern sector which includes units cropping out along the western margin of the Rombak Window. Letters shown in parentheses after unit names denote the abbreviations used in Plate 1.

Western Sector -- Autochthon and Parautochthon

Structural basement in the Aefjord culmination consists almost entirely of the Tysfjord granite gneiss (pCt) of Foslie (1941). Mineralogically a true granite, this lithology commonly contains accessory magnetite, fluorite, epidote, apatite, and hastingsitic amphibole. No radiometric ages have been obtained to date for this unit. Similarities between the Tysfjord and Rombak granite gneisses (see below) suggest that the two are correlative (Gustavson, 1966). If so, then the 1707 ± 40 m.y. Rb-Sr isochron obtained by Heier and Compston (1969) for the Rombak granite gneiss would also be applicable to the Tysfjord granite gneiss.

The Forsa Complex (fc) is a zone of tectonic slices developed during emplacement of the main Caledonian allochthon onto the Tysfjord basement terrain. Lithologies present in this unit as complexly deformed slices include: 1) orthoquartzite, impure marble, rusty-weathering pelitic schist, and biotite-quartz-garnet-schist of probable Storvann Group affinity (see below); 2) garnet-quartz-muscovite schist and amphibolite of

probable main Caledonian allochthon affinity; and 3) minor protomylonitic Tysfjord granite gneiss.

The Storvann Group (first described by Bartley, 1981) forms an autochthonous transgressive cover sequence for the Western Gneiss Terrain basement gneisses on eastern Hinnoy. This sequence is considered to be broadly correlative with similar Cambrian platformal sequences found in the Baltic foreland at this latitude (Bartley, 1981). Autochthonous Storvann Group lithologies have been traced onto the mainland as far south as Hafjell (Figure 2; Tull et al., in press). Near Forsa, Storvann Group lithologies are parautochthonous and occur as: 1) discontinuous thrust slices within the Forsa Complex; and 2) a coherent, isoclinally folded package sandwiched between the Forsa Complex below and the main Caledonian allochthon structurally above. Two Storvan Group units occur in this package; 1) a biotite-quartz-garnet schist (labeled as S1 on the accompanying geologic map; the "quartz-garnet schist" member of Bartley, 1981); and 2) a rusty-weathering pelitic schist (labeled as S2 on the geologic map; the "pelitic schist" member of Bartley, 1981).

Western Sector -- Allochthon

The Reppi "schist" (rs) of Foslie (1941) is a reddish brown, quartz-plagioclase-garnet-biotite rock which characteristically contains large (up to 2 cm.) clinozoisite porphyroblasts which are randomly oriented within cleavage planes. The overall texture of this lithology varies from schistose to granofelsic depending on the ratio of phyllosilicates to framework silicates in any given sample.

The name "Skjafjell schist" (sks) is proposed here for a

tectonostratigraphic unit cropping out extensively on the southern end of the mountain Skjafjell within the Aefjord-Sitasjaure area. This garnet-biotite-quartz-muscovite schist is characteristically silver-gray to dark-gray in outcrop. Quartz stringers and veinlets up to 0.5 m. in length are common, and generally oriented parallel to the predominant schistosity in the rock.

The Hjertvatnet migmatitic gneiss (hm) is named for the lake Hjertvatnet in the central portion of the area, where it is exposed on both limbs of the large, Reppi-cored isocline mentioned earlier. On the northern limb, this unit is bounded on either side by probable pre-metamorphic thrusts. Here it can be subdivided into a predominate garnet-quartz-hornblende-plagioclase-biotite melanosome and a subordinate microcline-garnet-muscovite-biotite-quartz-plagioclase leucosome. The proportion of leucosome to melanosome on the northern limb is variable but rarely exceeds 1:3. As this unit is followed along strike into the hinge area of the isocline and beyond to its southern limb, the leucosome becomes increasingly predominate. In southern limb exposures near Hjertvatnet, the ratio of leucosome to melanosome approaches 10:1 and the unit takes on the character of a trondhjemitic to tonalitic gneiss with elongate xenoliths of melanosome. The contact between the Hjertvatnet migmatitic gneiss and the Skjafjell schist is considered to be premetamorphic thrust on this limb of the fold as well. The contact between this unit and the Rauvatn complex is much more irregular and is tentatively believed to be intrusive. The Hjertvatnet gneiss as described here is in part correlative with the Gicce gneiss of Foslie (1941), although Foslie's unit appears to have included lithologies which are

described below as Sjurvatnet schist.

The Rauvatn complex (rc; named for a small lake between Hjertvatnet and Geitvatn) is a tectonic melange consisting of pods and lenses of impure marbles, amphibolites, trondhjemites, and serpentinized peridotites in a quartz-garnet-muscovite-biotite schist matrix. The marbles occur as elongate stringers which are sometimes up to several kilometers in length and commonly show complex internal deformation. The amphibolite bodies occupy large tracts of Rauvatn complex exposures and often contain large numbers of trondhjemite dikes which exhibit crosscutting relationships suggestive of multiple generations of dike emplacement. The ultramafic pods are generally small (up to about 2500 m².) and spatially associated with the amphibolites. They are almost always completely altered to serpentinite and orthoamphibolite, and most are enveloped by a veneer of talc schist.

A garnet-plagioclase-biotite-quartz-muscovite schist which occupies large tracts in the vicinity of Sjurvatnet is here called the Sjurvatnet schist (ss). This brownish-gray pelitic schist commonly contains porphyroblasts of kyanite up to several centimeters in length, and subhedral staurolite porphyroblasts occur rarely. Small quartz veins and pods (occasionally containing accessory plagioclase, muscovite and kyanite) permeate the unit. In some outcrops, the Sjurvatnet schist exhibits a striking augen schist texture in which the "eyes" are plagioclase porphyroblasts or plagioclase + quartz composites up to 2 cm. in their longest dimension.

Two prominent horizons occur within the Sjurvatnet schist sequence. The Melkedal marble (mm) of Foslie (1941) is a thin (3-15 m.), laterally

extensive bed of bluish-gray, phlogopite-calcite marble. The Sjurvatnet quartzite (sq; described here for the first time) is a 20-200 m. thick horizon of tan, impure quartzite which parallels the outcrop trace of the Melkedal marble on the geologic map.

Foslie (1941) described the Elvenes conglomerate as a calcareous mica schist containing pebbles and cobbles of quartzite and trondhjemite. In this study, two distinct facies of conglomerate were identified. The first is an amphibolite-matrix conglomerate (ec1) containing pebbles and cobbles (up to 30 cm. in their longest dimension) of tonalite or trondhjemite, metagabbro, calcite marble, and orthoamphibolite, listed in approximate order of decreasing abundance. The second facies is a "carbonate" (biotite-calcite-quartz schist)-matrix conglomerate (ec2) with quartz, trondhjemite or tonalite, and carbonate clasts, again in order of decreasing abundance. The average clast size for ec2 is conspicuously smaller than that for ec1.

Stratigraphic relationships between the two facies are not always clear. As pointed out by Foslie (1941), the Elvenes conglomerate as a whole is discontinuous along strike. Within the map area, both facies are discontinuous, and the amphibolite-matrix conglomerate appears both structurally above and below the carbonate-matrix facies. There is no evidence for folds or faults which might be responsible for this configuration, although exposures are poor in this area. The relationship is tentatively attributed to rather large-scale, stratigraphic interfingering of the two facies.

Tull et al., (in press) suggest that the Elvenes conglomerate represents a regional unconformity at the base of the Salangen Group of Gustavson (1966). Relationships in this area support that conclusion,

although evidence for regional discordance is generally equivocal. The Elvenes Conglomerate is interpreted to be upright based on : 1) the lack of abundant marble clasts within the conglomerates, which might have been expected if the conglomerate had developed above the Salangen Group marbles; and 2) the presence of a suitable source for the observed clasts in the underlying Sjurvatnet schist unit.

Only the basal units of the Salangen Group marbles (sm) occur in the Aefjord-Sitasjaure area; for more comprehensive descriptions of these lithologies, see Gustavson (1966) or Steltenpohl (1982). Salangen Group carbonates mapped in this study are tan to bluish-white calcite and phlogopite-calcite marbles.

In addition to the amphibolites which are a major constituent of the Rauvatn Complex, small hornblende amphibolite bodies (a) occur throughout most of the tectonic stratigraphy of the western sector. Pegmatite dikes are common in the Storvann, Reppi, Skjafjell and Sjurvatnet units. A small tonalite body (tgn) occurs in the upper Sjurvatnet schist, just beneath the Elvenes conglomerate.

With the exception of the Tysfjord granite gneiss, which is considered to be Proterozoic by analogy with the Rombak granite gneiss, and the Storvann Group, which is thought to be Cambrian by Bartley (1981), the ages of units within the western sector tectonic stratigraphy are unknown.

Eastern Sector --Autochthon/Parautochthon

The predominant lithology in the western Rombak window is the Rombak granite gneiss (pCr). This unit was named and first described by Vogt (1942), although it was alluded to by Foslie (1942) as the Skjomen

granite. Predominate minerals in the gneiss include biotite, plagioclase, microcline, and quartz. Magnetite, fluorite, epidote, apatite and zircon are common accessories. Heier and Compston (1969) obtained a four-point Rb-Sr isochron for the Rombak granite gneiss which corresponds to an age of 1707 ± 40 m.y.. The Rombak and Tysfjord granite gneisses are strikingly similar in both hand specimen and thin section. Gustavson (1966) presents major-element chemical analyses for the two gneisses which reinforce the conclusion of Vogt (1942) that the units are correlative.

The Storriten Complex, named here for exposures on the mountain Storriten, is a zone of tectonic slicing which developed between two late-stage thrusts. It consists of large plates or schuppen of mylonitized granitic gneisses (stm) in a predominately phyllonitic matrix (stp). Based on mineralogical similarities between the mylonitic gneisses and the Rombak-Tysfjord granitic gneisses, the schuppen are considered to be slices of Precambrian basement. The matrix for these slices is a strongly sheared, graphite-biotite-chlorite-muscovite-quartz schist. Garnet is prevalent at certain horizons. Stringers and lenses of light gray orthoquartzite and dark gray impure quartzite up to a few meters in outcrop length are commonly interspersed within the phyllonite.

No fossils have been observed within the Storriten Complex schists, leaving their age a mystery. The graphitic nature of this unit suggests a lithologic correlation with the Middle Cambrian, organic-rich, "alum" shales which occur in the upper part of the "Hyolithus zone" sequence, the autochthonous, sedimentary cover in the Baltic foreland at this latitude (Kulling, 1964).

STRUCTURAL DEVELOPMENT OF THE AEFJORD-SITASJAURE AREA

Mapping of the tectonic stratigraphy described above permits the recognition of three phases of thrusting and four phases of folding in the Aefjord-Sitasjaure area (Table 1). Inspection of the tectonic map shown in Figure 4 reveals that all of these events resulted in macroscopic structures, and many of the temporal relationships between structural events can be deduced directly from map-scale interference patterns.

In the following discussion, structures are numbered to correspond with the deformational event during which they developed. For example, the first fold phase, which developed during the second deformational event, is termed F_2 .

D1 -- Thrusts within the Main Caledonian Allochthon

Except for the unconformity marked by the Elvenes conglomerate, contact relationships between tectonostratigraphic units in the main Caledonian allochthon are largely obscured by regional metamorphism which occurred subsequent to their development. The chaotic nature of the Rauvatn Complex is in strong contrast, however, to the monotony of the Skjafjell and Sjurvatnet schists above and below it, and these contacts are considered to be T_1 thrusts. Although no mylonitic fabrics were observed along these contacts, subunits within the Rauvatn Complex are commonly truncated along them. Moreover, the Rauvatn Complex is completely cut out south of Melkevatnet by T_1 thrusts and does not reappear in the northern limb of the F_2 , Reppi-cored fold.

As alluded to previously, the contact between the Hjertvatnet migmatitic gneiss and Rauvatn Complex is considered to be intrusive. In

contrast to the irregular, even diffuse contact between the Hjertvatnet and Rauvatn units, contacts between the Hjertvatnet migmatite and the Skjafjell and Sjurvatnet schists are relatively sharp and characterized by a high strain gradient through which melanosome "islands" within the leucosome become highly attenuated over a distance of a few meters. These contacts are also interpreted as T_1 thrusts. Thus, it would appear that the Rauvatn Complex and the Hjertvatnet migmatitic gneiss which intrudes it form a distinct, thrust-bound structural package interposed between the Sjurvatnet and Skjafjell schist units. Other tectonostratigraphic contacts in the allochthon may be T_1 thrusts, but the available evidence is equivocal. The age of T_1 thrusting is not well constrained, but the lack of metamorphic discontinuities across these thrusts require that they are older than the regional metamorphic event.

D2 -- Isoclinal Folding and Development of the Forsa Thrust

One of the most prominent structural features in the Aefjord-Sitasjaure area is the large isoclinal F_2 fold which is cored by the Reppi schist. Repetition of characteristic units such as the Hjertvatnet migmatitic gneiss and the Skjafjell schist on either side of the Reppi schist constitutes the primary evidence for this structure. The earliest and most predominant penetrative cleavage observed in the western sector is everywhere subparallel to lithostratigraphic contacts except immediately northeast of Forsa in the nose of the Reppi-cored fold. Here, relationships between lithostratigraphic contacts and the predominant cleavage are consistent with this cleavage being axial planar with respect to the fold, and therefore it is interpreted as S_2 . Unfortunately, outcrop is very poor in the vicinity of the fold closure, and it is

impossible to determine with certainty whether the structure is antiformal or synformal. It is shown as synformal in the geologic cross-sections (Plate II), an interpretation consistent with its being a large drag feature developed during eastward translation along the subjacent Forsa thrust, which will be discussed below. Regardless of its closure direction, the northern limb of this fold must be upright since the Elvenes conglomerate outcrops in that limb are upright. This observation implies that all units within the allochthon south and west of the Reppi schist lie in the overturned limb of this fold, and the T_1 thrusts occurring in this limb are consequently shown as overturned on the geologic and tectonic maps.

Mesoscopic F_2 folds are common throughout the area. These folds are always similar with height-to-width ratios (following the terminology of Hansen, 1971) in excess of two. The orientation of F_2 fold axes and axial planes are highly scattered (Figure 5a,b), reflecting the effects of three superimposed folding events. No consistent vergence was observed for mesoscopic F_2 folds.

The basal contact between the main Caledonian allochthon and the Tysford granite gneiss in this region is the Forsa thrust. It is marked by an abrupt intensification of the S_2 cleavage in the allochthon and the development of a blastomylonitic to protomylonitic cleavage in the subjacent Tysfjord granite gneiss. Both the mylonitic and penetrative S_2 cleavages are consistently subparallel to the thrust. There is no indication that transposition of the S_2 cleavage by a later, thrust-related fabric was responsible for its intensification near the thrust; consequently, the Forsa thrust is assigned a D_2 age.

The amount of translation which occurred along the Forsa thrust is

unknown but must have been large. Upper plate units such as the Rauvatn complex are unlikely to have been derived from the platformal to miogeosynclinal sedimentary sequences characteristic of the Baltic margin in pre-Caledonian time. Hodges et al., (in preparation, a) present arguments that the main Caledonian allochthon must have been derived from west of the Lofoten-Vesteralen archipelago. Thus, a generally eastward transport direction is inferred for the Forsa thrust.

The age of the D₂ event is constrained by the observation that the S₂ cleavage was synkinematic with respect to the growth of major porphyroblasts during regional metamorphism; for example, sigmoidal S₂ cleavage traces are common in rolled garnets of the Sjurvatnet schist sequence. Hodges et al., (in preparation, b) obtained K-Ar cooling ages of 449±19 m.y. for amphiboles which defined the S₂ cleavage in metabasites from the area. This age may be considered a minimum for the development of D₂ structures.

D₃ -- Tight to Isoclinal Folding

Mesoscopic F₃ folds are similar and commonly overturned to recumbent. Most are isoclinal, although a significant fraction of those which developed in more competent lithologies are tight. Height-width ratios vary between one and two. Vergence is inconsistent. F₃ axes generally plunge gently, although axial orientations are variable (Figure 5d). Macroscopic F₃ folds are rare in the Aefjord-Sitasjaure area; the best example is an antiformal recumbent isocline cored by the Skjafjell schist NE of Geitvatn.

An axial planar S₃ schistosity is commonly well-developed throughout

the eastern sector and in the southern part of the western sector. S_3 strongly transposes S_2 , and rootless, intrafolial F_2 folds are frequently encountered in the eastern sector. Poles to S_3 cleavage are scattered in stereographic projection (Figure 5c), although a maximum corresponding to a NNW strike and shallow NE dip is apparent. This maximum represents measurements taken in the western sector where the effects of later folding events are relatively subdued.

D₄ -- Cross-Folding

The Aefjord basement culmination is the most striking macroscopic example of F_4 cross-folds. Mesoscopic F_4 folds are similar, generally broad to open, and either upright or overturned to the southwest. Height-width ratios are commonly less than one. F_4 folds are markedly disharmonic on all scales. Stereographic projections of F_4 axes are scattered in a fashion consistent with refolding about F_6 axes (Figure 5f; see below). No cleavage of D_4 age was observed.

D₅ -- Basement-Involved Thrusting

The D_5 deformational event resulted in the development of the Storriten complex schuppenzone between two major T_5 thrusts -the Frostisen and Mereftasfjell thrusts (Figure 4).

The Frostisen thrust, which juxtaposes the Storriten complex onto the Rombak basement terrain, is named for a large glacier north of the map area. Near the glacier, the immediate lower plate of the thrust consists of light gray orthoquartzites which constitute a tectonic remnant of the autochthonous, Caledonian stratigraphic cover of the Tysfjord-Rombak gneissic terrain. Along strike to the south, the thrust cuts down-section

in the lower plate until it places the Storriten complex directly on Rombak granite gneiss in the Aefjord-Sitasjaure area. Several hundred meters structurally below the thrust, the Rombak gneiss exhibits a weakly developed penetrative cleavage which strikes roughly N-S and dips steeply to the west. Two to ten centimeter-wide ductile shear zones which are roughly parallel to the cleavage also occur at this level. As the Frostisen thrust is approached from below, these elements are progressively rotated to shallower westward dips. Intensification of the penetrative cleavage leads to the development of a pronounced augen texture in the granite gneiss immediately beneath the thrust surface. At this structural level the cleavage is distinctly protomylonitic and parallel to the thrust surface; the discrete shear zones are either no longer present or impossible to discern due to the intensity of the mylonitic cleavage development. It is presently unclear whether the penetrative cleavage and ductile shear zones are related to the development of the Frostisen thrust or are preexisting elements which are rotated into parallelism with D_5 structures. A. Andresen and J. Tull (in Tull et al., in press) describe similar penetrative cleavage and shear zones in the northern part of the Rombak window which are truncated by the apparent continuation of the Frostisen thrust. Based on these observations, the features in the Aefjord-Sitasjaure area are also considered to be pre- D_5 and may be pre-Caledonian in age.

Structurally above the Frostisen thrust, the predominant phyllonitic cleavage in the Storriten complex matrix is slightly anastomosing but generally subparallel to the protomylonitic cleavage within the basement schuppen (compare Figure 5 g and h). Both are concordant with the Frostisen thrust and are thus considered to be D_5 fabrics. The

phyllonitic cleavage commonly crosscuts and occasionally transposes both S_3 and S_2 penetrative cleavages. Despite broad refolding about F_6 folds, both the mylonitic and phyllonitic cleavages maintain a relatively constant, roughly N-S strike and a subhorizontal to slightly east or west-directed dip. In addition to the mylonitic cleavage, Storriten complex basement schuppen also commonly exhibit a well-developed stretching lineation with a mean orientation of $10^\circ; N58^\circ W$. This lineation is interpreted as indicative of the direction of tectonic transport for the Frostisen-Mereftasfjell thrust complex.

Although the Mereftasfjell thrust crops out poorly in the Aefjord-Sitasjaure area, its presence is marked by a general intensification of the Storriten complex phyllonitic cleavage (to which it must be subparallel, based on its general outcrop pattern) and a distinct metamorphic discontinuity. Upper plate, Skjafjell schist lithologies were metamorphosed to kyanite grade, whereas lower plate, Storriten complex schists attained only garnet grade.

The presence of this metamorphic break corroborates the evidence provided by cross-cutting S_5 - S_3 cleavage relationships for a post- D_3 age for the Frostisen-Mereftasfjell thrust complex. Moreover, refolding of S_5 by F_6 requires a pre- D_6 age for these structures. Unfortunately, relationships between this thrust complex and F_4 cross-folds are less clear. A striking feature of the regional map shown in Figure 2 is that the basement-cover contact along the western edge of the Rombak window (the Frostisen-Mereftasfjell thrust complex) appears unfolded by the large, F_4 cross-fold responsible for the Aefjord culmination. This might be taken as evidence for a post- D_4 age for the thrust complex, but the strongly disharmonic nature of F_4 folds makes this evidence less than

compelling. An alternative interpretation -that the F_4 folds and the thrust complex are part of the same deformational event -requires the development of folds with axial trends subparallel to the transport direction of coeval thrusting. This relationship has been reported from elsewhere in Scandinavia (Kvale, 1960; Hansen, 1971), but it is usually associated with early developed structures. Development of the Frostisen and Mereftasfjell thrusts and the intervening Storriten complex are tentatively assigned to a unique post- D_4 deformational event (D_5), although a syn-or even pre- F_4 cross-fold age is not inconsistent with the available evidence.

The occurrence of large slices of Proterozoic granite gneiss within the Storriten complex strongly suggests significant basement involvement in T_5 thrusting. In addition, the Frostisen-Mereftasfjell thrust complex, which dips shallowly westward beneath the main Caledonian allochthon in the eastern sector, does not reappear at the surface within the western sector. This observation requires that the thrust complex must root into the Rombak-Tysfjord basement terrain beneath the area. Age relations further necessitate that these D_5 structures truncate the D_2 Forsa thrust at depth. The geologic cross-section shown in Plate II illustrates my interpretation of the thrust geometry beneath the Aefjord-Sitasjaure area. Note that the available data do not constrain: a) the interplay between the Mereftasfjell and Frostisen thrusts at depth; b) the down-dip extent of the Storriten complex; or c) the exact location of the truncation of the Forsa thrust by the D_5 structures. The cross-section merely illustrates the broad geometry of thrust interaction in a manner consistent with but not required by field observations.

D₆ -- Back-folding

Broad to open, roughly concentric D₆ folds are common macroscopic structures in the Aefjord-Sitasjaure area. Mesoscopic F₆ folds are generally upright to slightly overturned, and fold morphology varies from broad in quartz-rich lithologies to chevron in more schistose rocks. Height-width ratios are generally less than one. F₆ axes trend NNW and plunge shallowly (Figure 5j). Vergence is consistently westward. Both mesoscopic and macroscopic F₆ folds are clearly disharmonic. The most striking example of this is the F₆ fold whose axis runs roughly down the center of Hjertvatnet. Note that the amplitude of this fold progressively decreases passing from north to south.

A penetrative S₆ crenulation cleavage is commonly developed in more schistose lithologies. Microfold or crenulation axes are subparallel to mesoscopic F₆ axes and the two are plotted together on Figure 5j.

North of Sjurvatnet, the Elvenes conglomerate units are truncated by a presumed high-angle fault in the core of a macroscopic F₆ fold. Exposures are very poor in this area, and the fault surface was not directly observed; hence, the sense and magnitude of displacement along the fault could not be determined. Because of its orientation and position in the core of an F₆ fold, this fault has been tentatively assigned a D₆ age.

KINEMATIC ANALYSIS

While geometric analysis of structural fabrics is a powerful method

of characterizing general transport directions (using present-day coordinates) in areas with relatively simple structural histories, it becomes increasingly difficult in areas with long and complex histories. Nevertheless, integration of mesoscopic fabric analysis with macroscopic observations permits some general conclusions concerning the kinematics of structures in the Aefjord-Sitasjaure area.

Comparison between Figure 5f and 5j shows that F_4 axes form a rough, small-circle distribution which is approximately centered on the maximum concentration of F_6 axial orientations. This geometry is consistent with a predominantly flexural-slip mechanism for F_6 folds (Clifford, 1960). Although there is some scatter in the orientations of F_6 axes, the vergence of these folds is consistently to the west, precluding use of the separation angle method of Hansen (1971) to constrain the "slip-line" or a kinematic axis of F_6 folding. However, this same consistency of vergence strongly suggests net WSW tectonic transport associated with these folds.

Two lines of evidence suggest the general transport direction of T_5 thrusts. First, the rotation of ductile shear zones in the Rombak granite to progressively more shallow westward dips near the Frostisen thrust suggests a NW to SE transport direction. Second, the orientation of stretching lineations in mylonitic basement schuppen within the Storriten complex indicate a transport vector of approximately $S60^\circ E$.

The slip line for F_4 folds is more poorly known. F_3 axes define a great-circle on Figure 5d which is consistent with their being refolded about shear or slip folds with roughly E-W trending axes (Turner and Weiss, 1963; p.486), in this case F_4 . The intersection between this

great circle and the mean axial plane of F_4 folds should uniquely determine the slip line for F_4 folding (Ramsay, 1960). Unfortunately, stereographic projections of poles to F_4 axial planes are scattered in Figure 5e as a result of superimposed F_6 folding. Figure 6 illustrates how the F_4 a axis might be constrained somewhat. If we assume a flexural-slip model for F_6 folds, poles to F_4 axial planes should define a great circle centered on the mean F_6 axial orientation (Turner and Weiss, 1963; p.478). The pole to the original F_4 axial plane must be within the spread of measured data along this great circle. This constrains the original axial plane to be within the two "limiting" planes shown in Figure 6. Intersection between this region and the great circle of F_3 axes defines an "arc" within which the F_4 slip line should lie. This is not a particularly satisfying result, since the resulting "arc" is several tens of degrees in length. The possibilities are narrowed further by the assumptions: a) that the initial F_4 axis should lie within the present small-circle configuration of F_4 axes; b) that this axis should be coincident with the pole to the great circle defined by F_3 axes; and c) that this axis should lie along the initial F_4 axial plane. These constraints suggest that the slip line should lie somewhere in the northern segment of the "arc". Although far from exact, this approach leads to the general conclusion that the slip vector for F_4 cross-folds was generally NE or SW-directed. Note that this direction is significantly different from the transport direction inferred from stretching lineations for T_5 thrusts, implying that development of cross-folds and the Merefstasfjell-Frostisen thrust complex were probably not coeval.

Poles to S_2 schistosity, although understandably scattered, define a

distinct maximum on Figure 5a. Considering the intensity of F_4 and F_6 folding, it is perhaps surprising to find that the plane perpendicular to this maximum roughly approximates the great-circle distribution of F_3 axes. This suggests that the roughly N-S strike and shallow dip of this plane approximates the initial orientation of F_3 axial planes. In the eastern sector, where F_4 and F_6 are less pronounced, F_3 axes trend generally NNE and plunge less than 20° , and this is taken as the "best guess" for initial F_3 axial orientations. Attempts at slip line determinations for these folds are frustrated by the lack of consistent vergence and the large scatter in F_2 axial orientations. D_3 tectonic transport is inferred to have been approximately perpendicular to the trend of F_3 folds and thus ~ESE-directed.

The maximum in Figure 5a is very similar to that defined by D_3 planar fabrics. This is at least in part due to the common transposition of S_2 by S_3 . F_2 axes are highly scattered in Figure 5b, making it difficult to speculate on the relationship between the maximum shown in Figure 5a and the initial orientation of F_2 axial planes. D_2 structures are least modified by subsequent events in the extreme northwestern part of the map area near Forsa. Here, the Forsa thrust strikes ~N-S, subparallel to the axial trace of the Reppi-cored fold. The moderate eastward dip of both the thrust and the axial plane of the fold are not considered primary; rather, these are interpreted as reflecting broad F_6 upwarping. However, the ~N-S trend of the Reppi-cored fold in this area remains the best estimate for the primary trend of F_2 folds. Tectonic transport during D_2 is considered to have been roughly orthogonal to this trend, a conclusion which is compatible with derivation of the allochthonous rocks in the

upper plate of the Forsa thrust from west of the Lofoten-Vesteralen Islands.

The lack of associated tectonite fabrics and the cryptic nature of T_1 thrusts prohibits kinematic analysis of the D_1 structural event.

IMPLICATIONS AND DISCUSSION

Timing of Deformational Events

The Caledonian orogeny in Scandinavia is commonly subdivided into two distinct episodes: the late Cambrian-early Ordovician Finnmarkian phase, and the middle Silurian-early Devonian (?) Scandian phase (Roberts, 1971; Gee and Wilson, 1974; Ramsay and Sturt, 1976; Sturt et al., 1978). The ~450 m.y. K-Ar hornblende cooling ages obtained by Hodges et al., (in preparation) for samples from the Aefjord-Sitasjaure area suggest that D_2 deformation occurred at a time almost exactly midway between the two "phases". K-Ar mineral ages commonly reflect the time of cooling through some critical closure temperature for a given mineral-isotopic system rather than the true age of crystallization (e.g., Armstrong, 1966), and some might argue that the Aefjord-Skjomenes "ages" reflect slow cooling from a Finnmarkian metamorphic event. Using discordant hornblende and biotite K-Ar ages from this area and the equation derived by Dodson (1973) relating mineral-isotopic system closure temperatures to cooling rate, Hodges et al., (in preparation) derived a K-Ar hornblende closure temperature of ~475°C and a cooling rate over the temperature interval between this temperature and that of biotite K-Ar closure of ~3°C/m.y.. Hodges and Royden (in preparation) concluded that peak metamorphic

temperatures in the area reached at least 680°C based on garnet-biotite geothermometry. Simple extrapolation from the K-Ar hornblende closure temperature back to the peak metamorphic temperature using the 3°C/m.y. cooling rate yields a crystallization age of ~520 m.y.. This age is decidedly Finnmarkian. The clear fallacy in this approach lies in the implicit assumption that the cooling rate of a regionally metamorphosed terrain is constant through several hundred degrees centigrade. If any generalities can be made concerning this subject, an exponential rather than linear cooling function might be expected. In this case, the calculated crystallization age would be considerably less than 520 m.y.. Without more detailed information on the form of the function, it is impossible to say just how much less.

An alternative explanation of the 450 m.y. age would be that the analyzed hornblendes yield anomalously old ages due to excess radiogenic argon incorporated during crystallization, and that the metamorphism was Scandian. Excess argon has been documented in metamorphic amphiboles and biotites from the Sulitjelma area in the central Norwegian Caledonides (Wilson, 1972). The problem with this argument is that the ~450 m.y. age reported by Hodges et al., (in preparation) represents the mean of three statistically indistinguishable hornblende ages obtained for samples from outcrops up to 12 km. apart. As pointed out by Wilson (1972), discordance between K-Ar dates for the same mineral within a small area is symptomatic of excess argon. In the Aefjord-Sitasjaure area, hornblendes give consistent K-Ar ages over a relatively large area. If these ages are anomalously old due to excess argon, then we are left in the unfortunate position of finding a mechanism for generating and maintaining high and

uniform Ar partial pressures over a large area during amphibole crystallization.

Yet another interpretation (and the one which I prefer) is that D₁₋₂ deformation and coeval metamorphism occurred during neither the Finnmarkian nor the Scandian but sometime in between. Indeed, Rb-Sr whole-rock isochrons for post-and syn-tectonic intrusives in the central and northern Scandinavian Caledonides often yield ages suggestive of tectonic activity during the interval between the lower Ordovician and the middle Silurian (Gee and Wilson, 1974; Reymer, 1978; Claesson, 1979, 1980; Cribb, 1981; Wilson, 1981). In most of these cases, the deformation and metamorphism in question can be demonstrated to be "intra-allochthon" phenomena; none of the data seriously threaten the conclusion of Gee and Wilson (1976) that final emplacement of the main Caledonian allochthon onto the Baltic shield structural basement occurred during the Silurian. The Forsa thrust, on the other hand, is clearly a synmetamorphic feature. If the hornblende cooling ages are taken at face value, it is inescapable that initial emplacement of the main Caledonian allochthon onto the Baltic shield occurred at least 449 m.y. ago in the Aefjord-Sitasjaure area.

Interpretation of geochronologic data from multiply deformed terrains is never easy, and more comprehensive isotopic studies are required before definitive statements concerning the timing of deformational events in this segment of the Scandinavian Caledonides are warranted. For the time being, it seems prudent to suggest that the Caledonian orogeny in Scandinavia might best be looked at in terms of a continuum of deformation and metamorphism rather than two temporally distinct pulses.

Regional Nappe Correlations

Nicholson and Rutland (1969), Binns (1978), Gustavson (1978), and Zwann and Roberts (1978) have all presented regional nappe correlations for this portion of the Caledonides. Unfortunately, most of these suffer from the adoption of Gustavson's (1966, 1972) postulated thrust at the "base" of the Reppi schist, and some infer a tectonic contact at the base of the Salangen Group. Any attempts at regional nappe correlations involving allochthonous units in the Aefjord-Sitasjaure area must recognize: 1) that any tectonic discontinuities within the amphibolite grade, main Caledonian allochthon of this area are premetamorphic; 2) that a rough, "mirror-image" stratigraphy occurs on either side of the Reppi schist; 3) that there is no apparent tectonic discontinuity between the Salangen Group marbles and the underlying Sjurvatnet schist (part of the Narvik Group of Gustavson, 1966); and 4) that all of the units in the main Caledonian allochthon in this area must be older than the late Ordovician hornblende cooling ages.

Nicholson and Rutland's (1969) correlation between the Fauske Marble Group in the Bodo-Sulitjelma area (~150 km. south of the study area) and the Salangen Group seems reasonable in light of similarities in lithology and tectonic position between the two. It is tempting to correlate the units below the Salangen Group in the main Caledonian allochthon with the Sulitjelma schists structurally beneath the Fauske Marble Group. In particular, the Sulitjelma sequence includes the Sulitjelma ophiolite (Mason, 1967; Boyle et al., 1979), which may provide concrete evidence for the oceanic terrain only hinted at by the Rauvatn complex. One potential problem with this correlation lies in Nicholson's (1974) assertion of

structural discontinuity between the Fauske Marble Group and Sulitjelma schists, although Nicholson and Rutland (1969) argued structural continuity between the two. A more serious complication concerns the Furulund Group, which underlies the Sulitjelma schist/ophiolite sequence, and its relationship with those units. Kautsky (1953), Nicholson and Rutland (1969), Henley (1970), and Findlay (1980) have argued for a major thrust between the Sulitjelma and Furulund sequences. Boyle et al., (1979) and Boyle et al., (1981) suggest that the entire Sulitjelma-Furulund system is overturned and that the Furulund Group was deposited unconformably onto the Sulitjelma sequence. The unconformity interpretation is initially appealing in that certain horizons within the Furulund Group sound similar to the Reppi schist based on published descriptions (e.g., Findlay, 1980). Unfortunately, low grade portions of the Furulund Group near the Swedish-Norwegian border and correlative rocks northeast and southwest of Sulitjelma in Sweden contain late Caradocian to Silurian fossils (Catenipora sp.; Wilson, 1970). If the Sulitjelma and Furulund sequences form a coherent tectonic unit as suggested by Boyle et al., (1981), then the presence of late Ordovician-Silurian fossils within this unit prohibits correlation with the main Caledonian allochthon in the Aefjord-Sitasjaure area which was metamorphosed prior to or during the early Caradocian. Still, considering: a) the general disagreement in structural interpretations for the Sulitjelma area; b) the similarities between the Sulitjelma and Aefjord-Sitasjaure lithologies; and c) the possibility (however remote) that the Aefjord-Sitasjaure K-Ar ages reflect excess argon; the main Caledonian allochthon in the study area is tentatively correlated with the Fauske + Sulitjelma (+ Furulund ?) sequence in the Sulitjelma area.

The Fauske + Sulitjelma sequence was termed the Gasak Nappe by Kautsky (1953). The Gasak is in turn broadly correlative with the Rosingsfjall Nappe of Kulling (1955). Kulling (1964), in a paper concerning the northern Norrbotten mountains of Sweden (immediately east of the study area), correlated units in the Aefjord-Sitasjaure area with the Seve-Koli Nappe complex which occurs structurally below the Rodingsfjall Nappe. On the other hand, Kulling (1972; p.258) places units which are clearly correlative with the main Caledonian allochthon in the study area (Foslie, 1942) in his Stipok Klippe of the Rodingsfjall Nappe. Based on Kulling's (1964, 1972) and Foslie's (1942) lithologic descriptions, I favor the Rodingsfjall Nappe correlation.

Regional correlation of the Storriten complex is comparatively easy. The Swedish portion of the complex was mapped by Kulling (1964) as his "Middle Thrust Rocks" of Abisko Nappe. However, rocks of the Storriten complex bear little resemblance to the banded tectonites ("hardskiffer") characteristic of the Abisko Nappe in its type area. From Kulling's (1964) lithologic descriptions, it seems equally likely that the Storriten complex rocks could be correlative with his "Lower Thrust Rocks." Thus, I regard the Storriten complex as broadly correlative with Kulling's Middle and Lower thrust packages. This unit is also clearly correlative with the Akkajaure complex of Kautsky (1953).

Structural Style

Most tectonic models of the Scandinavian Caledonides have emphasized the importance of westward-thinning thrust sheets with high aspect ratios in the structural architecture (e.g., Gee, 1975; Nicholson and Rutland, 1969; Binns, 1978). While thrusting was indisputably an important

shortening mechanism, large fold nappes may be more common and more significant than generally supposed. Early, large-amplitude recumbant folds have been described in the central and northern Scandinavian Caledonides by Olesen (1971), Boyle et al., (1979), Graversen et al., (1981), Bartley (in press), and in this report. It seems reasonable to suspect that large-scale lithostratigraphic inversions may be common within the main Caledonian allochthon.

This report also presents evidence for three distinct episodes of thrusting (D_1 , D_2 , and D_4) within the Aefjord-Sitasjaure area. On eastern Hinnoy, west of the study area, Hakkinen (1977) and Bartley (1982; in press) recognized yet another thrusting event which is approximately time-correlative with the D_3 event of this report. Of these four thrusting events, the first is premetamorphic, the second and third are broadly synmetamorphic, and the third and fourth involve Baltic shield basement lithologies. Hodges et al., (in preparation, a) interpreted the transition from basement non-involvement to basement involvement as the consequence of continued subduction of the Baltic craton beneath the Greenland craton during continent-continent collision. It is becoming increasingly clear from studies here and elsewhere in the north-central Scandinavian Caledonides (e.g., Thelander, 1980) that the Baltic cratonal basement was much more significantly involved in Caledonian thrusting and folding than has been commonly assumed.

Gee (1980) has emphasized the importance of upper and middle Cambrian, organic-rich shales of the Baltic platformal to miogiosynclinal sequence in providing major decollement horizons for translation of the main Caledonian allochthon onto the Baltic margin. If the graphitic

phyllites which constitute much of the Storriten complex are correlative with the middle Cambrian "alum" shale of Kulling (1964), it would appear that these shales also provide important "secondary" detachment surfaces for basement-involved thrusts such as the Mereftasfjell as they ramp up-section into the stratigraphic cover from their "primary" detachment surfaces within the basement.

CONCLUSIONS

Geologic mapping at a scale of 1:50,000 in the Aefjord-Sitasjaure area permits subdivision of the main Caledonian allochthon at this latitude into seven tectonostratigraphic units. Contact relationships between these units are often unclear due to their premetamorphic development, but the Rauvatn complex (of probable oceanic affinity) is clearly thrust-bounded, and the underlying Sjurvatnet schist is an unconformity marked by the Elvenes conglomerate. Whatever their initial contact relationships, these units appear to have behaved as a coherent mass during their synmetamorphic emplacement onto the Baltic craton structural basement. Based on similarities with units at this structural level in the Sulitjelma area, the main Caledonian allochthon at this latitude is considered to be correlative with the Rodingsfjall Nappe.

Six deformational episodes were recognized in the area. D₁ involved stacking of tectonostratigraphic units within the main Caledonian allochthon. D₂ included the development of large-scale fold nappes and emplacement of the main Caledonian allochthon onto the Tysfjord-Rombak

basement terrain along the Forsa thrust. D₃ and D₄ resulted in ~N-S isoclinal and ~E-W upright folding (repectively) of structural basement and cover. D₅ marks the development of the Mereftasfjell and Frostisen thrusts which imbricated the Tysfjord-Rombak basement terrain and led to further translation of the main Caledonian allochthon toward the Baltic foreland. The Storriten complex, a schuppenzone developed in between the Mereftasfjell and Frostisen thrusts during D₅, is considered equivalent to the Abisko complex of Kulling (1964) and the Akkajaure complex of Kautsky (1953). D₆ resulted in roughly N-S trending upright folds.

K-Ar ages for hornblendes defining the S₂ schistosity in metabasic rocks in both the structural basement and cover suggest that initial emplacement of the main Caledonian allochthon onto the Aefjord-Rombak terrain occurred at least 449±19 m.y. ago.

REFERENCES

- Armstrong, R.L. 1966. K-Ar dating of plutonic and volcanic rocks in orogenic belts. In: Potassium Argon Dating (edited by Schaeffer, O.A., and Zahringer, J.). Springer-Verlag, 117-133.
- Bartley, J.M. 1981. Lithostratigraphy of the Storvann Group, East Hinnoy, north Norway, and its regional implications. *Norg. geol. Unders.* 370, 11-24.
- Bartley, J.M. 1982. Limited basement involvement in Caledonian deformation, Hinnoy, north Norway, and tectonic implications. *Tectonophysics* 83, 185-203.
- Bartley, J.M. in press. Structural evolution of East Hinnoy, north Norway. *Jour. Struct. Geol.*
- Binns, R.E. 1978. Caledonian nappe correlation and orogenic history in Scandinavia north of lat67°N. *Geol. Soc. Amer. Bull.* 89, 1475-1490.
- Boyle, A.P., Griffiths, A.J., and Mason, R. 1979. Stratigraphical inversion in the Sulitjelma area, central Scandinavian Caledonides. *Geol. Mag.* 116, 393-402.
- Boyle, A., Hansen, T.S., Kollung, S., and Mason, R. 1981. A new tectonic perspective of the Sulitjelma region. *Terra Cognita* 1, 36.
- Claesson, S. 1979. Pre-Silurian orogenic deformation in the north-central Scandinavian Caledonides. *Geol. For. Stockh. Forh.* 101, 353-356.
- Claesson, S. 1980. A Rb-Sr isotope study of granitoids and related mylonites in the Tannas Augen Gneiss Nappe, southern Swedish Caledonides. *Geol. For. Stockh. Forh.* 102, 403-420.
- Clifford, P. 1960. The geological structure of the Loch Luichart area, Ross-shire. *J. geol. Soc. Lond.* 115, 365-386.
- Cribb, S.J. 1981. Rb-Sr geochronological evidence suggesting a reinterpretation of part of the north Norwegian Caledonides. *Norsk geol. Tidsskr.* 61, 97-110.
- Dewey, J.F. 1969. Evolution of the Appalachian/Caledonide orogen. *Nature* 222, 124-129.
- Dodson, M.H. 1973. Closure temperature in cooling geochronological and petrological systems. *Contr. Miner. Petrol.* 40, 259-274.
- Findlay, R.H. 1980. A regional lithostratigraphy for southern and eastern Sulitjelma, north Norway. *Norsk geol. Tidsskr.* 60, 223-234.
- Foslie, S. 1941. Tysfjords geologi. *Norg geol. Unders.* 149, 1-298.

- Foslie, S. 1942. Hellemobotn og Linnajavrre. Norg. geol. Unders. 150, 1-119.
- Gee, D.G. 1975. A tectonic model for the central part of the Scandinavian Caledonides. Am. J. Sci. 275A, 468-515.
- Gee, D.G. 1978. Nappe displacement in the Scandinavian Caledonides. Tectonophysics 47, 393-419.
- Gee, D.G. 1980. Basement-cover relationships in the central Scandinavian Caledonides. Geol. For. Stockh. Forh. 102, 455-474.
- Gee, D.G., and Wilson, M.R. 1974. The age of orogenic deformation in the Swedish Caledonides. Am. J. Sci. 274, 1-9.
- Gee, D.G., and Wilson, M.R. 1976. A reply. Am. J. Sci. 276, 390-394.
- Graversen, O., Marker, M., and Sovegjarro, U. 1981. Precambrian and Caledonian nappe tectonics in the central Scandinavian Caledonides, Nordland, Norway. Terra Cognita 1, 47.
- Gustavson, M. 1966. The Caledonian mountain chain of southern Troms and Ofoten areas, Part I: Basement rocks and Caledonian metasediments. Norges geol. Unders. 239, 1-162.
- Gustavson, M. 1972. The Caledonian mountain chain of southern Troms and Ofoten areas, Part III: Structures and structural history. Norges geol. Unders. 283, 1-56.
- Gustavson, M. 1974. 1:250,000 berggrunnsgeologisk kart over Narvik. Norges Geologiske Undersokelse.
- Gustavson, M. 1978. Caledonides of north-central Norway. Geol. Surv. Canada 78-13, 25-30.
- Hakkinen, J.W. 1977. Structural geology and metamorphic history of Western Hinnoy and adjacent parts of Eastern Hinnoy, north Norway. Unpub. Ph.D. thesis, Rice University, Houston, 161p.
- Hansen, E. 1971. Strain Facies. Springer-Verlag, 207p.
- Heier, K.S., and Compston, W. 1969. Interpretation of Rb-Sr age patterns in high-grade metamorphic rocks, north Norway. Norsk geol. Tidsskr. 49, 257-283.
- Henley, K.J. 1970. The structural and metamorphic history of the Sulitjelma region, Norway, with special reference to the nappe hypothesis. Norsk geol. Tidsskr. 50, 97-136.
- Hodges, K.V., Bartley, J.M., and Burchfiel, B.C. In preparation, a. Structural evolution of an A-type subduction zone, Lofoten-Rombak area, northern Scandinavian Caledonides.

- Hodges, K.V., Bartley, J.M., Krueger, H.W., and Hodges, L.R. In preparation, b. The use of discordant apparent mineral ages in determining closure temperatures and cooling rates in geologic environments.
- Hodges, K.V., and Royden, L. In preparation. Geothermometry and geobarometry of retrograded metamorphic rocks: an indication of the uplift trajectory of a portion of the northern Scandinavian Caledonides.
- Kautsky, G. 1953. Der Geologische bau des Sulitelma-Salojauregebietes in den Nordscandinavischen Kaledoniden. *Sverges geol. Unders.* 528, 1-228.
- Kulling, O. 1955. Den kaledoniska fjällkedjans berggrund inom Västerbottens län. Beskrivning till berggrundskarta över Västerbottens län, 2. *Sverges geol. Unders.* Ca 37, 101-296.
- Kulling, O. 1964. Oversikt över Norra Norrbottensfjällens kaledon-berggrund. *Sverges geol. Unders.* Ba 19, 1-165.
- Kulling, O. 1972. The Swedish Caledonides. In: *Scandinavian Caledonides* (edited by Strand, T., and Kulling, O.), Wiley Interscience, 302p.
- Kvale, A. 1953. Linear structures and their relation to movement in the Caledonides of Scandinavia and Scotland. *Jl. geol. Soc. Lond.* 109, 51-73.
- Mason, R. 1967. The field relations of the Sulitjelma Gabbro, Nordland. *Norsk geol. Tidsskr.* 47, 237-248.
- Nicholson, R., and Rutland, R.W.R. 1969. A section across the Norwegian Caledonides; Bodo to Sulitjelma. *Norges geol. Unders.* 260, 1-86.
- Olesen, N.O. 1971. The relative chronology of fold phases, metamorphism and thrust movements in the Caledonides of Troms, northern Norway. *Norsk geol. Tidsskr.* 51, 355-377.
- Ramsay, D.M., and Sturt, B.A. 1976. The syn-metamorphic emplacement of the Mageroy Nappe. *Norsk geol. Tidsskr.* 56, 291-308.
- Ramsay, J.G. 1960 The deformation of early linear structures in areas of repeated folding. *J. Geol.* 68, 75-93.
- Ramsay, J.G. 1981. Tectonics of the Helvetic Nappes. In: *Thrust and Nappe Tectonics* (edited by Price, N.J., and McClay, K.R.), Blackwell, 293-310.
- Reymer, A. 1978. Precambrian elements in the Seve Nappe. In: *XIII Nordiske geologiske vintermode, Abstracts* (edited by Berthelsen, A., and Hansen, M.), Kobenhavns Universitet, 52.

- Roberts, D. 1971. Timing of Caledonian orogenic activity in the Scandinavian Caledonides. *Nature Physical Science* 232, 22-23.
- Steltenpohl, M.G. 1982. Structural and stratigraphic relationships of the Ofoten synform, North Norway. Unpub. M.S. thesis. University of Alabama. Tuscaloosa.
- Sturt, B.A., Pringle, I.R., and Ramsay, D.M. 1978. The Finnmarkian phase of the Caledonian orogeny. *Jl. geol. Soc. Lond.* 135, 597-610.
- Thelander, T., Bakker, E., and Nicholson, R. 1980. Basement-cover relationships in the Nasafjället Window, central Swedish Caledonides. *Geol. For. Stockh. Forh.* 102, 569-580.
- Tornebohm, A.E. 1896. Grunddragen af det centrala Skandinaviens bergbyggnad. *Kongliga Svenska Vetenskaps Akademiens Handlingar* 28, 1-210.
- Tull, J.F., Bartley, J.M., Hodges, K.V., Andresen, A., Steltenpohl, M.G., and White, J.M. In press. Overview of the tectonic evolution of the Caledonides in the Ofoten region (68°-69°N), North Norway. In: IGCP Caledonides Symposium Volume, Uppsala.
- Turner, F.J., and Weiss, L.E. 1963. Structural Analysis of Metamorphic Tectonites. McGraw-Hill. 545p.
- Vogt, T. 1942. Trekk av Narvik-Ofoten traktens geologi. *Norges geol. Unders.* 21, 198-213.
- Wilson, M.R. 1970. The timing of orogenic activity in the Bodo-Sulitjelma tract. *Norges geol. Unders.* 269, 184-190.
- Wilson, M.R. 1972. Excess radiogenic argon in metamorphic amphiboles and biotites from the Sulitjelma region, central Norwegian Caledonides. *Earth Planet. Sci. Lett.* 14, 403-412.
- Wilson, M.R. 1981. Geochronological results from Sulitjelma, Norway. *Terra Cognita* 1, 82.
- Zwann, K.B., and Roberts, D. 1978. Tectonostratigraphic succession and development of the Finnmarkian nappe sequence, North Norway. *Norges geol. Unders.* 343, 53-71.

TABLE 1. DEFORMATIONAL SEQUENCE IN THE AEFJORD-SITASJAURE AREA

	Elements	Inferred Vergence or Transport Direction	Age
D ₁	Unnamed T ₁ thrusts within the main Caledonian allochthon	?	?
D ₂	The Forså ⁰ thrust (T ₂)	E	> 449 m.y.
	Recumbent folds (F ₂)	E	> 449 m.y.
	Axial-planar schistosity (S ₂)	--	> 449 m.y.
D ₃	Recumbent folds (F ₃)	ESE	?
	Axial-planar schistosity (S ₃)	--	?
D ₄	Upright cross-folds (F ₄)	NE or SW	?
D ₅	The Frostisen and Mereftasfjell thrusts (T ₅)	S60°E	?
	The Storriten complex schuppenzone	S60°E	?
D ₆	Upright back-folds (F ₆)	WSW	?
	Crenulation cleavage (S ₆)	--	?
	High-angle fault (?)	?	?

FIGURE CAPTIONS

- Figure 1. Generalized tectonic map of the Scandinavian Caledonides showing the distribution of structural cover (patterned) and structural basement.
- Figure 2. Generalized tectonic map of the Ofoten region, western Scandinavia showing distribution of structural cover (patterned) and structural basement. The Aefjord-Sitasjaure area, covered by the geologic map shown in Plate 1, is outlined. Hi - Hinnoy; Ha - Hafjell; Ac - Aefjord Culmination; Rw - Rombak Window.
- Figure 3. Tectonic stratigraphy of the Aefjord-Sitasjaure area indicating correlations with other stratigraphies proposed for this area by Foslie (1941) and Gustavson (1966).
- Figure 4. Tectonic map of the Aefjord - Sitasjaure area.
- Figure 5. Equal-area stereographic contour diagrams. a) Poles to S_2 cleavage and F_2 axial planes; b) F_2 fold axes; c) Poles to S_3 cleavage and F_3 fold axes; d) F_3 fold axes; e) Poles to F_4 axial planes; f) F_4 fold axes; g) Poles to phyllonitic cleavage, Storriten complex; h) Poles to mylonitic cleavage in basement slices, Storriten complex; i) Poles to S_6 cleavage and F_6 axial planes; j) F_6 fold axes.
- Figure 6. Graphical method of constraining the kinematic a axis for F_4 folds. See text for explanation.

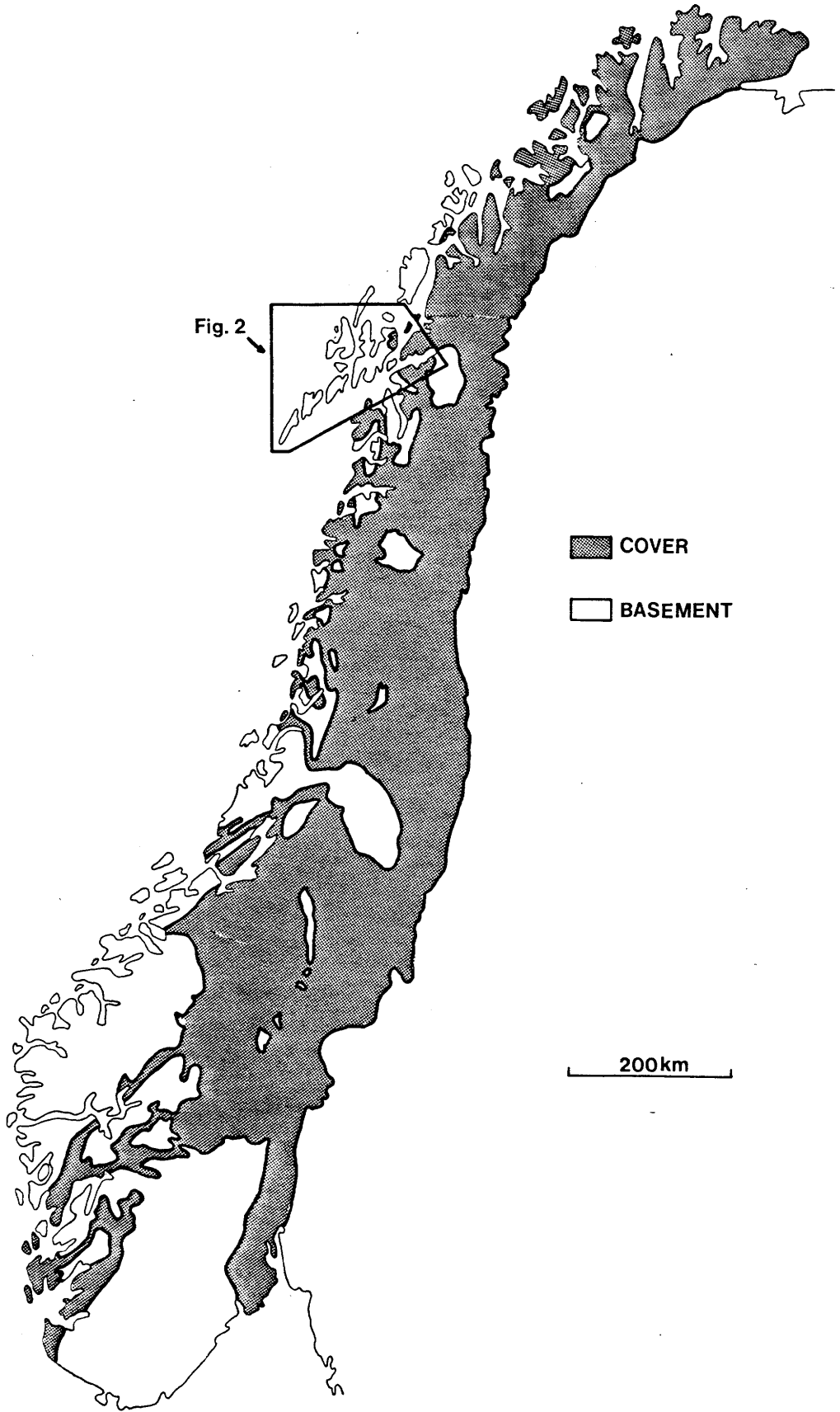
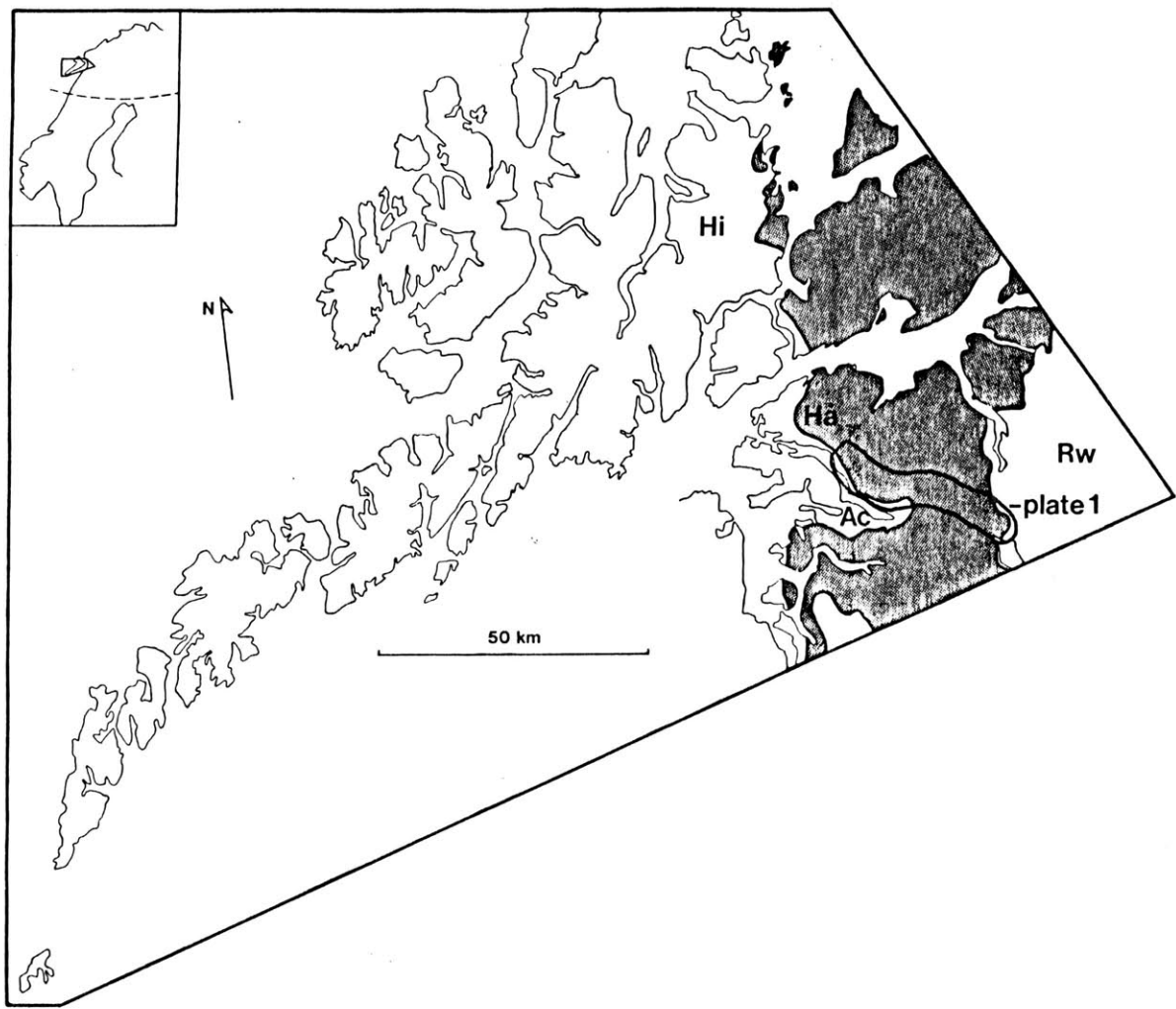


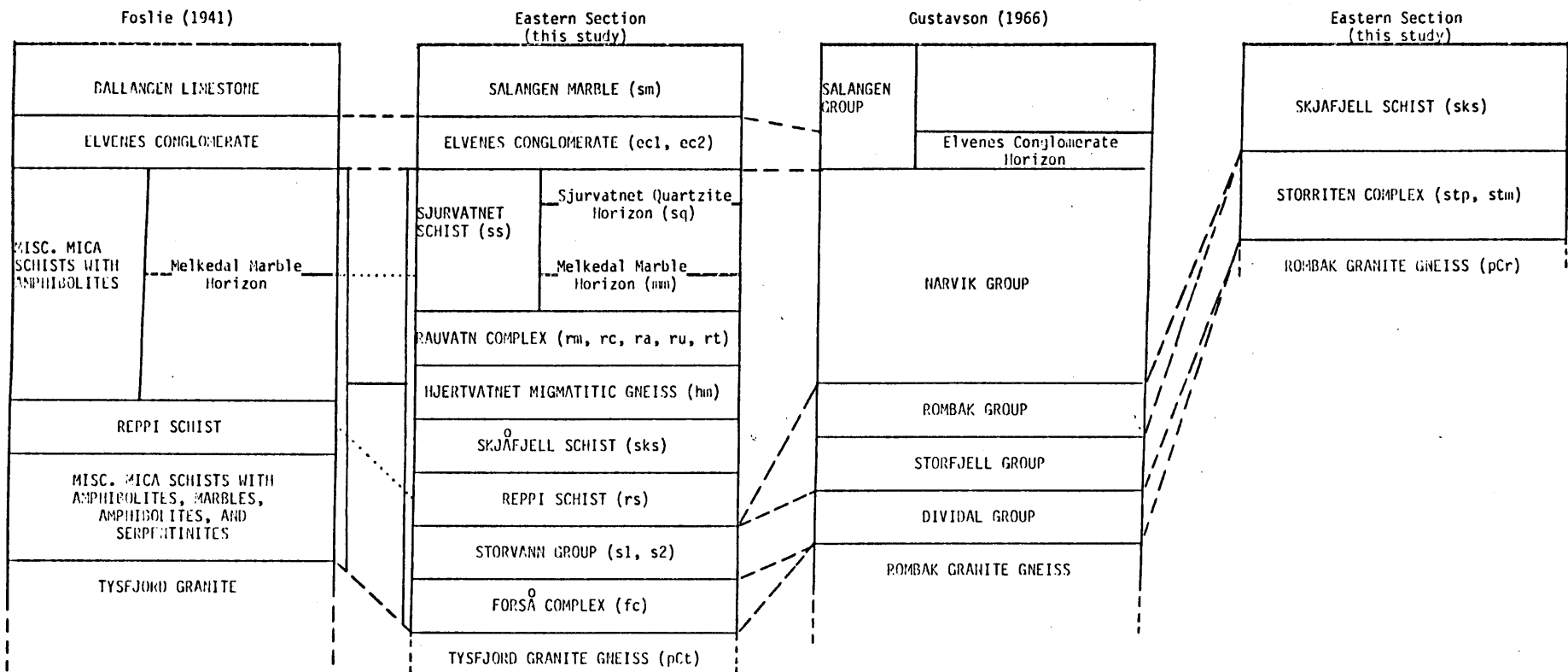
Fig. 2

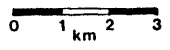
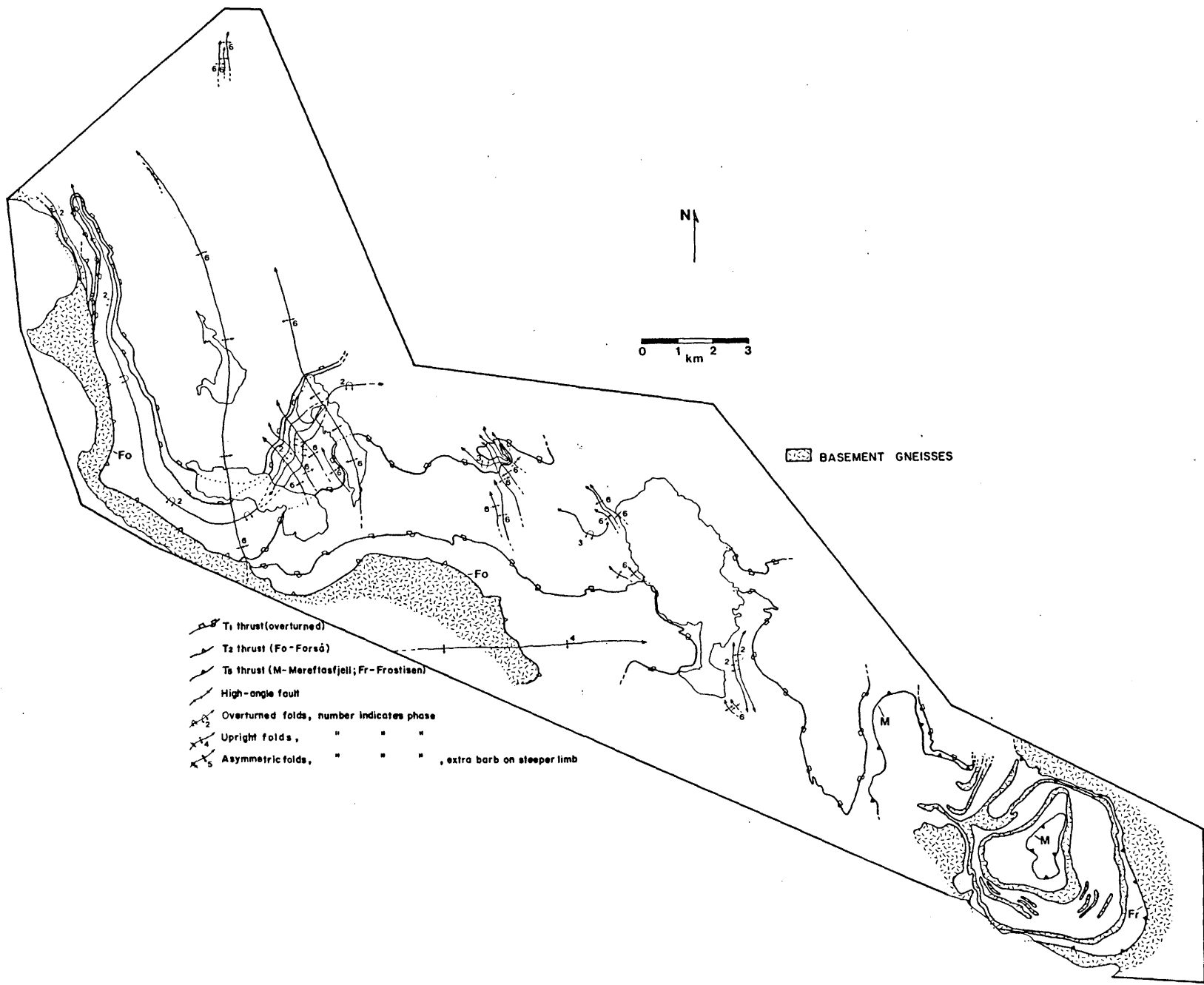
COVER

BASEMENT





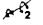
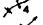

200km



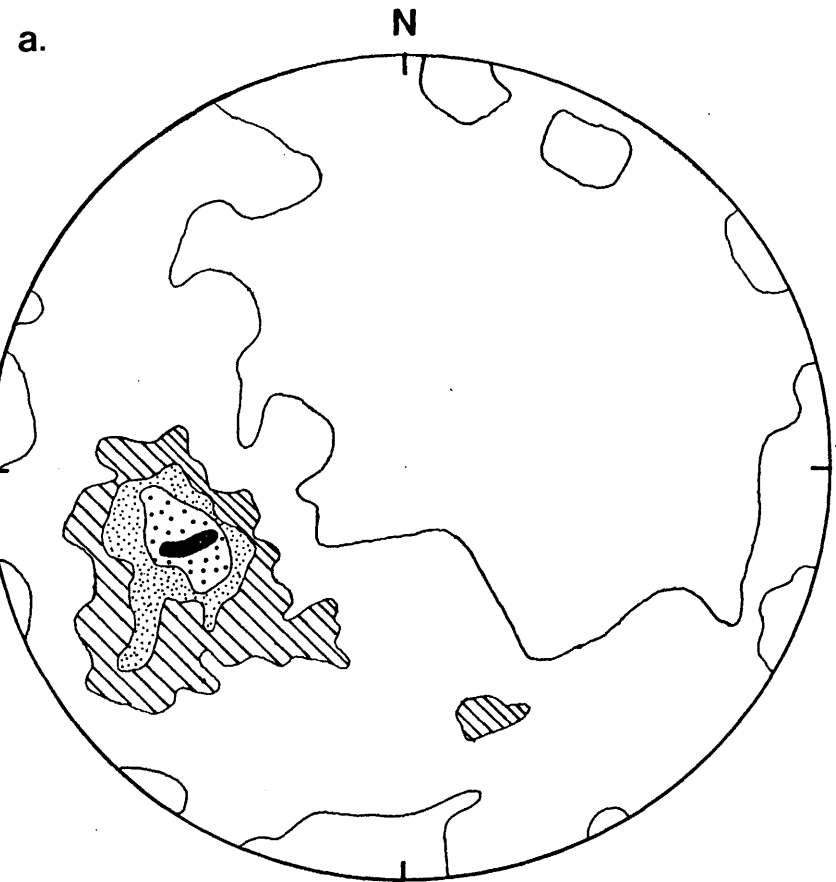




 BASEMENT GNEISSES

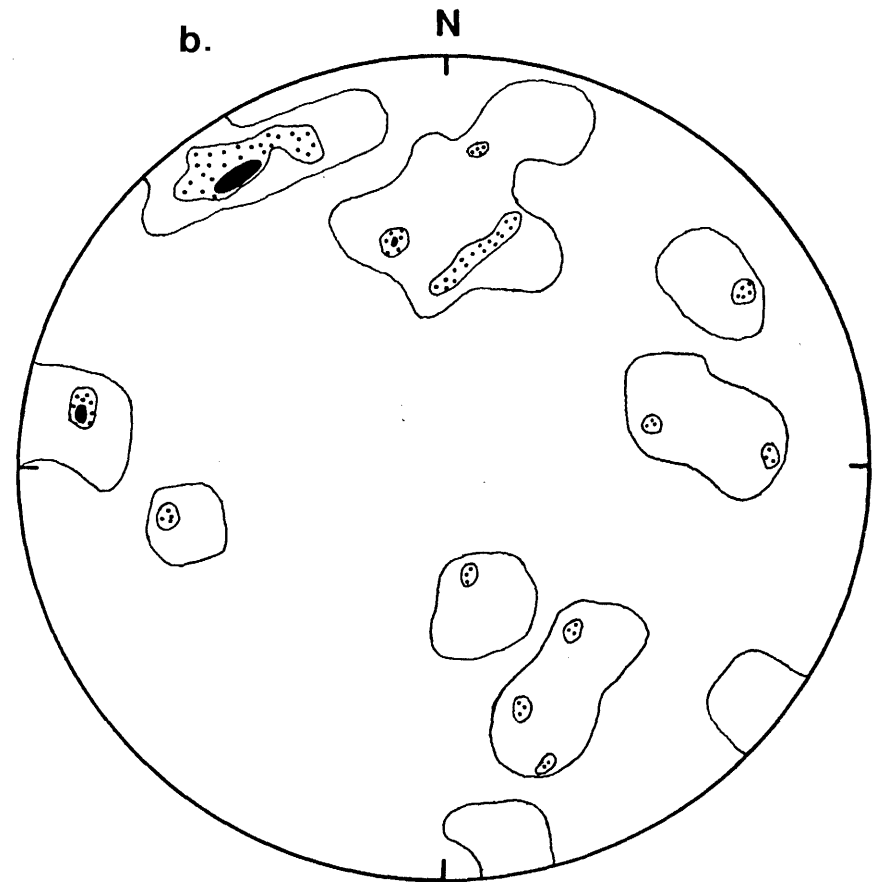
-  T₁ thrust (overturned)
-  T₂ thrust (Fo-Forsá)
-  T₃ thrust (M-Merettasfjell; Fr-Frostisen)
-  High-angle fault
-  Overturned folds, number indicates phase
-  Upright folds, " " "
-  Asymmetric folds, " " " , extra barb on steeper limb

**S₂ CLEAVAGE
F₂ AXIAL PLANES**



**117 POLES TO PLANES
C.I. = 4%/area**

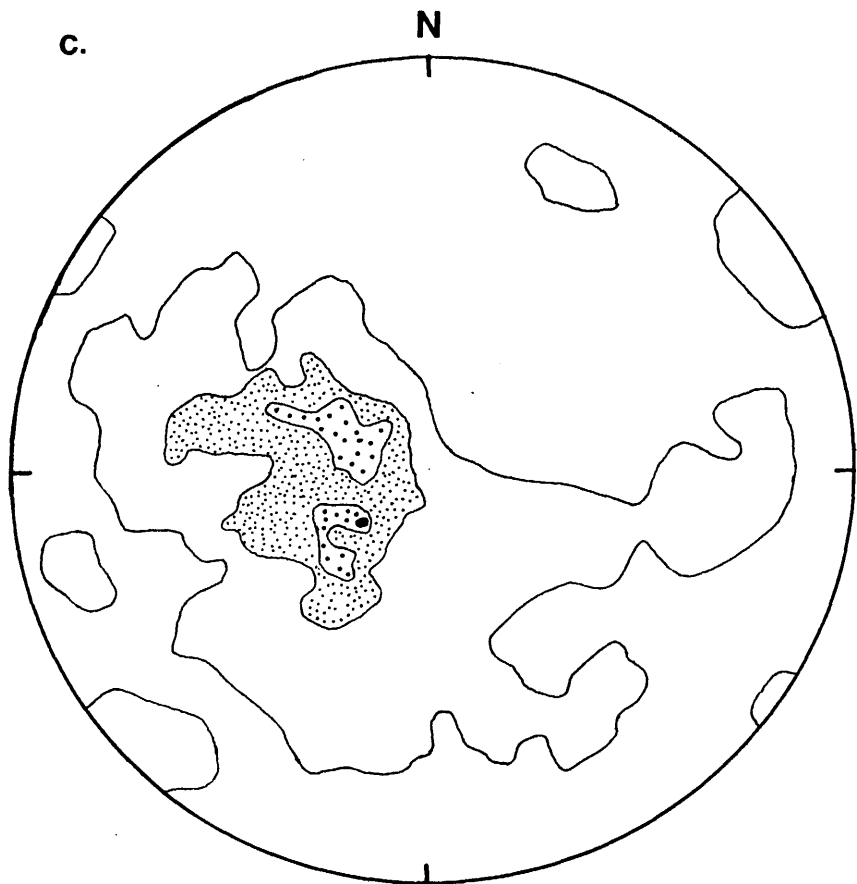
F₂ AXES



**20 AXES
C.I. = 5%/area**

**S₃ CLEAVAGE
F₃ AXIAL PLANES**

c.

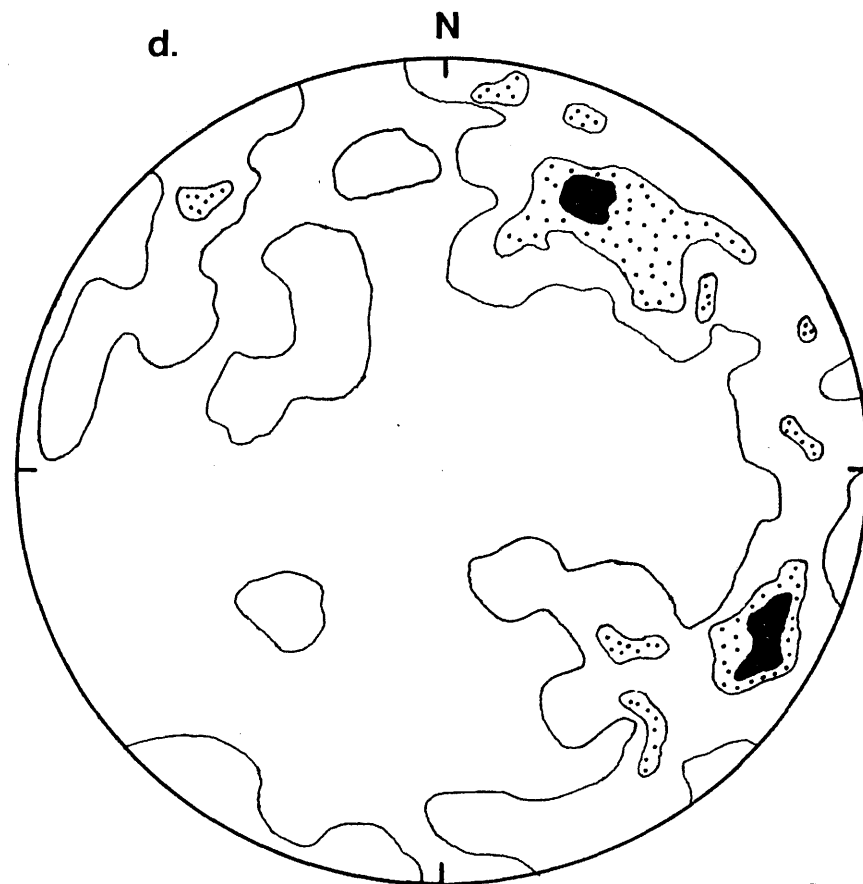


103 POLES TO PLANES

C.I. = 5% / % area

F₃ FOLD AXES

d.

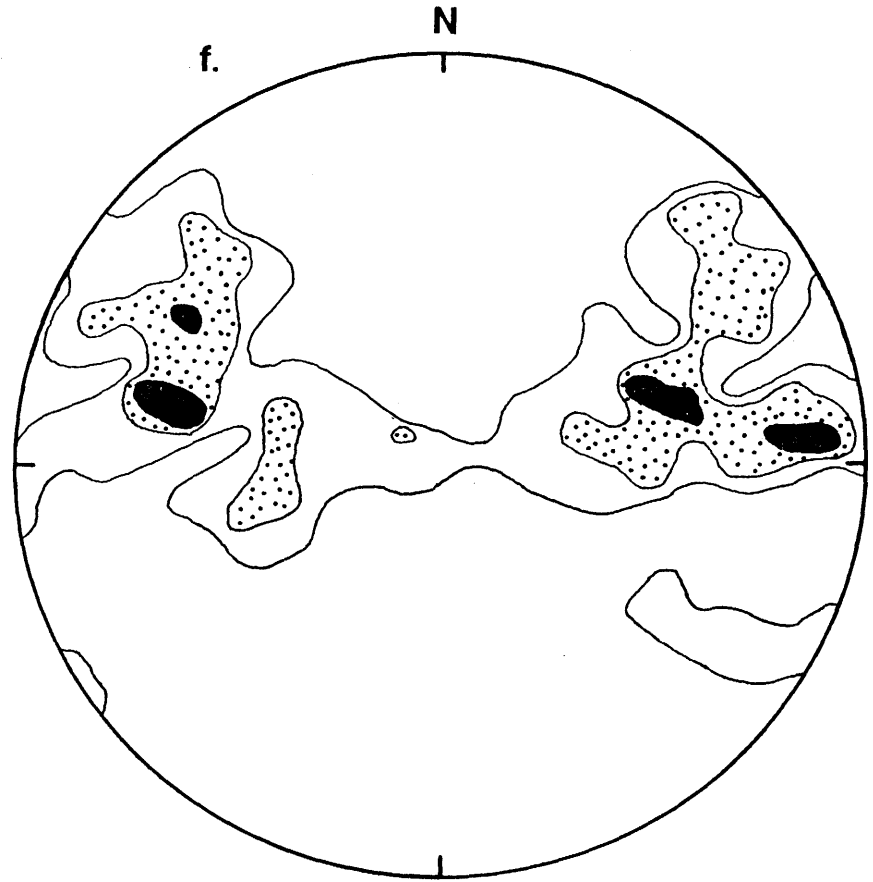
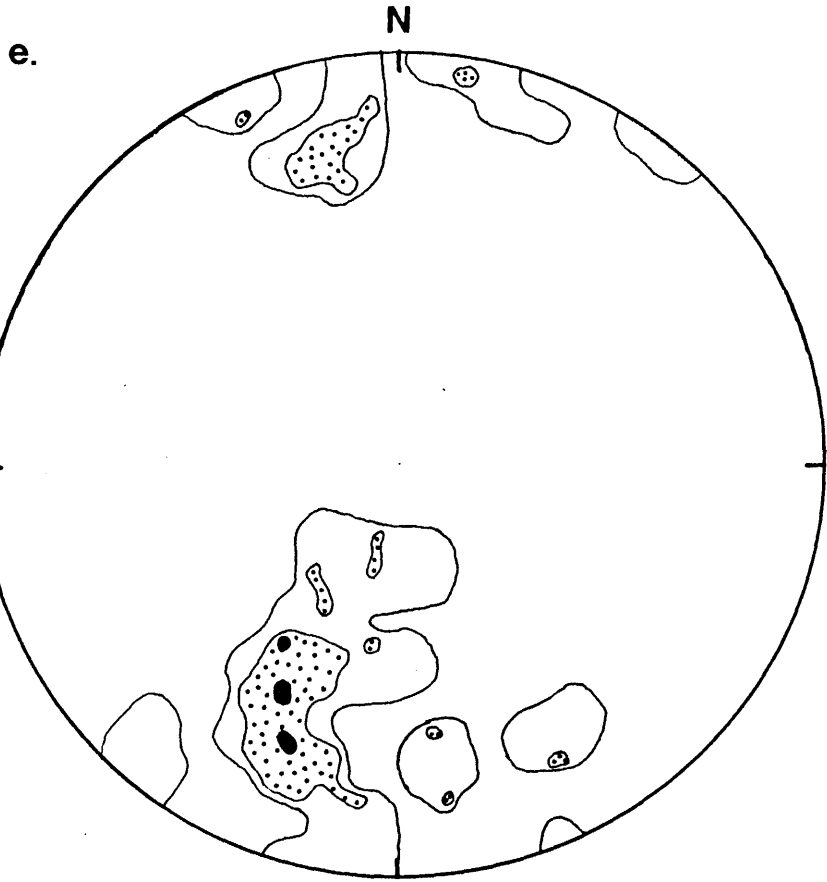


70 AXES

C.I. = 4% / % area

F₄ AXIAL PLANES

F₄ FOLD AXES



22 POLES TO PLANES

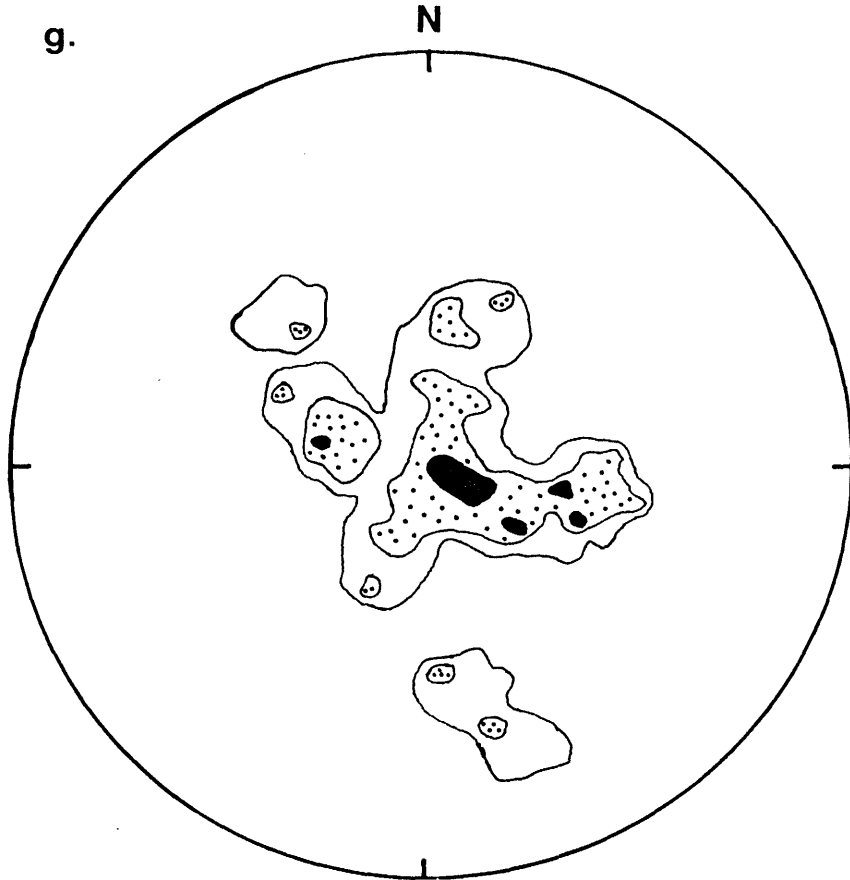
C.I. = 10% / % area

43 AXES 55

C.I. = 4% / % area

**PHYLLONITIC CLEAVAGE
STORRITEN COMPLEX**

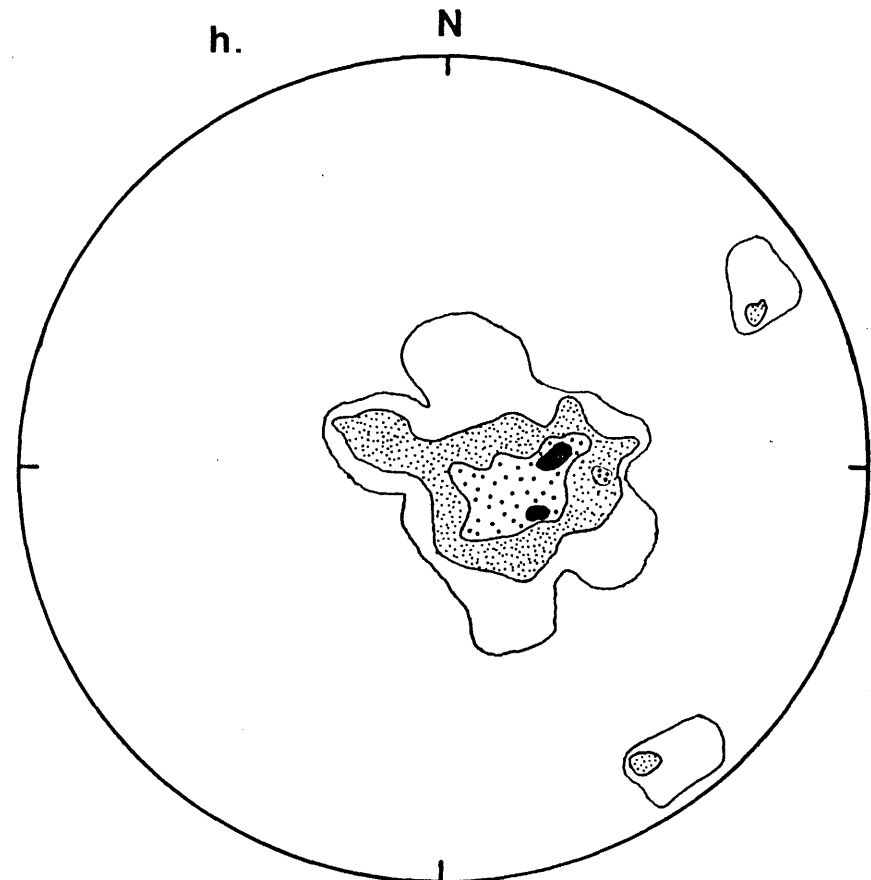
g.



**19 POLES TO PLANES
C.I. = 11%/% area**

**MYLONITIC CLEAVAGE
STORRITEN COMPLEX**

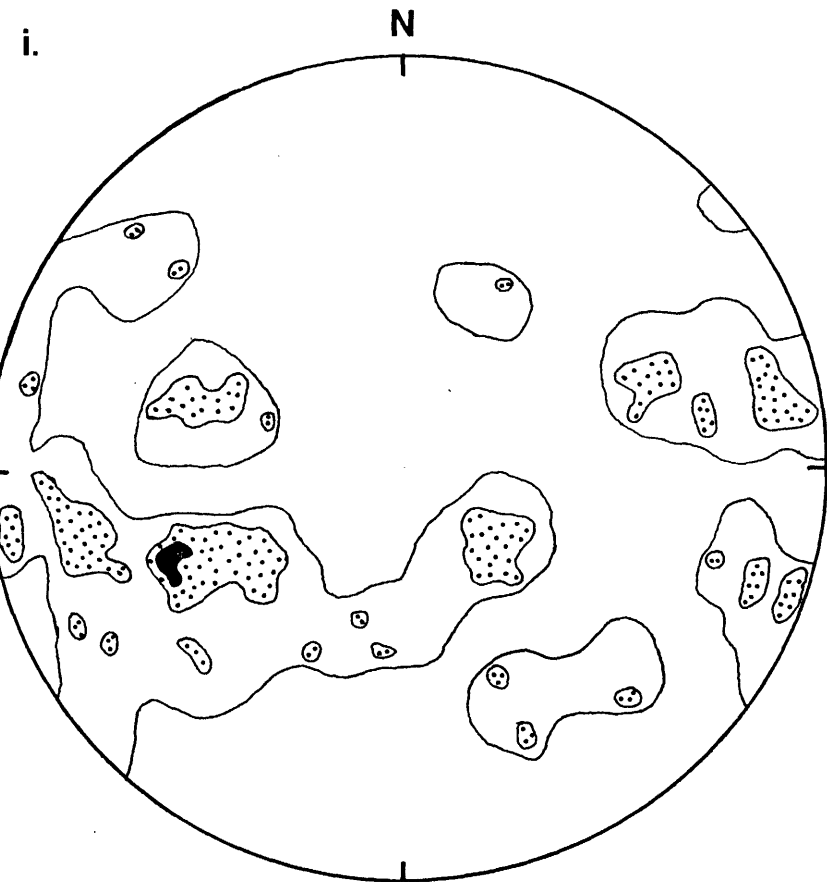
h.



**22 POLES TO PLANES
C.I. = 10 %/% area**

S₆ CLEAVAGE

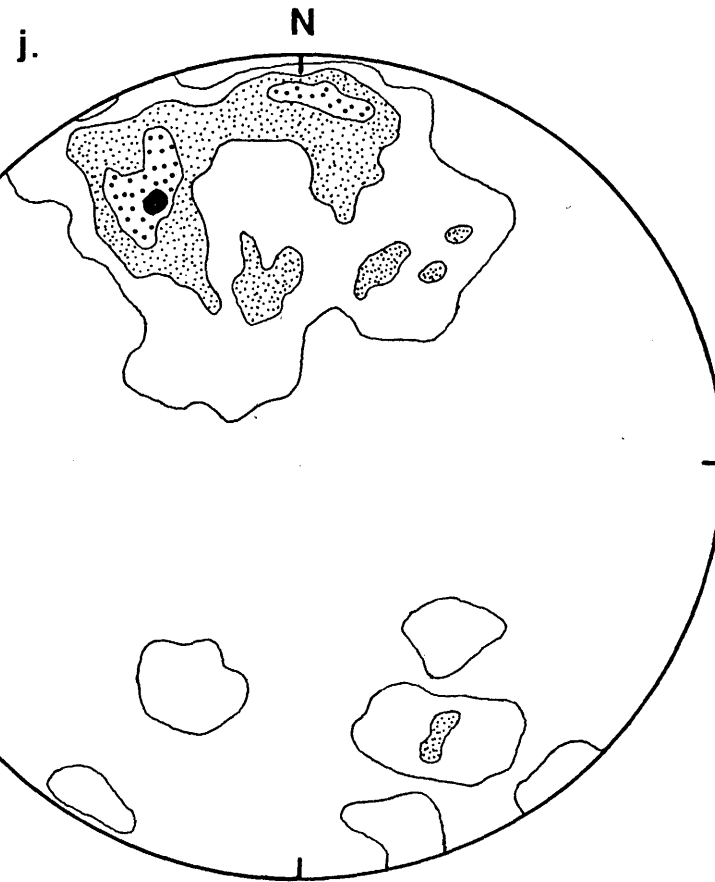
F₆ AXIAL PLANES



35 POLES TO PLANES

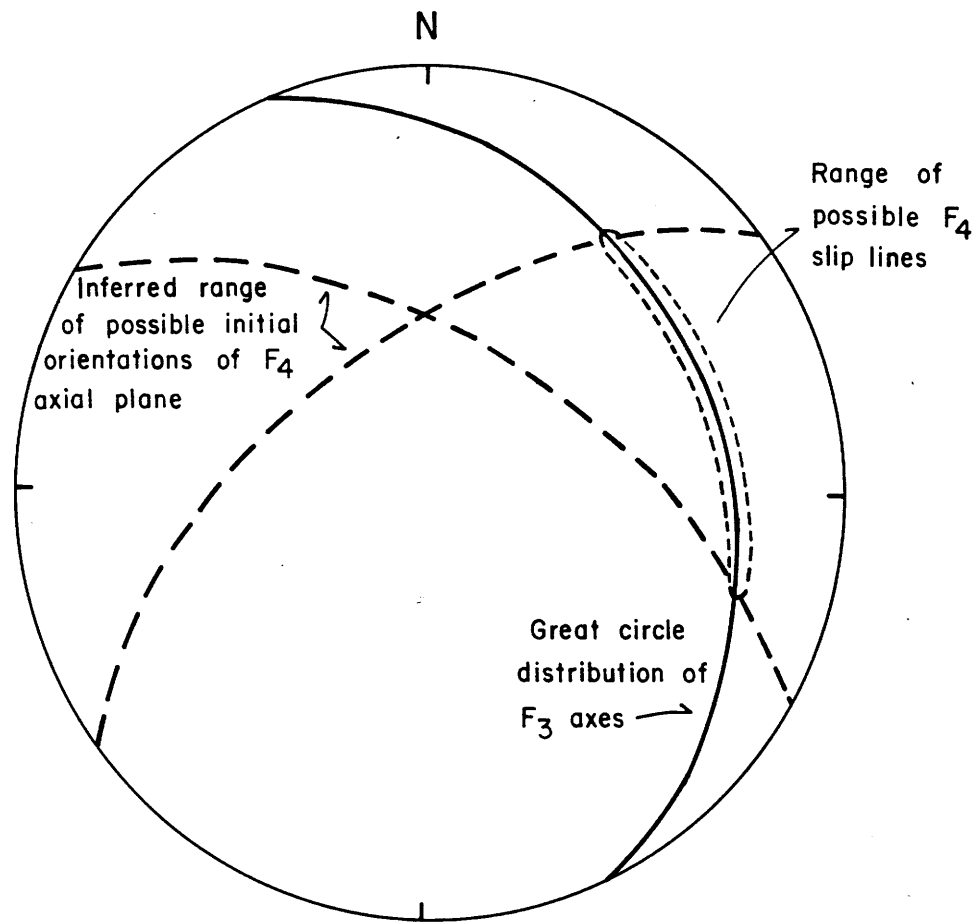
C.I. = 5%/% area

F₆ FOLD AXES



53 AXES 57

C. I. = 4%/% area



PART II

THE USE OF DISCORDANT APPARENT MINERAL AGES IN DETERMINING CLOSURE
TEMPERATURES AND COOLING RATES IN GEOLOGIC ENVIRONMENTS

THE USE OF DISCORDANT APPARENT MINERAL AGES IN DETERMINING CLOSURE
TEMPERATURES AND COOLING RATES IN GEOLOGIC ENVIRONMENTS

ABSTRACT

Use of the equation derived by Dodson (1973) to calculate closure temperatures for geochronological systems requires the assumption of a cooling rate. In slowly cooling instances (cooling rate $< 10^{\circ}\text{C}/\text{my}$), small errors in assumed cooling rate can lead to significant errors in calculated closure temperatures. When two discordant mineral ages are available for a particular area, we show that it is possible to determine uniquely the closure temperatures for each mineral-isotopic system, and the average cooling rate over the interval between closure of the two systems. Application of this technique using discordant metamorphic hornblende and biotite K-Ar ages from the Aefjord area in the northern Norwegian Caledonides yields closure temperatures of $473 (+11/-7)^{\circ}\text{C}$ and $263 (+10/-5)^{\circ}\text{C}$ for hornblende and biotite respectively, and an average cooling rate of $3.0 (+2.9/-1.0)^{\circ}\text{C}/\text{my}$ over the interval of discordancy.

INTRODUCTION

The calculated isotopic age of a rock or mineral reflects that point in time at which it became an effectively closed system with respect to gain or loss of the radiogenic isotope used for dating. Ideally, this age corresponds to the crystallization age of the sample. Even in the early years of geochronology, however, it became clear that mineral ages in geologic terrains with complex thermal histories often greatly underestimated the true age of crystallization (Tilton et al., 1958; Goldich et al., 1961). Hart (1964) found major discordancies in K-Ar and Rb-Sr ages for a variety of minerals in a contact metamorphic aureole and attributed these discrepancies to variations in the temperatures required to "reopen" the mineral systems to loss of radiogenic daughter products. Armstrong (1966); Armstrong et al., (1966); and Harper (1967) concluded that discordant mineral ages in regional metamorphic terrains could be similarly explained by slow cooling through a series of critical closure temperatures which varied from one mineral-isotopic system to another. Ultimately, Dodson (1973), using the assumption that volume diffusion of the radiogenic daughter product controls closure of mineral systems, derived a mathematical relationship between the closure temperature of a geochronological system, the solid-state diffusion parameters governing mobility of the daughter product during cooling, and the absolute cooling rate.

Although mineral ages are only minimum estimates of crystallization ages in igneous and metamorphic terrains, they provide a wealth of information concerning the cooling history of those areas. Mineral ages have been used to constrain uplift rates in regional metamorphic terrains

(Clark and Jager, 1969; Dallmeyer et al., 1975; Dallmeyer, 1978) and to construct detailed cooling curves for igneous intrusions (Harrison et al., 1979; Harrison and McDougall, 1980a). The closure temperatures used in such studies are based on: i) the metamorphic grade of samples whose isotopic systematics were disturbed by metamorphism (e.g., Jager et al., 1967); ii) the variation of apparent mineral ages in deep drill holes (e.g., Turner and Forbes, 1976); and/or iii) solutions of Dodson's (1973) closure temperature equation using empirically or experimentally derived diffusion parameters. Although potentially the most powerful of these methods, direct calculation of a closure temperature using Dodson's equation requires the assumption of a cooling rate. Large errors in assumed cooling rates can lead to potentially significant errors in calculated closure temperatures. In this paper we describe a technique by which this problem can be circumvented. It requires two discordant mineral ages from a given terrain and results in the direct calculation of a closure temperature for each mineral-isotopic system as well as an average cooling rate over the interval of discordancy. As an example of the usefulness of this technique in constraining the cooling history of regional metamorphic terrains, it is applied to discordant hornblende and biotite K-Ar ages from a small area in the northern Scandinavian Caledonides.

METHOD

Figure 1 illustrates a hypothetical cooling history for an area in which discordant mineral ages have been obtained. In this example, we assume that the age discordance can be attributed to slow cooling rather

than multiple heating events. Following Dodson (1973, 1979), we can write an equation of the form:

$$T_c = \frac{E}{R \ln \left(\frac{AD_0RT_c^2}{a^2\dot{T}} \right)} \quad (1)$$

for each mineral isotopic system. Here, T_c is the closure temperature; D_0 and E are the frequency factor and activation energy which describe self-diffusion of the radiogenic daughter product in the mineral; A is a constant describing the geometry of diffusive loss in the mineral; a is the characteristic dimension of the system; R is the gas constant; and \dot{T} is the average cooling rate over the interval of transition between completely open and completely closed system behavior.

Equation (1), which can be solved iteratively for T_c , is exact only if inverse temperature increases linearly with time over the transition interval. If the closure temperatures of the two systems illustrated in Figure (1) are sufficiently close, we introduce small error by making three critical assumptions: i) that the cooling rates for the transition intervals for each system are substantially the same; ii) that these cooling rates can be adequately approximated by the average cooling rate over the interval between closure of the two systems (hereafter called the "discordancy interval"); and iii) that this average cooling rate can be reasonably approximated by a linear cooling function, such that:

$$\dot{T} = \frac{T_a - T_b}{t_a - t_b} \quad (2)$$

where T_a and T_b are the closure temperatures of systems a and b, and t_a and t_b are their measured apparent ages.

Thus, for the hypothetical situation shown in Figure 1, we have a system of three equations {two of the form of Equation (1); one of the form of Equation (2)} to describe three unknowns: T_a , T_b and \dot{T} . We have not yet found an analytical solution for this system; fortunately, a graphical solution is easy (Figure 2). Equation (1) can be used to graph T_c vs. \dot{T} for each of the mineral systems. The difference between the two resulting curves can be graphed as $(T_a - T_b)$ vs. \dot{T} . Equation (2) describes a straight line on this final plot with a slope of $(t_a - t_b)$. Intersection of the two curves constitutes a simultaneous solution of the system of equations and uniquely defines the closure temperature of each mineral-isotopic system as well as the average cooling rate over the discordancy interval.

APPLICATION

Ideally, this method can be applied using any two mineral-isotopic systems for which accurate diffusion data are available. In the following geologic application we will use discordant hornblende and biotite K-Ar ages.

Evaluation of Parameters

To solve for hornblende and biotite ^{40}Ar closure temperatures we must specify a variety of parameters pertaining to argon diffusion in

these systems. Our choice of parameters is given in Table 1, but many bear further justification here.

Excellent data are now available for ^{40}Ar self-diffusion in hornblende and biotite. Harrison (1980) has combined the results of his hydrothermal experiments on ^{40}Ar diffusion in biotite with the deep borehole data of Brookins et al., (1977) to arrive at an activation energy (E) of 40.3 ± 0.9 kcal/mol and a frequency factor (D_0) of $0.0026 + 0.0042/-0.0016$ cm²/sec. By integrating geologic data on ^{40}Ar loss in hornblendes from a metamorphic aureole in New Zealand with laboratory data, Harrison and McDougall (1980b) obtained $E = 63.3 \pm 1.7$ kcal/mole and $D_0 = 0.022 (+0.048/-0.010)$ cm²/sec.

We have assumed that diffusion of ^{40}Ar in the biotite structure can be modeled as radial diffusion in an infinite cylinder (Giletti, 1974; Hofmann et al., 1974). Following Harrison and McDougall (1980b), we model ^{40}Ar diffusion in hornblende as radial diffusion in a sphere. These assumptions lead to values of 27 and 55 for A of biotite and hornblende respectively.

The characteristic diffusion distance (a) is often taken as the grain radius or half-size of a mineral system. However, there is increasing evidence that diffusion in many minerals may be controlled by some dimension substantially smaller than physical grain size (Evernden et al., 1960; Hart, 1964; Hanson and Gast, 1967; Harrison and McDougall, 1980b). Although diffusion theory predicts a direct relationship between grain size and apparent age, Dodson (1973) gives an Alpine example of 30 cm biotites yielding the same apparent ages as nearby 1 mm biotites. The

simplest explanation of such phenomena is that mineral grains are often subdivided by crystal defects and cleavage planes which can serve as fast diffusion paths. Since diffusion rates in the "pristine" crystal structure are much slower than along these paths, and thus limit the rate of daughter product loss during cooling, closure of mineral-isotopic systems should depend on the distance between fast diffusion paths rather than physical grain size. Harrison and McDougall (1980b) suggest an "effective" dimension of 0.008 cm for ^{40}Ar diffusion in hornblendes, and we have adopted this in our calculations. Preliminary experimental data of Harrison (personal communication, 1981) suggest an effective dimension of 0.015 cm for ^{40}Ar diffusion in biotite, which compares favorably with Hanson and Gast's (1967) estimates of 0.02 to 0.05 cm. We have used a value of 0.02 cm in the calculations below. In choosing these values for a , we recognize that effective diffusion dimensions (EDD) are probably not constant for a given mineral-isotopic system; differences in thermal and deformational histories may lead to significant differences in EDD. The possible consequences of error on our choice of a will be discussed in a later section.

The Aefjord Area, Northern Norway - a regional metamorphic example

Rocks of the Aefjord area ($68^{\circ}15'\text{N}$, $16^{\circ}45'\text{E}$) were complexly deformed and metamorphosed at kyanite grade during the early Paleozoic Caledonian orogeny (Hodges, in preparation). The area includes the basal Caledonian thrust in this region, which places allochthonous metasedimentary and metaigneous lithologies over parautochthonous (?) Proterozoic granite gneisses of Baltic Shield affinity (Figure 3).

Six samples from this area were chosen for a reconnaissance K-Ar

study aimed at obtaining: i) a minimum estimate of the age of metamorphism; and ii) a better understanding of the cooling history of the area. Sample locations are shown in Figure 3 and descriptions are given in the Appendix.

For the cooling rate calculated here to be geologically meaningful, temperature history through the interval of interest must approximately have followed a linear function (Fig. 1; Eq. 2). In particular, the age recorded by the biotites in the Aefjord area must not reflect re-opening of the biotite isotopic systems by re-heating, following a hypothetical early cooling episode which closed both the hornblende and biotite systems. It is difficult to prove conclusively that no such reheating occurred, but geologic evidence does not support it. Regional tectonic considerations indicate that the metamorphism of the Aefjord area resulted from tectonic burial due to abortive westward subduction of the Baltic continental margin during early Paleozoic collision with North America (Caledonian orogeny; see Gee, 1975, 1978; Hodges et al., in prep.). Cooling of the Aefjord area resulted from uplift and erosion of the tectonic stack during progressive eastward and downward stepping of thrust faulting, which thus thickened the crust under the rocks considered here (Bartley, 1981; Hodges, 1981; Hodges et al., in preparation). No late-or post-metamorphic igneous intrusions, which might reheat the rocks in the study area following the regional metamorphic peak, are known anywhere in the Scandinavian Caledonides. Retrograde metamorphism in this area is considered to reflect minor back-reaction during cooling (Hodges and Royden, in preparation) rather than a second heating for which there is no independent evidence.

Consequently, the simple thermal history assumed here is geologically probable.

Analytical Technique

Amphibole and biotite mineral separates were prepared and purified using standard mechanical and heavy liquid techniques. Sample purity is estimated at greater than 98%. Argon analyses were performed in duplicate on separate aliquots of each sample using an AEI MS-10 mass spectrometer and conventional techniques. Potassium analyses were done by flame photometry after fusion of the samples with LiBO_3 . The constants used for calculating ages are those recommended by Steiger and Jager (1977).

Analytical Results

Table 2 shows the results of our analyses. All hornblende ages are concordant within the stated error brackets (mean age 449 +/- 19 my), as are all biotite ages (mean age 379 +/- 15 my). Figures 4a and 4b are graphs of Equation (1) for hornblende and biotite K-Ar systems using the diffusion parameters given in Table 1. Figure 4c shows the difference between the two curves plotted in $(T_h - T_b)$ vs. \dot{T} space. The mean apparent hornblende and biotite ages from Aefjord yield the linear cooling function: $(T_h - T_b) = 70\dot{T}$, also shown in Figure 4c. By taking into account the assumed error on the mineral ages, we find that the slope of the cooling function can range from 36 to 104. The range of intersections in Figure 4c yields a cooling rate as well as its estimated error: $\dot{T} = 3.0 (+2.9/-1.0)^\circ\text{C}/\text{my}$. From Figures 4a and 4b, these cooling rates yield: $T_h = 473 (+11/-7)^\circ\text{C}$ and $T_b = 263 (+10/-5)^\circ\text{C}$.

DISCUSSION

Comparison of Calculated T_c and \dot{T} with Other Estimates

Based on metamorphic mineral assemblages in the Central Alps, Steiger (1966) estimated the closure temperature of hornblende as something less than 540°C. Since then, estimates of T_h for slow cooling regional metamorphic terrains have included 525°C (Dallmeyer, 1975; Dallmeyer et al., 1975), 480°C (Dallmeyer, 1978), and 750-620°C (Berger and York, 1981). Biotite closure temperature estimates for slow cooling situations include 350-200°C (Jager et al., 1967), 325°C (Dallmeyer, 1975; Dallmeyer et al., 1975), 177°C (Turner and Forbes, 1976), 300 +/- 50°C (Wagner et al., 1977), 345-300°C (Dallmeyer, 1978) and 400-350°C (Berger and York, 1981). Our hornblende and biotite closure temperature estimates for Aefjord agree reasonably well with most of these estimates except those of Berger and York (1981). Possible explanations for the discrepancy between our results and those of Berger and York include: i) errors introduced by improper choice of diffusion parameters on our part (discussed further below); and ii) errors in Berger and York's estimates due to mineral instability during the vacuum extraction process they used to obtain diffusion coefficients for T_c calculations (see Harrison and McDougall, 1980b, for discussion).

Using hornblende and biotite age determinations and closure temperature estimates from Dallmeyer (1975), Dallmeyer et al., (1975), Dallmeyer (1978), and Berger and York (1981), Equation (2) yields average cooling rates of 2.9, 1.8, 5.4, and 5.3°C/my, respectively, for the regional metamorphic terrains dealt with in those papers. These values

are similar to our estimate for the Aefjord area.

Effects of Errors in Choice of Diffusion Parameters and Other Assumptions

The errors reported by Harrison (1980) and Harrison and McDougall (1980b) for hornblende and biotite D_0 and E have little effect on T_c and \dot{T} estimates using our method. For example, allowing for the complete range of estimated errors for D_0 and E leads to a range of 2.3 to 3.0°C/my for \dot{T} , 462 to 473°C for T_h , and 262 to 265°C for T_b using the Aefjord data. A potentially more serious problem concerns the universal applicability of these D_0 and E values. Although the diffusion parameters of Harrison (1980) and Harrison and McDougall (1980b) are by far the best available for these mineral-isotopic systems, they were obtained for a rather limited range of mineral compositions. Gerling et al., (1968) and O'Nions et al., (1969) report a strong compositional dependence for Ar retentivity in amphiboles. Harrison (1980) found a strong correlation between mole fraction annite and activation energy for ^{40}Ar diffusion in biotite. The Aefjord hornblendes and biotites which we studied span a range of compositions, including compositions for which Harrison's and Harrison and McDougall's diffusion parameters should be strictly valid. Until compositional effects on D_0 and E for these mineral-isotopic systems are better quantified, it is difficult to assess the error they may have introduced to our closure temperature and cooling rate estimates.

Our choices of effective diffusion dimensions, though reasonable, are admittedly somewhat arbitrary. Figure 5, drawn for hornblende using diffusion parameters from Harrison and McDougall (1980b) and $\dot{T} = 5^\circ\text{C/my}$, illustrates the strong dependence of closure temperature on choice of

diffusion dimension. The average grain half-size for the Aefjord hornblendes is ~ 0.09 cm. From Figure 5, this value yields $T_h \sim 575^\circ\text{C}$ compared with the $\sim 480^\circ\text{C}$ predicted using an EDD of 0.008 cm. We applied our method to the Aefjord samples using the average grain half-sizes of biotite (0.04 cm) and hornblende rather than the assumed EDD and obtained $\dot{T} = 4.0 (+4.0/-1.3)$, $T_h = 570 (+15/-9)$, and $T_b = 287 (+10/-6)$. Although these closure temperatures are significantly higher than those calculated using the assumed EDD, the cooling rates are quite similar. The EDD closure temperature for hornblende compares more favorably than the 0.09 cm temperature with most other estimates (see above), whereas the 0.04 cm biotite closure temperature is actually more consistent with previously published values. It will be difficult to predict diffusion dimensions with confidence until we develop a better understanding of effective diffusion dimensions and their dependence on the thermal and deformational histories of geochronological systems.

The assumption of linear cooling over the discordancy interval is probably a reasonable first approximation over the narrow temperature range in question. More complicated cooling functions would be required for larger time-temperature intervals representing a greater proportion of the cooling history of a sample, and such functions could be easily substituted for Equation (2) in our technique.

CONCLUSIONS

We have shown how two discordant mineral ages can be used to calculate closure temperatures for the mineral-isotopic systems studied

and the average cooling rate over the discordancy interval. This technique has been applied to mineral ages from the Aefjord area in Norway to obtain closure temperatures and a cooling rate which are generally consistent with estimates made using other methods. The principal advantage of this approach over more conventional uses of Dodson's (1973) equation is that the cooling rate need not be assumed in order to calculate closure temperatures. The principal disadvantages of this approach are those inherent to Dodson's relationship; specifically, it requires assumptions of effective diffusion dimensions, and diffusion parameters are still poorly known for many mineral-isotopic systems. As the EDD concept becomes better understood and more experimental diffusion data for geochronological systems becomes available, this method has the potential of providing extremely detailed records of cooling histories in a variety of tectonic settings.

REFERENCES

- Armstrong R.L. (1966) K-Ar dating of plutonic and volcanic rocks in orogenic belts. In Potassium Argon Dating (eds. O.A. Schaeffer and J. Zahringer), pp. 117-133, Springer-Verlag.
- Armstrong R.L., Jager E., Eberhardt P. (1966) A comparison of K-Ar and Rb-Sr ages on Alpine biotites. *Earth Planet. Sci. Lett.* 1, 13-19.
- Berger G.W. and York D. (1981) Geothermometry from $^{40}\text{Ar}/^{39}\text{Ar}$ dating experiments. *Geochim. Cosmochim. Acta.* 45, 795-811.
- Brookins, D.G., Forbes R.B., Turner D.L. Laughlin, A.W., and Naser C.W. (1977) Rb-Sr K-Ar, and fission-track geochronological studies of samples from LASL drillholes Gt-1, Gt-2, and EE-1, Los Alamos Information Report La-6829, 27 pp.
- Clark S.P. and Jager E. (1969) Denudation rates in the Alps from geochronologic and heat flow data. *Am. J. Sci.* 267, 1143-1160.
- Dallmeyer R.D. (1975) Incremental $^{40}\text{Ar}/^{39}\text{Ar}$ ages of biotite and hornblende from retrograded basement gneisses of the Southern Blue Ridge: their bearing on the age of Paleozoic metamorphism. *Am. J. Sci.* 275, 444-460.
- Dallmeyer R.D. (1978) $^{40}\text{Ar}/^{39}\text{Ar}$ incremental-release ages of hornblende and biotite across the Georgia Inner Piedmont: their bearing on Late Paleozoic - Early Mesozoic tectono-thermal history. *Am. J. Sci.* 278, 124-149.
- Dallmeyer R.D., Sutter J.F., and Baker D.J. (1975) Incremental $^{40}\text{Ar}/^{39}\text{Ar}$ ages of biotite and hornblende from the north-eastern Reading Prong: Their bearing on late Proterozoic thermal and tectonic history. *Geol. Soc. Am. Bull.* 86, 1435-1443.
- Dodson M.H. (1973) Closure temperature in cooling geochronological and petrological systems. *Contrib. Mineral. Petrol.* 40, 259-274.
- Dodson M.H. (1979) Theory of cooling ages. In Lectures in Isotope Geology (eds. E. Jager and J.C. Hunziker), pp. 210-217, Springer-Verlag.
- Evernden J.F., Curtis G.H., Kistler R., and Obradovich J. (1960) Argon diffusion in glauconite, microcline, sanidine, leucite, and phlogopite. *Am. Jour. Sci.* 258, 583-604.
- Gerling E.K., Kol'tsova T.V., Petrov B.V., and Zul'fikarova Z.K. (1968) On the suitability of amphiboles for age determination by the K-Ar method. *Geochim. Int.* 2, 148-154.
- Giletti B.J. (1974) Studies in diffusion, I. Argon in phlogopite mica. In Geochemical Transport and Kinetics (eds. A.W. Hofmann et al.), pp. 107-115, Carnegie Inst. of Washington.

- Goldich S.S., Nier A.O., Baadsgaard H., Hoffman J.H. and Krueger H.W. (1961) The Precambrian geology and geochronology of Minnesota. Minn. Geol. Surv. Bull. 41.
- Hanson G.N. and Gast P.W. (1967) Kinetic studies in contact metamorphic zones. *Geochim. Cosmochim. Acta* 31, 1119-1153.
- Harper C.T. (1967) The geologic interpretation of potassium-argon ages of metamorphic rocks from the Scottish Caledonides. *Scott. J. Geol.* 3, 46-66.
- Harrison T.M. (1980) Thermal histories from the $^{40}\text{Ar}/^{39}\text{Ar}$ age spectrum method. Unpub. Ph.D. Thesis, Australian National University.
- Harrison T.M., Armstrong R.L., Naeser C.W., and Harakal J.E. (1979) Geochronology and thermal history of the Coast Plutonic complex, near Prince Rupert, B.C. *Can. J. Earth Sci.* 16, 400-410.
- Harrison T.M. and McDougall I. (1980a) Investigations of an intrusive contact, northwest Nelson, New Zealand - I. Thermal, chronological and isotopic constraints. *Geochim. Cosmochim. Acta* 44, 1985-2003.
- Harrison T.M. and McDougall I. (1980b) Investigations of an intrusive contact, northwest Nelson, New Zealand - II. Diffusion of radiogenic and excess ^{40}Ar in hornblende revealed by $^{40}\text{Ar}/^{39}\text{Ar}$ age spectrum analysis. *Geochim. Cosmochim. Acta* 44, 2005-2020.
- Hart S.R. (1964) The petrology and isotopic-mineral age relations of a contact zone in the Front Range, Colorado, *J. Geol.* 72, 493-525.
- Hodges K.V. (in prep.) Tectonic stratigraphy and structural evolution of the Aefjord-Sitasjaure area, northern Scandinavian Caledonides
- Hodges K.V., Bartley J.M. and Burchfiel B.C. (in prep.) Structural evolution of an A-type subduction zone, northern Scandinavian Caledonides.
- Hodges K.V. and Royden L. (in prep.) Geothermometry and geobarometry of retrograded metamorphic rocks: an indication of the uplift trajectory of a portion of the northern Scandinavian Caledonides.
- Hofmann A.W., Gilletti B.J., Hinthorne J.R., Anderson C.A., and Comaford D. (1974) Ion microprobe analysis of a potassium self-diffusion experiment in biotite. *Earth Planet. Sci. Lett.* 24, 48-52.
- Jager E., Niggli E., and Wenke E. (1967) Rb-Sr alters bestimmungen an glimmern der Zentralalpen. *Beitrage zur Geologischen Karte der Schweiz. Lieferung* 134, 1-67.
- O'Nions R.K., Smith D.G.W., Baadsgaard H., and Morton R.D. (1969) Influence of chemical composition on argon retentivity in metamorphic calcic amphiboles from south Norway. *Earth Planet. Sci. Lett.* 5, 339-345.

- Steiger R.H. (1966) Dating of orogenic phases in the central Alps by K-Ar ages of hornblendes. *J. Geophys. Res.* 71, 1721-1733.
- Steiger R.H. and Jäger E. (1977) Subcommittee on geochronology: convention on the use of decay constants in geo- and cosmochronology. *Earth Planet. Sci. Lett.* 36, 359-362.
- Tilton G.R., Wetherill G.W., Davis G.L., and Hopson C.A. (1958) Ages of minerals from the Baltimore Gneiss near Baltimore, Maryland. *Geol. Soc. Am. Bull.* 69, 1469-1474.
- Turner D.L. and Forbes R.B. (1976) K-Ar studies in two deep basement drill holes: a new geologic estimate of argon blocking in biotite (abstract). *EOS* 57, 353.
- Wagner G.A., Reimer G.M., and Jäger E. (1977) Cooling ages derived by apatite fission-trace, mica Rb-Sr and K-Ar dating: the uplift and cooling history of the Central Alps. *Memorie di Padova* XXX.

APPENDIX: Sample Descriptions

- 79-1G Tysfjord granite gneiss. Quartz, microcline, plagioclase, muscovite, biotite, magnetite, zircon, sphene. Biotite occurs as euhedral plates up to 0.05cm in length.
- 79-3H Amphibolite dike in Tysfjord granite gneiss. Biotite, hornblende, plagioclase, quartz, sphene, opaque. Biotite occurs as subhedral to euhedral plates and platy aggregates up to 0.19cm in length. Hornblende occurs as subhedral prismatic grains up to 0.3cm in length. Hornblende and biotite form coarse intergrowths.
- 79-5C Mylonitic Sjurvatnet schist. No thin section available. Hand specimen contains obvious quartz, muscovite, biotite, garnet, and plagioclase. Biotite grain size <<0.1cm.
- 79-7D Amphibolite body within Rauvatn complex. Hornblende, plagioclase, biotite, quartz, garnet, sphene, opaque. Hornblende occurs as subhedral prismatic grains up to 0.12cm in length.
- 79-12E Sjurvatnet schist. Quartz, muscovite, biotite, garnet, plagioclase, kyanite, opaque, tourmaline, zircon. Biotite occurs as mats of subhedral plates intergrown with muscovite. Maximum grain size is 0.07cm.
- 79-14D Amphibolite body within Sjurvatnet schist. Hornblende, biotite, plagioclase, quartz, garnet, sphene, opaque, zircon. Hornblende occurs as euhedral to subhedral prisms up to 0.25cm in length, often intergrown with biotite.

LIST OF TABLES

Table 1. Diffusion Parameters

Table 2. Aefjord K-Ar data

TABLE 1
DIFFUSION PARAMETERS

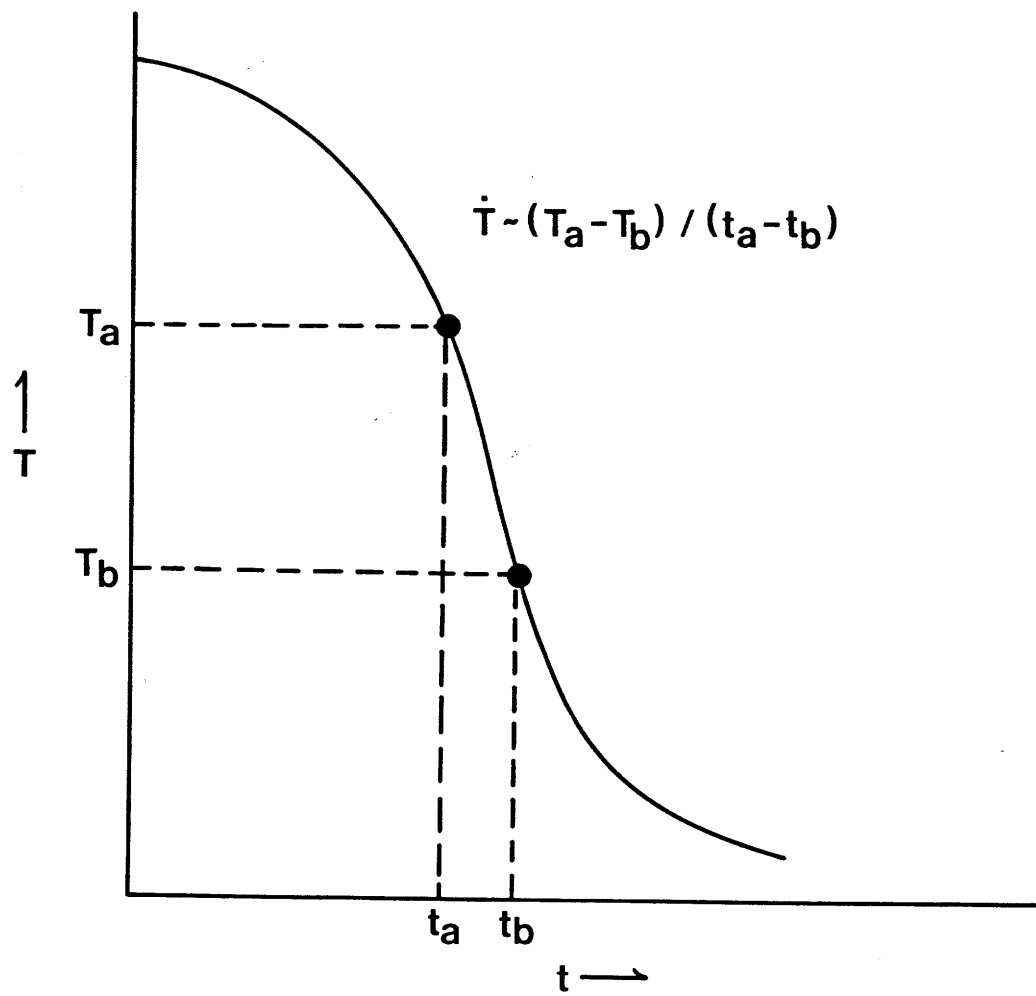
Parameter	Value	Source
<i>Hornblende</i>		
D_0	0.022 (+0.048/-0.010) cm^2/s	} Harrison and McDougall (1980b)
E	63300 (+/-1700) cal/mol	
A	55	
a	0.008 cm	
<i>Biotite</i>		
D_0	0.0026 (+0.0042/-0.0016) cm^2/s	Harrison (1980)
E	40300 (+/-900) cal/mol	Harrison (1980)
A	27	Giletti (1974); Hofmann et al, (1974)
a	0.02 cm	Harrison (pers. comm., 1981); Hanson and Gast (1967)
R	1.987 cal/mol $^\circ\text{K}$	

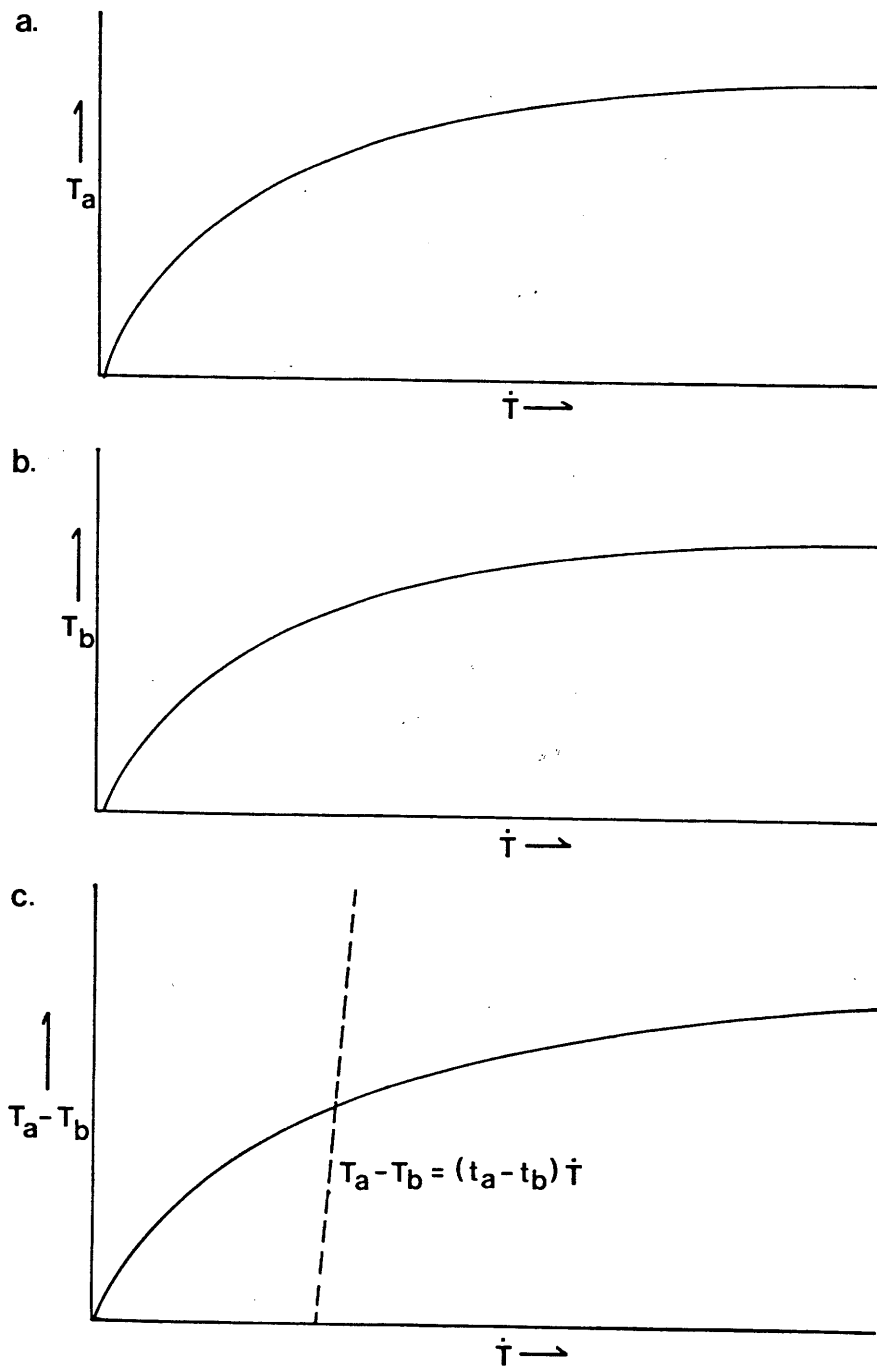
TABLE 2
AEFJORD K-Ar DATA

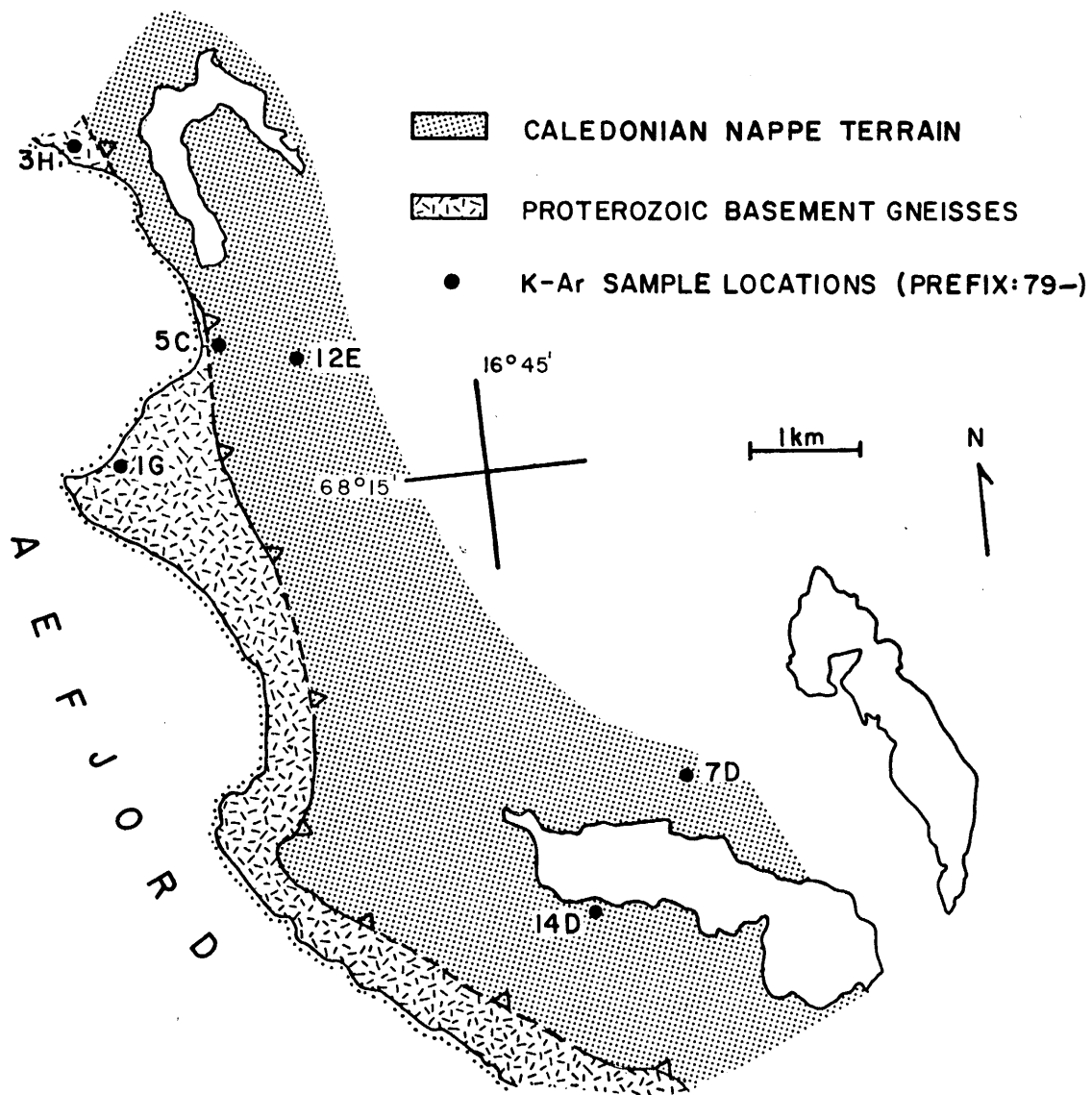
<u>Sample #</u>	<u>Mineral</u>	<u>Mesh Size</u>	<u>Wt. % K</u>	<u>$^{40}\text{Ar}^*$ ppm</u>	<u>$^{40}\text{Ar}^*/^{40}\text{Ar tot.}$</u>	<u>Apparent Age (my)</u>
79-1G	Bio	-60/+100	7.582	0.2202	0.8990	376 (+/-16)
79-3H	Bio	-100/+200	7.160	0.2188	0.8610	393 (+/-13)
79-3H	Hbl	-100/+200	0.953	0.0350	0.7230	463 (+/-19)
79-5C	Bio	-100/+200	7.322	0.2133	0.9620	377 (+/-16)
79-7D	Hbl	-100/+200	0.922	0.0316	0.7340	436 (+/-18)
79-12E	Bio	-80/+200	6.948	0.1979	0.9500	369 (+/-16)
79-14D	Hbl	-100/+200	0.647	0.0229	0.7975	448 (+/-20)

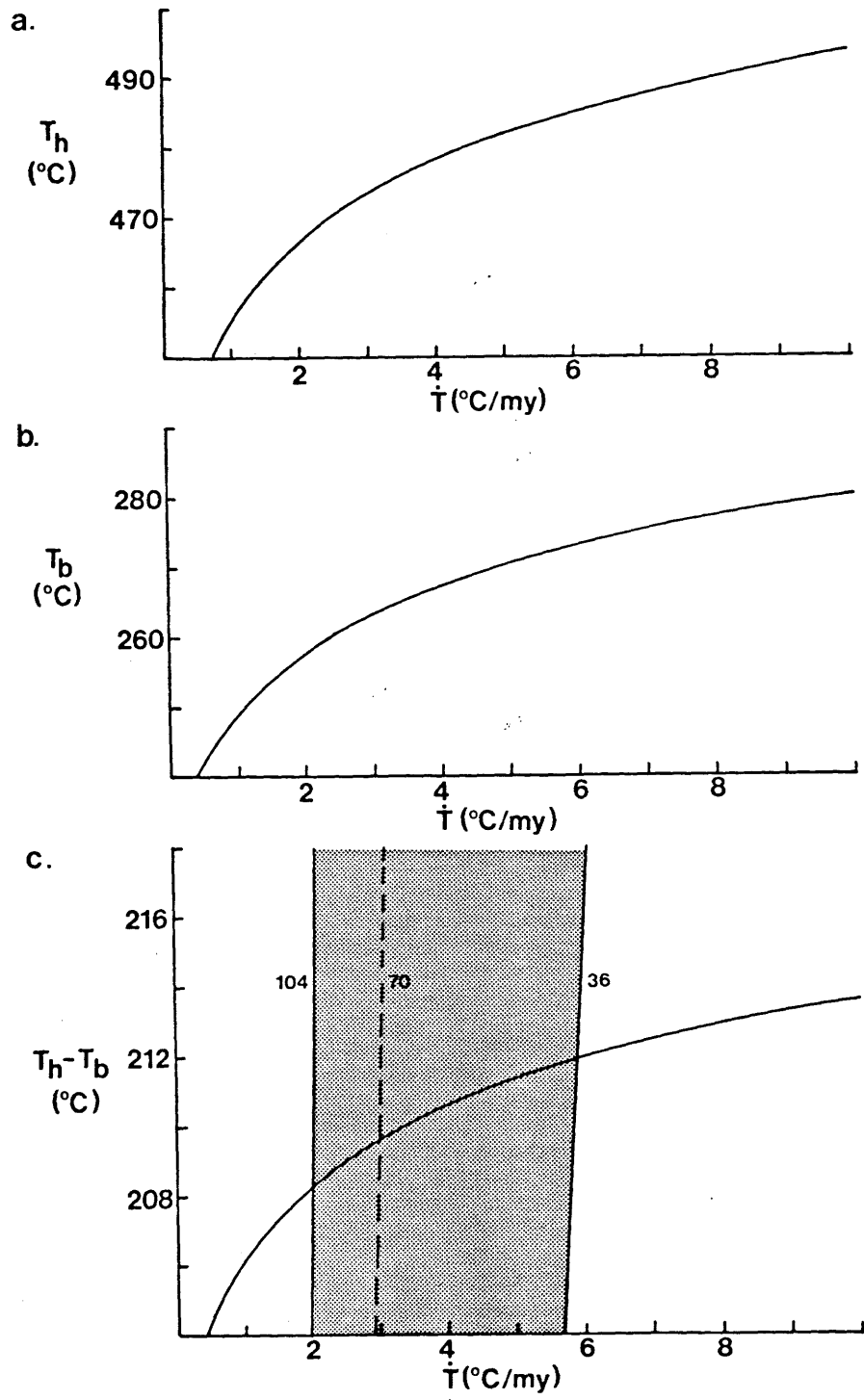
FIGURE CAPTIIONS

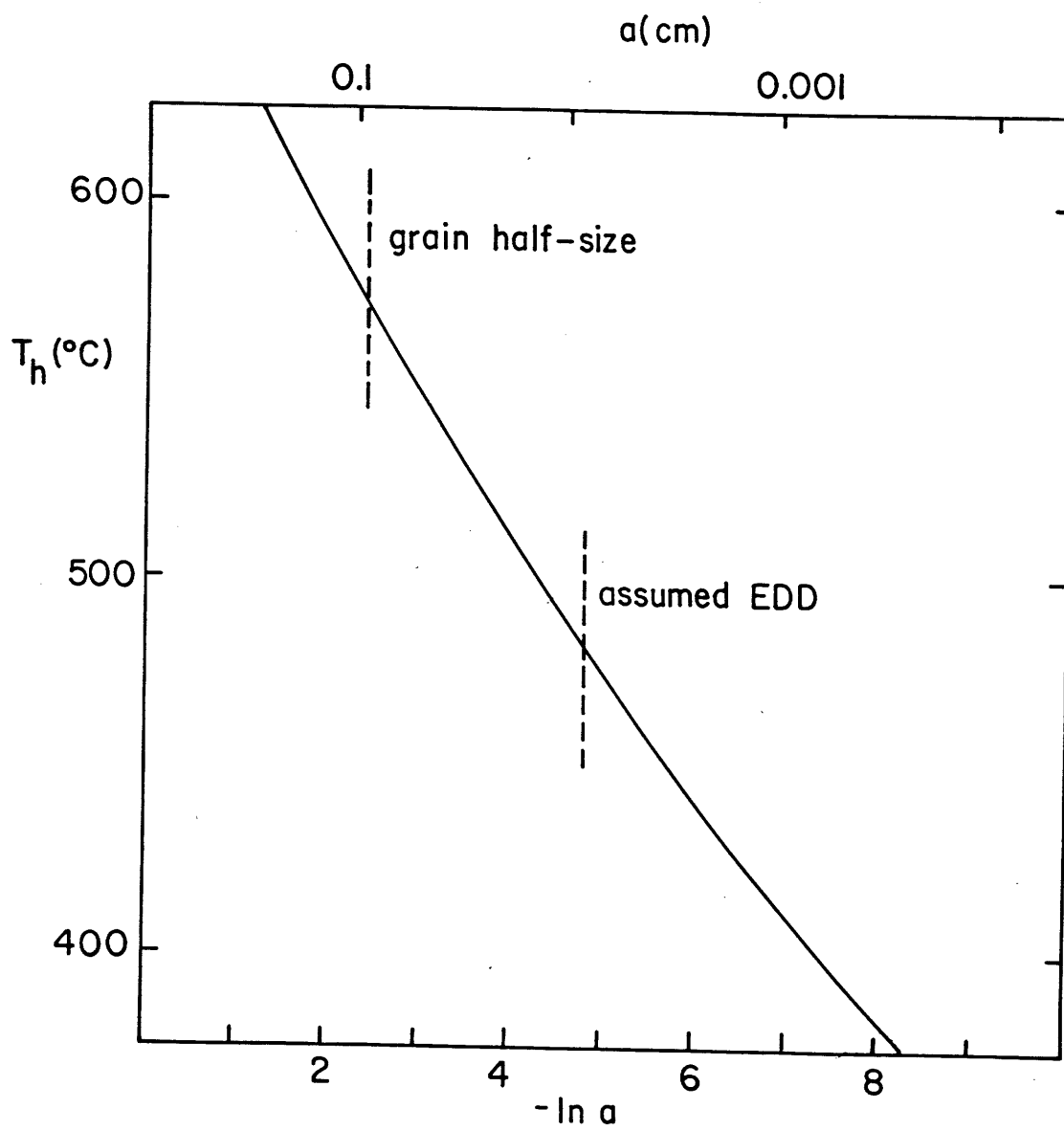
- Figure 1. Hypothetical cooling curve for a regional metamorphic terrain. Mineral-isotopic systems a and b yield discordant apparent ages t_a and t_b as a result of slow cooling through their respective closure temperatures T_a and T_b . When T_a and T_b are sufficiently close, the cooling rate (\dot{T}) over the interval of discordancy can be approximated by $(T_a - T_b) / t_a - t_b$.
- Figure 2. Graphical solutions for the closure temperatures of two discordant mineral-isotopic systems and the average cooling rate over the interval of discordancy. a) Plot of closure temperature vs. cooling rate (generated using Equation (1)) for mineral-isotopic system a in Figure 1. b) A similar plot for mineral-isotopic system b. In Figures 2 a and b, note that the dependence of closure temperature on cooling rate is much greater for slow cooling rates than for fast cooling rates. c) The result of subtracting the curve in 2b from the curve in 2a, shown in $(T_a - T_b)$ vs. \dot{T} space. The linear cooling function for this mineral-isotopic pair (generated using Equation 2) is also plotted. Intersection of the two curves defines \dot{T} , T_a , and T_b .
- Figure 3. Simplified tectonic map of the Aefjord area, northern Norway showing K-Ar sample localities.
- Figure 4. Graphical solution for \dot{T} , T_h , and T_b for the Aefjord samples. a) Graph of T_h vs. \dot{T} generated using hornblende diffusion parameters from Table 1. b) A similar graph of T_b vs. \dot{T} . c) Difference between hornblende and biotite closure temperature curves plotted along with the linear cooling function defined by the interval of discordancy (70my). Shaded region indicates the range of possible lengths of the discordancy interval (36 to 104my) based on the stated errors in apparent hornblende and biotite cooling ages.
- Figure 5. Plot of T_h vs. $-l\eta$ using diffusion data from Harrison and McDougall (1980b) and $\dot{T} = 5^\circ\text{C}/\text{my}$. Shown for reference are the assumed EDD for the Aefjord hornblendes (0.008cm) and the average grain half-size of these samples (0.09cm).











PART III

GEO THERMOMETRY AND GEOBAROMETRY OF RETROGRADED METAMORPHIC ROCKS:
AN INDICATION OF THE UPLIFT TRAJECTORY OF A PORTION OF THE
NORTHERN SCANDINAVIAN CALEDONIDES

GEO THERMOMETRY AND GEOBAROMETRY OF RETROGRADED METAMORPHIC ROCKS:
AN INDICATION OF THE UPLIFT TRAJECTORY OF A PORTION OF THE
NORTHERN SCANDINAVIAN CALEDONIDES

Abstract

Kyanite grade pelitic schists from the Aefjord area (68°15'N, 16°45'E), northern Norway, show abundant textural evidence of retrograde reequilibration during late-orogenic uplift and cooling of this part of the Scandinavian Caledonides. Graphical analysis of mineral compositions in seven samples that show a range of retrograde textures indicates that they reached final chemical equilibrium under non-uniform pressure-temperature conditions. Three element partitioning geothermometers and geobarometers yield consistent P-T estimates in individual samples, which together define a linear trend in P-T space. The sample showing the fewest signs of retrogression yields the highest pressure and temperature estimates, whereas samples exhibiting abundant reequilibration textures give lower P-T estimates. We suggest that the trend indicated by these samples reflects a portion of the P-T trajectory assumed by the Aefjord area during uplift. Thus, the judicious use of element partitioning geothermometers and geobarometers on samples showing signs of retrograde metamorphism may yield important new information concerning the late tectonic evolution of metamorphic terrains.

Introduction

Most metamorphic applications of major element partitioning geothermometers and geobarometers have been aimed at estimating "peak" metamorphic temperatures and pressures (e.g., Ghent, 1975; Tracy, Robinson and Thompson, 1976; Ghent, Robbins and Stout, 1979; Ferry, 1980). An increasing body of evidence, however, suggests that many commonly used geothermometers and geobarometers are susceptible to retrograde reequilibration during the uplift and slow cooling of intermediate to high grade regional metamorphic terrains (e.g., Dahl, 1979; Bohlen and Essene, 1980; Hodges and Spear, in press). This unfortunate development suggests that our capability of accurately determining peak metamorphic conditions in such terrains may be quite limited despite the ever-increasing quality of experimental calibration for the equilibria used. Still, it may be possible to use the reequilibration of geothermometers and geobarometers to our advantage in the study of uplift histories in orogenic terrains. If, for example, different samples from a single metamorphic terrain last reequilibrate at different times during uplift, then the use of mineral assemblages in these samples for geothermometry and geobarometry could yield an indication of the P-T trajectory assumed by the area during uplift and erosion.

Pelitic schists from a 10km² area near Aefjord in northern Norway (68°15'N, 16°45'E) were uniformly metamorphosed to kyanite grade during the early Paleozoic Caledonian orogeny. Subsequent to the metamorphic peak, the area was subjected to retrograde metamorphism during late-orogenic uplift and erosion.

Petrographic study of pelitic schists from the area shows that the degree of retrograde recrystallization varies from outcrop to outcrop. To test the possibility that geothermometers and geobarometers might be used to constrain the P-T history of the Aefjord area during uplift, seven samples showing variable degrees of retrogression were selected for detailed petrographic and electron microprobe study.

Geologic Setting

Figure 1 is a tectonic map of the Aefjord area, approximately 40 km southwest of Narvik, Norway. A detailed discussion of the structural evolution of this area will appear elsewhere (Hodges, in preparation).

The most striking tectonic feature of the Aefjord area is the Forsa thrust (designated as T₂ on Figure 1), which forms the primary contact between structural basement and cover in this part of the Scandinavian Caledonides. In the lower plate and to the west of the Forsa thrust lies the Proterozoic Tysfjord granite gneiss of probable Baltic Shield affinity and its parautochthonous - autochthonous, Caledonian stratigraphic cover, the Storvann Group of Bartley (1981). In the upper plate and to the east of the thrust lies an allochthonous nappe complex that has been subdivided into a seven-unit tectonic stratigraphy by Hodges (in preparation). The entire nappe complex was folded into a large amplitude, F₂ isocline, cored by the Reppi schist, which developed during T₂ thrusting. Relationships between tectonite fabrics and porphyroblast growth suggest that development of the T₂ Forsa thrust was roughly synchronous with prograde metamorphism. The estimated minimum

age of metamorphism in the Aefjord area is 449 ± 19 my based on K-Ar hornblende ages (Hodges et al., in preparation, a).

The metamorphic grade appears remarkably uniform across the area (amphibolite facies, kyanite grade). Diagnostic low variance assemblages are common at two horizons within the nappe complex, the Sjurvatnet and Skjafjell schists.

Sample Selection and Analytical Technique

Seven pelitic samples from the Sjurvatnet and Skjafjell schists were chosen such that all contained the assemblage kyanite-garnet-muscovite-biotite-plagioclase-quartz (in order to maximize the number of applicable geothermometers and geobarometers), and such that they together represented the range of degrees of retrogradation observed in the Aefjord area. Sample localities form two distinct clusters on the tectonic map shown in Figure 1. Postmetamorphic folding has upended the nappe stratigraphy in this area, and surfaces of uniform structural level during metamorphism probably now strike parallel to the surface trace of the Reppi schist horizon and dip $< 60^\circ$ to the northeast. Thus, although the two clusters of sample localities are several kilometers apart, they were probably at approximately the same structural level during metamorphism. This in turn suggests that all of the samples were subjected to similar maximum pressures during orogenesis. The relationship between the peak temperatures obtained by the two clusters is less clear. Hodges et al. (in preparation, b) suggest that the Forsa thrust represents a continental subduction zone developed as the Baltic

craton (represented in this area by the Tysfjord granite gneiss) was underthrusting the Greenland craton during the Caledonian orogeny. If correct, this interpretation suggests that the thermal models for collisional orogens developed by Bird et al. (1975) might be applicable to the Aefjord area. Thus, we might expect synmetamorphic isotherms to have been roughly subparallel to the Forsa thrust, suggesting that the two clusters should have experienced similar temperatures since they are approximately the same distance structurally above the thrust. We conclude, therefore, that all of the analyzed samples probably reached similar peak metamorphic conditions during orogenesis. At any rate, the individual clusters are small enough (<3km) that peak temperatures and pressures almost certainly did not vary significantly within a cluster.

The automated Materials Analysis Corporation microprobe at the Massachusetts Institute of Technology (MIT) was used to analyze selected minerals. Garnet, plagioclase, biotite and muscovite were analyzed in all samples; in addition, staurolite was analyzed in sample 79-18A (Tables 1--3). Two to four domains were chosen in a polished thin section from each sample such that all of the minerals to be analyzed were in mutual contact or, in exceptional cases, less than 3 mm apart. In each domain, each mineral was analyzed two to four times as close as possible to its rim (within a few microns). Reproducibility was generally better than 3% for a given grain. These analyses were used to obtain average compositions for the minerals in each domain, and the domain averages were in turn used to compute an average mineral composition for the section. There was no significant difference in mineral composition from domain to domain within a single thin section,

suggesting that chemical equilibrium was attained in all samples, at least on the scale of a 2 cm diameter probe mount.

In addition to mineral rim analyses, compositional traverses were made for one garnet grain in each sample. The analyzed garnets were the largest in each sample to increase the probability of near-center sections. Only Mg, Ca, Mn and Fe were analyzed for the traverses, and raw counts/second (preset = 20s) were used to construct the qualitative profiles shown in Figure 6. Spot checks revealed no significant zonation in any of the other analyzed minerals.

Descriptive Mineralogy

Approximate modal proportions for the seven samples, based on 500 point counts per thin section, are given in Table 4.

Garnet occurs as subhedral grains ranging in diameter from 0.3 mm (79-8B) to 2.5 mm (79-18A). Inclusions are rare to absent in 79-8B and 79-12E. Quartz and ilmenite inclusions are common in 79-8C, 79-18A, 79-21A, 79-21C and 79-21F. Garnets in 79-21A, 79-21C and 79-21F also contain rare biotite inclusions. The largest garnet in 79-18A is optically zoned; its core is characterized by a helicitic pattern of quartz and ilmenite inclusions, whereas its outermost 0.2 to 0.8 mm includes randomly oriented quartz and epidote (Fig. 2a).

Biotite and muscovite occur as subhedral plates (up to 4 mm in length) which define an axial planar cleavage in the samples. In addition, fine-grained (<0.2 mm), randomly oriented muscovite surrounds

large subhedral to anhedral kyanite porphyroblasts in sample 79-18A, and optically continuous muscovites up to 4 mm include large subhedral to anhedral kyanites in 79-21C and 79-21F (Fig. 2d).

Kyanite occurs as subhedral porphyroblasts (up to 7 mm) showing patchy extinction. Inclusions of quartz, ilmenite and muscovite are common. Aluminosilicates also occur as small (< 0.4 mm) euhedra in all samples except 79-8B. Optical properties and occasionally well-developed cleavage suggest that these are also kyanite. These "second-stage" aluminosilicates commonly form epitaxial overgrowths on larger "first-stage" kyanites (Fig. 2c), or are intergrown with very fine-grained quartz (< 0.1 mm) around the edges of plagioclase grains, especially along garnet-plagioclase interfaces (Fig. 2b).

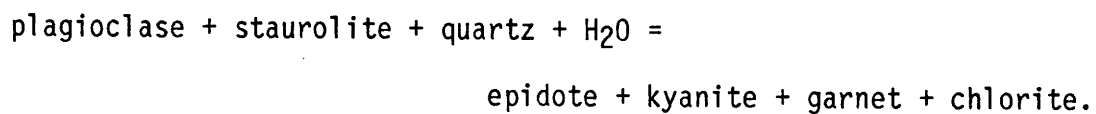
Plagioclase generally occurs as anhedral, highly strained porphyroblasts up to 8 mm. Albite twinning is common. Optical zonation is absent. Minor sericitization occurs in most grains.

Quartz forms anhedral to subhedral grains up to 5 mm showing patchy extinction, as well as polygonal, recrystallized grains up to 0.3 mm. The degree of quartz recrystallization varies from about 10% in 79-12E to about 60% in 79-21A.

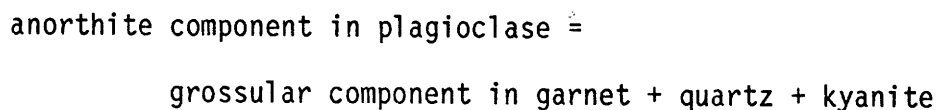
Staurolite occurs as rare, inclusion-free, anhedral porphyroblasts (up to 2 mm) in 79-18A. Subhedral to anhedral grains (up to 3 mm) of apparently secondary chlorite occur in samples 79-18A and 79-21A.

Petrographic Evidence for Retrogression

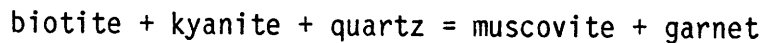
Textural evidence for retrograde metamorphism is common in all samples except 79-8B. Irregular staurolite porphyroblasts, secondary garnet rims with epidote inclusions, and secondary matrix kyanite, epidote and chlorite in sample 79-18A suggests a hydration reaction such as:



Common intergrowths of microcrystalline quartz and second-stage kyanite along garnet-plagioclase interfaces (Fig. 2b) are consistent with operation of the net transfer reaction:



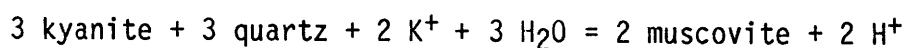
in response to decreasing temperature and/or pressure. Muscovite overgrowths on kyanite (Fig. 2d) might be explained by reactions such as:



which is also consistent with a decrease in P-T conditions.

Since all samples are from a geographically restricted area and approximately the same structural level, we can safely assume that all

experienced a similar P-T trajectory during uplift and cooling. However, retrograde textures are not developed to a uniform extent in all samples; no one sample shows all of the retrograde textures illustrated in Figure 2. Table 5 indicates the distribution of these textures. The variability of retrograde texture development suggests that the samples may have equilibrated at different times, and thus under different pressure and temperature conditions, during the uplift history of the Aefjord area. This may reflect local variations in the availability of fluids for hydration reactions, or kinetic effects not yet fully understood. It would be useful to be able to rank the samples in order of degree of retrogradation based solely on petrographic observations. Unfortunately, this proves very difficult. Although there is textural evidence for retrogression through net-transfer reactions, the extent of retrogradation through exchange reactions is impossible to determine petrographically. Thus, estimates of "percent retrogradation" based on the modal percentage of retrograde minerals are overly simplistic. This problem is compounded by the fact that the textures shown in Figure 2 could arise through many reactions other than those postulated above. For example, Carmichael (1969) suggests the formation of muscovite overgrowths on kyanite through:



Although it consumes H₂O, Carmichael considers this reaction to be part of a complex prograde reaction leading to the polymorphic inversion: kyanite = sillimanite. Both this reaction and that which we postulated

above are thermodynamically valid descriptions of the muscovite-kyanite relationship, but whether one or the other actually operated in a given sample makes a dramatic difference in the amount of muscovite produced from a given amount of kyanite; Carmichael's reaction gives two moles of muscovite for each mole of kyanite consumed, whereas our reaction yields one mole of muscovite for two moles of kyanite. Obviously, success at "quantifying" retrogression through modal proportions depends critically on determining the actual reaction responsible for an observed texture. It is entirely plausible that none of the reactions postulated above were actually responsible for the retrograde textures in the Aefjord samples, and thus attempts to rank them by degrees of retrogradation based solely on petrographic evidence seem fruitless. We can say with certainty, however, that the only sample which shows no textural signs of retrogradation is 79-8B.

Primary Mineral Compositions and Phase Equilibria

If the Aefjord samples did not reach final equilibrium at uniform pressure and temperature, then this should be reflected in the mineral chemistry. One way to evaluate the possibility of chemical disequilibrium is through the use of phase diagrams. Mineral assemblages are graphically represented in Figure 3 using planar Al-Fe-Mg and K-Na-Ca projections, and in Figure 4 using stereographic plots of the Mg-Al-Fe-H₂O (muscovite projection) and Mg-Ca-Fe-Na tetrahedra generated after the methods described by Spear (1980). The thermodynamic "legality" of using these projections as phase diagrams hinges on the assumptions: a) that the plotted assemblages equilibrated at uniform

pressure and temperature; b) that the chemical potentials of the phases through which the projections are made were constant in all of the assemblages; and c) that equilibrium between assemblages is not seriously affected by components neglected in the projections (Greenwood, 1975). Tie-lines or tie-planes will not cross on a "legal" projection. If they do then one or more of the above conditions were not met and the projection is "illegal." Garnet-biotite-kyanite assemblages from the Aefjord samples yield abundant crossing tie-line relationships (Fig. 3) when projected from quartz, muscovite and H₂O onto the Al-Fe-Mg plane (Thompson, 1957). The possibility that this might be explained by sample-to-sample variation in the activity of H₂O is evaluated in Figure 4a. Here, the same assemblages are projected through muscovite and quartz into the Al-Fe-Mg-H₂O tetrahedron, assuming stoichiometric H₂O in biotite. Although this projection does indicate variability in the activity of water, many tie-planes still intersect. Similar projections into Al-Fe-Mg-Ca and Al-Fe-Mg-Mn (not shown) also show crossing tie-plane relationships, indicating that the additional components Ca and Mn are not solely responsible for tie-line intersections in Figure 3.

The composition of staurolite in sample 79-18A is also shown on the Al-Fe-Mg plot in Figure 3a. The presence of four Al-Fe-Mg phases in 79-18A probably does not reflect the effects of additional components neglected in the projection; components such as Zn which could stabilize staurolite in such assemblages are only minor constituents of the 79-18A staurolites. A more likely explanation is that the chemical potential of

H₂O is internally buffered in this assemblage, invalidating a basic assumption in the use of Figure 3a as a phase diagram ($a_{\text{H}_2\text{O}}$ is constant in all assemblages).

The K-Na-Ca projection through quartz, kyanite and H₂O shows that muscovite-plagioclase assemblages in these samples also yield crossing tie-lines (Fig. 3b). Consideration of the possible effects of variable H₂O activity by projection of these assemblages from quartz and kyanite into the tetrahedron K-Na-Ca-H₂O (not shown) does not eliminate these relationships.

Hodges and Spear (in press) found a systematic increase in the calcium contents of coexisting garnet and plagioclase with decreasing Fe/Mg in the garnet in samples from Mt. Moosilauke, New Hampshire, which equilibrated at uniform P-T conditions near that of the aluminosilicate triple point. Figure 4b shows Sjurvatnet and Skajfjell garnet-biotite-plagioclase assemblages projected from quartz, muscovite, kyanite and H₂O into the Mg-Ca-Fe-Na tetrahedron. Again, tie-plane intersections are common, and there appears to be no systematic correlation between garnet-plagioclase Ca contents and garnet Fe/Mg, although increasing grossular component in garnet does correlate with increasing anorthite component in plagioclase.

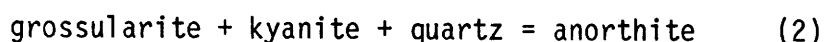
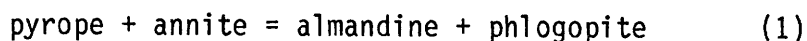
The phase diagrams in Figure 3 constitute strong evidence for chemical disequilibrium among the seven Aefjord samples. Other projections such as those in Figure 4 argue that the crossing tie-lines in Figure 3 are not simply due to the effects of additional components or variability in the activity of H₂O. Thus, these samples appear to have

reached final equilibration under different pressure and temperature conditions.

It is important to note that, despite abundant evidence for chemical disequilibrium between samples, there is no chemical evidence for disequilibrium within individual samples. Rim compositions of minerals were found to be remarkably uniform in all of the domains analyzed in each probe section, suggesting that chemical equilibrium was attained at least on the scale of a thin section.

Variations in Distribution Coefficients

Another approach to evaluating equilibrium between mineral assemblages is through the use of distribution coefficients (Kretz, 1959; Albee, 1965). Two equilibrium equations which will figure prominently in a later section on geothermometry and geobarometry are:



The first of these describes Fe-Mg exchange between coexisting garnet and biotite, and the second is the inverse of a net transfer reaction which was postulated previously as the reaction leading to the formation of k_2 secondary kyanite in the Aefjord samples. Assuming that quartz and kyanite are pure phases, we can define a distribution coefficient for each of these reactions:

$$K_d(1) = \frac{\left(\begin{matrix} \text{ga} \\ X \\ \text{py} \end{matrix} \right)^3 \left(\begin{matrix} \text{bi} \\ X \\ \text{ann} \end{matrix} \right)^3}{\left(\begin{matrix} \text{bi} \\ X \\ \text{ph} \end{matrix} \right)^3 \left(\begin{matrix} \text{ga} \\ X \\ \text{al} \end{matrix} \right)^3}$$

$$Kd(2) = \frac{\left(X_{an}^{pg} \right)^3}{\left(X_{gr}^{ga} \right)^3}$$

(See Table 6 for explanation of terms). Assuming ideal mixing and equilibration under uniform pressure and temperature conditions, then the Aefjord samples should define a straight line passing through the origin on plots of numerator vs. denominator for the above equations. The slope of this line is equal to the distribution coefficient. It is clear from Figure 5 that points shown do not define a unique straight line. Significant deviations from ideal mixing would lead to a regular-curved rather than straight-line distribution (Albee, 1965), but this is not observed either. We conclude from these figures that the Aefjord samples could not have reached final equilibrium under the same P-T conditions.

Garnet Zonation Evidence for Retrogression

Compositional profiles of garnets from the Aefjord samples are consistent with varying degrees of retrogradation (Fig. 6 a-g). Whereas the bell-shaped or essentially flat Mn profiles in the interior of these garnets is consistent with prograde garnet growth (Hollister, 1966; Anderson and Buckley, 1973), the dramatic increase in Mn near the rims in all samples except 79-18A suggests retrogression (Grant and Weiblen, 1971; Woodsworth, 1977). The margins of all garnets except 79-18A also

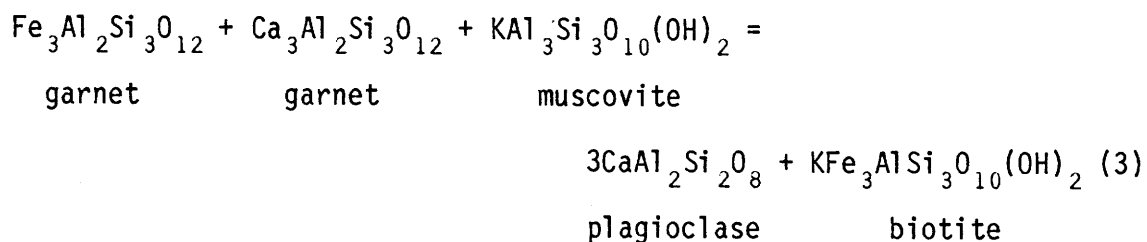
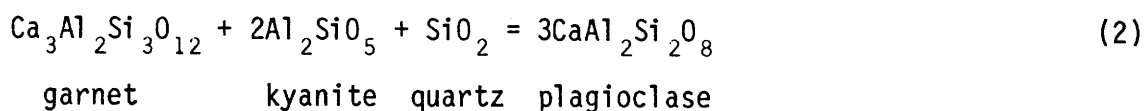
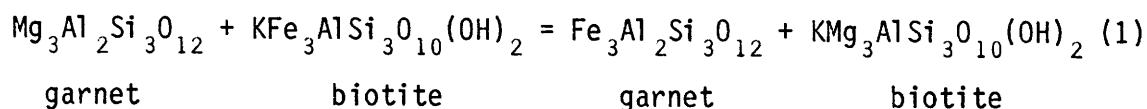
show a systematic increase in Fe/Mg which is consistent with Fe-Mg exchange between garnet and biotite in response to falling temperatures during uplift. Note that the garnet in 79-8B, the sample which shows no textural evidence for retrogradation, has the narrowest retrograde margin ($< 30 \mu\text{m}$).

Sample 79-18A contains a greater variety of retrograde assemblages and textures than the other samples and also shows strikingly different garnet compositional profiles. A well-defined discontinuity occurs in the profiles approximately 450-600 μm inward from the edge. This chemical discontinuity corresponds to the optical discontinuity which can be seen in thin-section (Fig. 2a). The Mn profile for the interior of this garnet compares favorably with those for garnets in other samples, suggesting that the core of the 79-18A garnet experienced similar prograde and retrograde histories to the other garnets. The outer 450-600 μm , however, reflects a second stage of garnet growth that does not appear to have occurred in the other samples.

Geothermometry and Geobarometry

The common Aefjord assemblage garnet-biotite-muscovite-plagioclase-quartz permits the application of three

widely used geothermometers and geobarometers to these samples:



Reaction (1) was calibrated empirically as a geothermometer by Thompson (1976) and Goldman and Albee (1977), and experimentally by Ferry and Spear (1978). Reaction (2) was calibrated as a geobarometer by Ghent (1976) using available thermochemical data, and his calibration was subsequently improved upon by Ghent, Robbins, and Stout (1979). Reaction (3) was empirically calibrated by Ghent and Stout (1981).

Hodges and Spear (in press) evaluated the inherent accuracy of these geothermometers and geobarometers by applying them to pelitic schist assemblages from the Mt. Moosilauke area, New Hampshire, where peak metamorphic conditions are constrained to be near those of the aluminosilicate triple point (Rumble, 1971). Ferry and Spear's (1978) calibration of reaction (1) and Ghent, Robbins, and Stout's (1979) calibration of reaction (2) yielded P-T estimates extremely consistent with Holdaway's (1971) aluminosilicate triple point. The Ghent and Stout (1981) calibration of reaction (3) yielded slightly (but consistently)

high pressure estimates.

The empirical calibration scheme used by Ghent and Stout (1981) involved a least-squares linear regression analysis similar to that of Thompson (1976). The equilibrium constant for equilibrium (3) was calculated for a variety of samples for which there were good estimates of pressure and temperature based on other geothermometers and geobarometers. Using a ΔV for reaction (3) calculated from thermochemical data in Helgeson et al. (1978), the samples were then plotted on a graph of $\{-RT \ln K_3 - (P-1)\Delta V\}$ vs. T . A best-fit line through these points permitted estimates of ΔH for reaction (3) from the y-intercept and ΔS from the slope. For their calibration, Ghent and Stout (1981) used samples from the Waterville-Vassalboro area, Maine (Ferry, 1980), and the Mica Creek area, British Columbia (Ghent, Simony and Knitter, 1980). Many of the temperature estimates used in their calibration were obtained from the garnet-biotite geothermometer. Hodges and Spear (in press) suggest that this geothermometer is highly susceptible to retrograde reequilibration down to temperatures of about 500-585°C. Unfortunately, many of the samples used by Ghent and Stout (1981) yield garnet-biotite temperatures in the range of 500-600°C, where the geothermometer may be unreliable. It seems prudent, therefore, to attempt a similar calibration using samples which crystallized at lower temperatures where the garnet-biotite geothermometer is more trustworthy. Although this may lower the spread of points used in the regression analysis, it is nonetheless worthwhile if we can circumvent the kinetic problems which could arise from the use of higher temperature samples.

Using samples from the Mt. Moosilauke area for which pressure and

temperature estimates were obtained using equilibria (1) and (2) (Hodges and Spear, in press), least-squares linear regression yields $\Delta H = 19569$ cal, and $\Delta S = 40.809$ cal/deg for equilibrium (3) with a correlation coefficient of 0.969. Our calibration of equilibrium (3) is in considerably better agreement with that which can be calculated from thermochemical data in Zen (1973) and Helgeson et al. (1978) ($\Delta H = 28849$ cal; $\Delta S = 37.23$ cal/deg) than is the calibration of Ghent and Stout (1981) ($\Delta H = 4124.4$ cal; $\Delta S = 22.061$ cal/deg). The reasonable consistency between our calibration and the one calculated from thermochemical data, as well as the statistical quality of our least-squares regression analysis, suggests that our calibration may be somewhat more accurate than that of Ghent and Stout (1981). A better calibration must await experimental study of equilibrium (3).

In order to estimate equilibrium pressures and temperatures for the Sjurvatnet samples, we will use the calibrations of Ferry and Spear (1978) and Ghent, Robbins and Stout (1979) for equilibria (1) and (2), and our calibration for equilibrium (3). Table 6 summarizes the pertinent thermodynamic values for these equilibria.

Using mineral composition data from Tables 1-3 and mole fraction formulations from Table 7, equilibrium constants were calculated for the three reactions. Errors in equilibrium constants were estimated by propagating an assumed standard error of 3% for the microprobe data through an error magnification equation in the manner of Hodges and Spear (in press).

Pressure and temperature curves for the three reactions, generated using the thermodynamic data in Table 6 and equilibrium constants for

each sample, are shown in Figure 7 a-g. The two curves shown for each equilibrium bracket \pm one standard deviation as calculated above.

The three equilibria yield very consistent P-T estimates for each sample. However, recorded pressures and temperatures vary significantly from sample to sample as shown in the summary diagram in Figure 8. The geothermometric and geobarometric data for the seven Sjurvatnet and Skjafjell samples define an essentially linear trend in P-T space for which $dP/dT \sim 20$ bars/ $^{\circ}\text{C}$.

Interpretation

We suggest that the pressure-temperature trend shown in Figure 8 reflects the P-T trajectory of the Aefjord area during late orogenic uplift and erosion. This interpretation is based on the following evidence.

First, the variation in recorded pressures and temperatures is probably not due to inaccuracies in the calibrations used for equilibria (1)-(3). Hodges and Spear (in press) found that the Ferry and Spear (1978) and Ghent, Robbins and Stout (1979) calibrations for equilibria (1) and (2) yielded extremely accurate results in the Mt. Moosilauke area, New Hampshire, where the pressure and temperature of metamorphism were well known. Equilibrium (3), although carrying with it large uncertainties due to the calibration method, yields pressure estimates extremely consistent with those made using equilibrium (2).

Second, the disagreement between calculated pressures and temperatures for the seven samples is not likely to be due to the effects of additional components on the geothermometers and

geobarometers used. For example, Albee (1965) and Ferry (1980) suggest that Mn and Ca in garnet can strongly affect the garnet-biotite Fe-Mg geothermometer. Figure 9 shows plots of $T(^{\circ}\text{C})$ vs. X_{Ca} and X_{Mn} for the Aefjord garnets. There is no strong correlation evident on either graph, suggesting that Mn and Ca did not strongly affect Fe-Mg partitioning between garnet and biotite.

Third, there is no evidence that the scatter in P-T estimates reflects disequilibrium in any of the samples. The consistency of primary mineral composition in all of the domains of each thin-section suggests that chemical equilibrium was attained in all samples.

Fourth, graphical analysis of phase equilibria (Figures 3, 4 and 5) prohibits the seven samples from having equilibrated for the last time at uniform pressure and temperature, consistent with the P-T variation recorded by equilibria (1)-(3).

Fifth, the geothermometry and geobarometry results are strongly supported by textural evidence for varying degrees of retrogradation in these samples. The sample which shows essentially no petrographic signs of retrogression (79-8B) also yields the highest pressure and temperature estimates. Moreover, several of the samples near the lower end of the P-T trend include direct textural evidence of equilibrium (2) having operated in a retrograde sense.

Sixth, major element zonation of garnets in these samples is consistent with retrograde reequilibration. The garnet profile for 79-8B (Figure 6) shows the narrowest retrograde margin. Garnets from samples yielding lower P-T estimates have more distinctive "rims." Note that, despite the secondary garnet growth in 79-18A which is apparent both in

Figure 2a and in Figure 6, P-T estimates for this sample lie reasonably well along the trend indicated by the other samples in Figure 8.

We suggest that the seven Sjurvatnet samples initially crystallized under similar pressure and temperature conditions. Based on the lack of reequilibration textures and the narrowness of retrograde garnet rims in sample 79-8B, peak metamorphic conditions probably did not greatly exceed those recorded by that sample. During subsequent uplift and cooling of the Aefjord area, the samples retrograded to varying extents and reequilibrated under different P-T conditions. Application of element partitioning geothermometers and geobarometers to these samples yields a roughly linear array in P-T space which apparently records a portion of the P-T trajectory of the area during uplift.

It could be argued that we are incorrect in our assumption that peak metamorphic conditions were uniform over the entire area. Even so, this would not significantly modify our interpretation of the P-T trajectory. Peak temperatures and pressures must have been relatively constant within each cluster of samples, and these subgroups illustrate the same P-T trend when considered individually. For example, samples 79-8B and 79-8C were collected less than 200m from each other, but they yield P-T estimates on opposite extremes of the trend.

The Closure Temperature Concept

Hodges and Spear (in press) argued that metamorphic geothermometers and geobarometers often underestimate peak metamorphic temperatures and pressures due to reequilibration during uplift and slow cooling. This reequilibration was treated as a problem in diffusion kinetics and

likened to the problem of closure of geochronological systems. Since diffusion in geologic materials appears to be far more sensitive to temperature than pressure (Misener, 1974), we can define a closure temperature (T_C) for a geothermometer or geobarometer as the temperature at which equilibrium was last attained between the participating mineral phases. Following Dodson (1973), T_C should be a function of: a) the frequency factor (D_0) and activation energy (E) which describe interdiffusion of the elements involved in reequilibration; b) the system dimensions; and c) the cooling rate. Hodges and Spear (in press) suggested closure temperatures for the garnet-biotite geothermometer of 585°C and 500°C for cooling rates of 1 and 100°C/my, respectively.

In the Aefjord area, closure temperatures for geothermometers and geobarometers varied widely from sample to sample, even though cooling rates were presumably uniform over such a small area. Why this should be so is not entirely clear. Part of the answer may lie in the observation that the system dimensions, or, in simpler terms, the distance between participating mineral phases probably varies from sample to sample. It has also been shown that D_0 and E are often compositionally dependent in silicates. The experimental data of Freer (1979) suggests that this is true for Fe-Mn interdiffusion in garnet, and Anderson and Buckley (1974) present a theoretical treatment of multicomponent diffusion in garnets which illustrates the complexity of the process. Furthermore, intergranular diffusion rates will clearly be affected by the presence or absence of an intergranular fluid, as well as the composition of this fluid.

Although the closure temperature concept is important in geothermometry and geobarometry, it is presently far from quantitative.

The study of multicomponent diffusion in heterogeneous geological systems is still in its infancy. Perhaps someday we can satisfactorily explain the T_c variability in the Aefjord area. For now, it seems reasonable to treat the array shown in Figure 7 as an empirical observation of part of the P-T trajectory of the Aefjord area during uplift and cooling.

Conclusions

Seven pelitic schist samples collected from a 10 km² area near Aefjord, northern Norway, contain similar prograde mineral assemblages suggesting similar peak metamorphic conditions. The samples show textural evidence for varying degrees of retrogradation which is supported by garnet compositional profiles. The consistency of prograde mineral compositions throughout individual samples suggests that chemical equilibrium was attained in each, although graphical analysis of the compositional data implies that the seven samples could not have reached final chemical equilibrium under uniform P-T conditions. The phase equilibria results are corroborated by three commonly used geothermometers and geobarometers, which yield significantly different P-T estimates for different samples. The geothermometric and geobarometric data form a linear array on a P-T diagram with $dP/dT \sim 20$ bar/°C. Consideration of the available petrographic and chemical data leads us to conclude that this array records part of the P-T trajectory of the Aefjord area during uplift.

The results of this study suggest that the careful application of geothermometry and geobarometry to retrograded samples from slowly

cooled, regional metamorphic terrains may yield important information concerning the latter stages of the tectonic evolution of orogenic terrains.

REFERENCES

- Albee, A.L., 1965a, Phase equilibria in three assemblages of kyanite-zone pelitic schists, Lincoln Mountain quadrangle, central Vermont: *Jour. Petrology*, v.6, p.246-301.
- Albee, A.L., 1965b, Distribution of Fe, Mg, and Mn between garnet and biotite in natural mineral assemblages: *Jour. Geology*, v.73, p.155-164.
- Anderson, D.E., and Buckley, G.R., 1973, Zoning in garnets -diffusion models: *Contr. Mineralogy Petrology*, v.40, p.87-104.
- Anderson, D.E., and Buckley, G.R., 1974, Modeling of diffusion controlled properties of silicates, in: Geochemical Transport and Kinetics (Hofmann, A.W. et al., editors), Carnegie Institution, Washington, p.31-52.
- Bird, P., Toksoz, M.N., and Sleep, N.H., 1975, Thermal and mechanical models of continent-continent convergence zones: *J. Geophys. Res.*, v.80, p.4405-4416.
- Bohlen, S.R., and Essene, E.J., 1980, Evaluation of coexisting garnet-biotite, garnet-clinopyroxene and other Fe-Mg exchange geothermometers in Adirondack granulites: *Geol. Soc. America Bull.* Pt. I, v.91, p.107-109.
- Dahl, P.S., 1979, Comparative geothermometry based on major-element and oxygen isotope distributions in Precambrian metamorphic rocks from southwestern Montana: *Am. Mineralogist*, v.64, p.1280-1293.
- Dodson, M.H., 1973, Closure temperature in cooling geochronological and petrological systems: *Contr. Mineralogy Petrology*, v.40, p.259-274.
- Ferry, J.M., 1980, A comparative study of geothermometers and geobarometers in pelitic schists from south-central Maine: *Am. Mineralogist*, v.65, p.720-732.
- Ferry, J.M., and Spear, F.S., 1978, Experimental calibration of the partitioning of Fe and Mg between biotite and garnet: *Contr. Mineralogy Petrology*, v.66, p.113-117.
- Freer, R., 1979, An experimental measurement of cation diffusion in almandine garnet: *Nature*, v.280, 220-222.
- Ghent, E.D., 1975, Temperature, pressure and mixed volatile equilibria attending metamorphism of staurolite-kyanite bearing assemblages, Esplande Range, British Columbia: *Geol. Soc. America Bull.*, v.86, p.1654-1660.

- Ghent, E.D., 1976, Plagioclase-garnet- Al_2SiO_5 -quartz: a potential geothermometer-geobarometer: *Am. Mineralogist*, v.61, p.710-714.
- Ghent, E.D., Robbins, D.B., and Stout, M.Z., 1979, Geothermometry, geobarometry and fluid compositions of metamorphosed calc-silicates and pelites, Mica Creek, British Columbia: *Am. Mineralogist*, v.64, p.874-885.
- Ghent, E.D., Simony, P.S., and Knitter, C.C., 1980, Geometry and pressure-temperature significance of the kyanite-sillimanite isograd in the Mica Creek area, British Columbia: *Contr. Mineralogy Petrology*, v.74, p.67-73.
- Ghent, E.D., and Stout, M.Z., 1981, Geobarometry and geothermometry of plagioclase-biotite-garnet-muscovite assemblages: *Contr. Mineralogy Petrology*, v.76, p.92-97.
- Goldman, D.J., and Albee, A.L., 1977, Correlation of Mg/Fe partitioning between garnet and biotite with $\text{O}^{18}/\text{O}^{16}$ partitioning between quartz and magnetite: *Am. Jour. Sci.*, v.277, p.750-761.
- Grant, J.A., and Weiblen, P.W., 1971, Retrograde zoning in garnet near the second sillimanite isograd: *Am. Jour. Sci.*, v.270, p.281-296.
- Greenwood, H.J., 1975, Thermodynamically valid projections of extensive phase relationships: *Am. Mineralogist* 60, 1-8.
- Helgeson, H.C., Delany, J.M., Nesbitt, H.W., and Bird, D.K., 1978, Summary and critique of the thermodynamic properties of rock-forming minerals: *Am. Jour. Sci.*, v.278A.
- Hodges, K.V., 1981, Basement-cover relationships in the Aefjord - Skjomenes area, northern Norway ($68^{\circ}15'N$, $16^{\circ}45'E$). *Geological Society of America Abstracts with Programs* 13, 7, 474.
- Hodges, K.V., Tectonic stratigraphy and structural evolution of the Aefjord-Sitasjaure area, northern Scandinavian Caledonides. In preparation.
- Hodges, K.V., Bartley, J.M., Krueger, H.W., and Hodges, L.R., The use of discordant apparent mineral ages in determining closure temperatures and cooling rates in geologic environments. In preparation, a.
- Hodges, K.V., Bartley, J.M., and Burchfiel, B.C., Structural evolution of an A-type subduction zone, Lofoten-Rombak area, northern Scandinavian Caledonides. In preparation, b.
- Hodges, K.V., and Spear, F.S., in press, Accuracy vs. reliability of element partitioning geothermometers and geobarometers: a study of the Mt. Moosilauke area, New Hampshire: *Am. Mineralogist*.
- Hollister, L.S., 1966, Garnet zoning: an interpretation based on the Rayleigh fractionation model: *Science*, v.154, p.1647-1651.

- Kretz, R., 1959, Chemical study of garnet, biotite, and hornblende from gneisses of southwestern Quebec, with emphasis on distribution of elements in coexisting minerals: *J. Geol.*, v.67, p.371-402.
- Misener, D.J., 1974, Cationic diffusion in olivine to 1400°C and 35kbar, in: Geochemical Transport and Kinetics (Hofmann, A.W. et al., editors), Carnegie Institution, Washington, p.117-130.
- Spear, F.S., 1980, Plotting stereoscopic phase diagrams: *Am. Mineralogist*, v.65, p.1291-1293.
- Thompson, A.B., 1976, Mineral reactions in pelitic rocks: II. Calculation of some P-T-X(Fe-Mg) phase relations: *Am. Jour. Sci.*, v.276, p.401-454.
- Thompson, J.B., Jr., 1957, The graphical analysis of mineral assemblages in pelitic schists: *Am. Mineralogist*, v.42, p.842-858.
- Tracy, R.J., Robinson, P., and Thompson, A.B., 1976, Garnet composition and zoning in the determination of temperature and pressure of metamorphism, central Massachusetts: *Am. Mineralogist*, v.61, p.762-765.
- Woodsworth, G.J., 1977, Homogenization of zoned garnets from pelitic schists: *Canadian Mineralogist*, v.15, p.230-242.
- Zen, E-an, 1973, Thermochemical parameters of minerals from oxygen-buffered hydrothermal equilibrium data: method, application to annite and almandine: *Contr. Mineralogy Petrology*, v.39, p.65-80.

TABLE CAPTIONS

- Table 1. Electron microprobe analyses of biotite and muscovite.
- Table 2. Electron microprobe analyses of garnet and staurolite.
- Table 3. Electron microprobe analyses of plagioclase.
- Table 4. Modal mineralogy
- Table 5. Distribution of retrograde textures
- Table 6. Thermodynamic data for geothermometry-geobarometry.
- Table 7. Activity formulations and equilibrium constant equations.

Table 1. Electron microprobe analyses of biotite and muscovite

	Biotite						Muscovite							
	8B	8C	12E	18A	21A	21C	21F	8B	8C	12E	18A	21A	21C	21F
SiO ₂	36.93	37.24	36.37	35.91	38.43	36.57	35.94	47.69	46.10	47.36	47.31	46.54	47.59	46.83
Al ₂ O ₃	18.87	19.29	19.07	18.05	18.63	18.75	19.13	35.45	34.66	34.03	33.25	33.21	33.39	32.24
TiO ₂	1.34	1.24	1.94	1.26	1.12	1.89	1.90	0.80	1.16	1.40	0.54	0.45	1.26	1.41
MgO	13.61	12.02	11.41	11.72	15.75	12.14	11.56	1.12	1.14	1.28	1.36	1.24	1.44	1.25
FeO	14.98	16.65	17.74	17.70	12.75	16.40	16.82	0.95	1.62	1.35	3.07	3.08	1.99	1.13
MnO	0.02	0.01	0.03	0.02	0.27	0.05	0.05	-	-	-	-	-	-	0.01
CaO	0.03	0.08	0.04	0.02	0.05	-	0.04	0.02	0.03	0.03	0.05	0.02	0.04	0.05
Na ₂ O	0.13	0.21	0.37	0.26	0.33	0.16	0.26	0.46	1.16	0.99	0.76	1.24	0.55	0.80
K ₂ O	8.61	8.91	8.39	8.83	8.38	8.99	8.77	9.56	9.80	9.54	10.20	9.45	10.19	9.77
total	94.52	95.68	95.36	93.77	95.71	94.96	94.47	96.45	95.67	95.98	96.54	95.23	96.44	93.49
CATIONS PER 22 OXYGENS														
Si	5.529	5.514	5.444	5.521	5.580	5.477	5.464	6.303	6.121	6.236	6.267	6.237	6.270	6.366
Al ^{IV}	2.471	2.476	2.556	2.479	2.420	2.523	2.536	1.697	1.879	1.764	1.733	1.763	1.730	1.634
Al ^{VI}	0.858	0.899	0.809	0.792	0.768	0.787	0.892	3.669	3.547	3.518	3.459	3.484	3.457	3.531
Ti	0.188	0.138	0.218	0.181	0.122	1.211	0.136	0.100	0.116	0.138	0.054	0.046	0.124	0.090
Mg	3.037	2.658	2.545	2.686	3.406	2.708	2.620	0.221	0.226	0.251	0.267	0.248	0.282	0.254
Fe	1.876	2.065	2.221	2.276	1.548	2.053	2.139	0.105	0.180	0.148	0.340	0.345	0.218	0.128
Mn	0.002	0.002	0.004	0.003	0.033	0.004	0.006	-	-	-	-	0.001	-	0.001
Σ VI	5.961	5.762	5.797	5.938	5.877	5.763	5.793	4.095	4.069	4.055	4.120	4.124	4.081	4.004
Ca	0.005	0.013	0.006	0.003	0.008	-	0.006	0.003	0.005	0.007	0.007	0.004	0.006	0.007
Na	0.036	0.069	0.107	0.007	0.135	0.044	0.076	0.222	0.298	0.195	0.195	0.321	0.140	0.211
K	1.644	1.687	1.603	1.731	1.551	1.714	1.701	1.612	1.660	1.724	1.724	1.615	1.713	1.691
ΣA	1.685	1.769	1.716	1.811	1.694	1.758	1.783	1.837	1.963	1.926	1.926	1.940	1.859	1.909

Table 2. Electron microprobe analyses of garnet and staurolite

	Garnet							Str
	8B	8C	12E	18A	21A	21C	21F	18A
SiO ₂	38.20	38.69	37.45	37.34	36.98	38.24	36.89	27.70
Al ₂ O ₃	21.81	21.58	20.86	20.91	21.59	21.38	21.24	51.09
TiO ₂	-	0.05	0.05	0.01	0.01	0.23	0.01	0.52
MgO	5.61	3.47	3.08	2.64	3.54	3.78	3.81	2.19
FeO	26.95	35.37	35.84	31.91	23.10	32.27	34.02	14.23
MnO	2.07	1.19	1.50	2.57	11.72	1.59	1.40	0.11
ZnO	nd	nd	nd	nd	nd	nd	nd	0.12
CaO	5.97	1.43	1.65	4.40	2.64	4.03	2.49	-
Total	100.61	101.78	100.43	99.78	99.58	101.52	99.86	95.96
	CATIONS PER 12 O							CATIONS
								PER 23 O
Si	2.977	3.037	3.007	3.008	2.968	3.001	2.965	3.944
Al	2.004	1.998	1.975	1.985	2.043	1.978	2.012	8.571
Ti	-	-	0.003	0.001	-	0.013	0.001	0.070
Mg	0.651	0.405	0.369	0.317	0.423	0.442	0.457	0.464
Fe	1.757	2.322	2.407	2.150	1.551	2.118	2.287	1.694
Mn	0.137	0.079	0.102	0.176	0.797	0.104	0.096	0.014
Zn	nd	nd	nd	nd	nd	nd	nd	0.013
Ca	0.498	0.121	0.142	0.364	0.227	0.337	0.214	-
<u>Fe</u>								
Fe+Mg	0.730	0.851	0.867	0.872	0.786	0.827	0.833	0.785
XAl	0.577	0.793	0.797	0.715	0.517	0.706	0.749	-
XPy	0.214	0.138	0.122	0.105	0.141	0.147	0.150	-
XGr	0.164	0.041	0.047	0.121	0.076	0.112	0.070	-
XSp	0.045	0.027	0.034	0.059	0.266	0.035	0.031	-
Σ	8.024	7.962	8.005	8.001	8.009	7.993	8.032	14.77

Table 3. Electron microprobe analyses of plagioclase

	8B	8C	12E	18A	21A	21C	21F
SiO ₂	54.49	64.67	62.99	60.52	61.20	60.81	61.32
Al ₂ O ₃	28.70	21.78	23.18	24.68	24.77	24.89	23.69
FeO	0.37	0.04	0.27	0.31	0.10	0.24	0.44
CaO	11.10	3.07	4.47	6.28	6.10	6.48	5.30
Na ₂ O	5.16	10.12	9.40	8.24	7.72	7.79	8.64
K ₂ O	0.07	0.06	0.07	0.06	0.05	0.14	0.06
Σ	99.89	99.74	100.38	100.09	99.94	100.35	99.45
CATIONS PER 8 OXYGENS							
Si	2.463	2.858	2.783	2.695	2.716	2.696	2.741
Al	1.530	2.858	1.207	1.295	1.296	1.301	1.249
Fe	0.014	1.135	0.010	0.012	0.002	0.009	0.017
Ca	0.538	0.001	0.212	0.300	0.290	0.307	0.254
Na	0.451	0.867	0.805	0.711	0.665	0.669	0.748
K	0.004	0.003	0.004	0.004	0.003	0.008	0.004
Σ	5.000	5.009	5.021	5.017	4.972	4.990	5.013
XAn	0.542	0.143	0.208	0.296	0.303	0.312	0.252
XAb	0.454	0.854	0.788	0.700	0.694	0.680	0.744
XOr	0.004	0.003	0.004	0.004	0.003	0.008	0.004

TABLE 4. MODAL MINERALOGY

	<u>79-8B</u>	<u>79-8C</u>	<u>79-12E</u>	<u>79-18A</u>	<u>79-21A</u>	<u>79-21C</u>	<u>79-21F</u>
Quartz	43%	38%	41%	34%	48%	28%	39%
Muscovite	13	22	16	7	10	9	18
Biotite	27	21	26	26	21	25	21
Garnet	5	10	5	3	2	16	10
Plagioclase	5	5	7	12	12	15	7
Kyanite	4	2	3	9	2	5	4
Staurolite	0	0	0	1	0	0	0
Chlorite	0	0	0	3	1	0	0
Other	3	2	20	5	4	2	1

Note: Modal percentages based on ~500 counts on a single polished section. "Other" denotes ilmenite and zircon in all samples; tourmaline in 79-8C, 79-18A, and 79-21F; allanite in 79-21A; and optically zoned epidote in 79-18A.

TABLE 5. DISTRIBUTION OF RETROGRADE TEXTURES

Sample	Texture present ?			
	(A)	(B)	(C)	(D)
79-8B	no	no	no	no
79-8C	no	yes	yes	no
79-12E	no	yes	no	no
79-18A	yes	yes	yes	no
79-21A	no	yes	yes	no
79-21C	no	yes	yes	yes
79-21F	no	yes	yes	yes

(A) -- Secondary garnet growth

(B) -- Second-stage kyanite along garnet-plagioclase interfaces

(C) -- Epitaxial second-stage kyanite on first-stage kyanite

(D) -- Muscovite "rims" on first-stage kyanite

TABLE 6. THERMODYNAMIC DATA FOR GEOTHERMOMETRY - GEOBAROMETRY

Equilibrium	ΔH (cal)	ΔS (cal/°K)	ΔV (cal/bar)	Source
(1)	12454	4.662	0.057	Ferry and Spear (1978)
(2)	14970	38.418	1.577	Ghent (1976); Ghent <u>et al.</u> (1979)
(3)	19569	40.809	1.802	this study

TABLE 7. ACTIVITY FORMULATIONS AND EQUILIBRIUM CONSTANT EQUATIONS

$$K_2 = \frac{\left(\frac{X_{ga}}{X_{py}} \right)^3 \left(\frac{X_{bi}}{X_{ann}} \right)^3}{\left(\frac{X_{bi}}{X_{ph}} \right)^3 \left(\frac{X_{ga}}{X_{al}} \right)^3}$$

$$K_2 = \frac{\left(\frac{X_{pg}}{X_{an}} \right)^3}{\left(\frac{X_{ga}}{X_{gr}} \right)^3} \times (2.5)$$

$$K_3 = \frac{\left(\frac{X_{pg}}{X_{an}} \right)^3 \left(\frac{X_{bi}}{X_{ann}} \right)^3}{\left(\frac{X_{mu}}{X_{mu}} \right) \left(\frac{X_{ga}}{X_{al}} \right)^3 \left(\frac{X_{ga}}{X_{gr}} \right)^3}$$

$$X_{al}^{ga} = \text{Fe}/\text{Fe}+\text{Mg}+\text{Ca}+\text{Mn}$$

$$X_{ga}^{py} = \text{Mg}/\text{Fe}+\text{Mg}+\text{Ca}+\text{Mn}$$

$$X_{ga}^{gr} = \text{Ca}/\text{Fe}+\text{Mg}+\text{Ca}+\text{Mn}$$

$$X_{ann}^{bi} = \text{Fe}/\text{Fe}+\text{Mg}+\text{Ti}+\text{AlVI}$$

$$X_{ph}^{bi} = \text{Mg}/\text{Fe}+\text{Mg}+\text{Ti}+\text{AlVI}$$

$$X_{an}^{pg} = \text{Ca}/\text{Ca}+\text{Na}+\text{K}$$

$$X_{mu}^{mu} = \left(\frac{X_{mu}}{K} \right) \left(\frac{X_{mu}}{\text{AlVI}} \right)^2$$

$$X_K^{mu} = \text{K}/\text{Ca}+\text{Na}+\text{K}$$

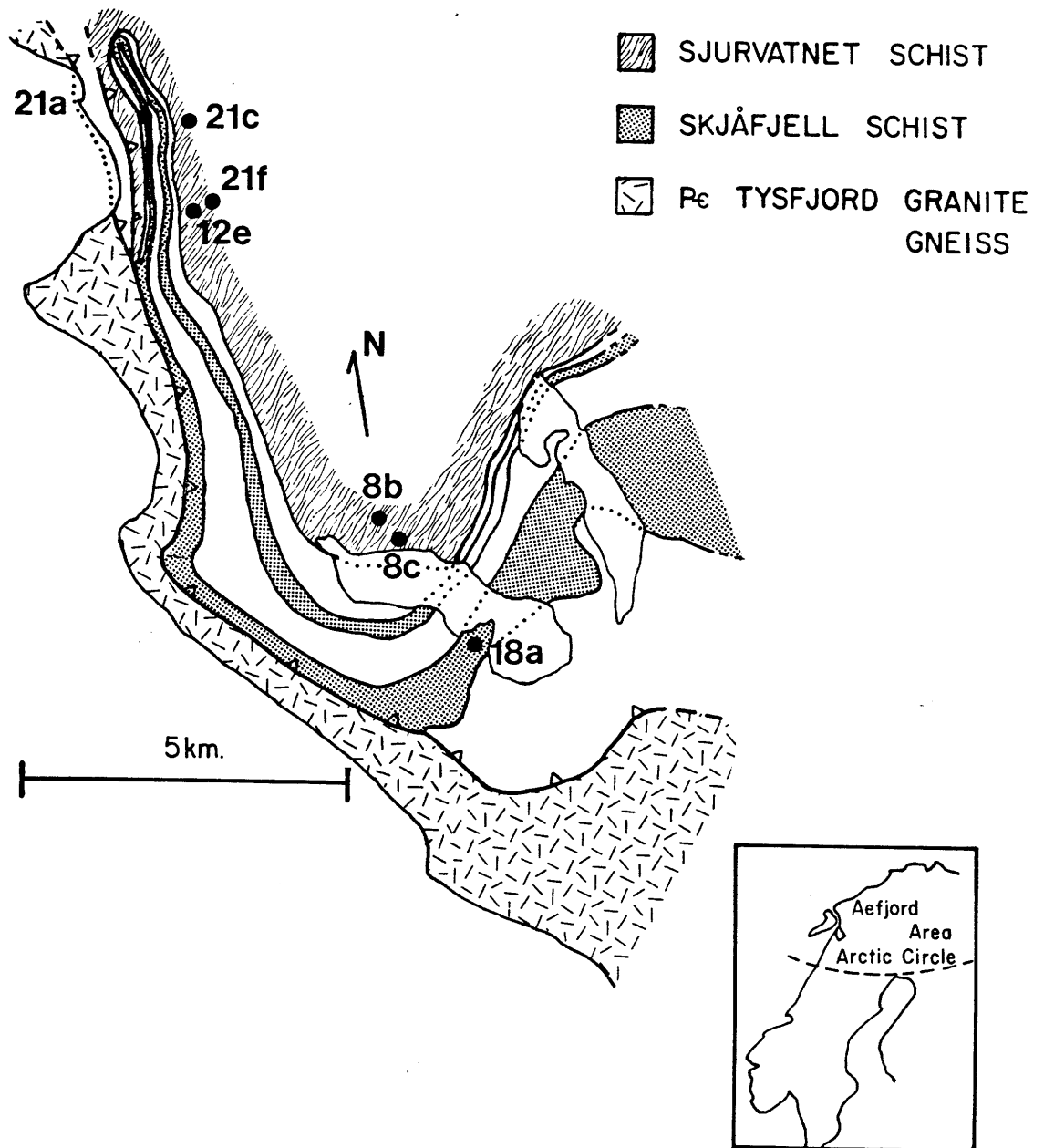
$$X_{AlVI}^{mu} = \text{AlVI}/\text{Fe}+\text{Mg}+\text{Mn}+\text{Ti}+\text{AlVI}$$

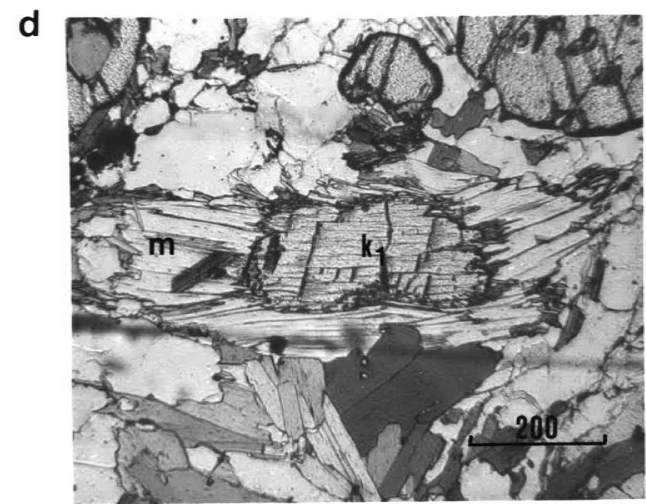
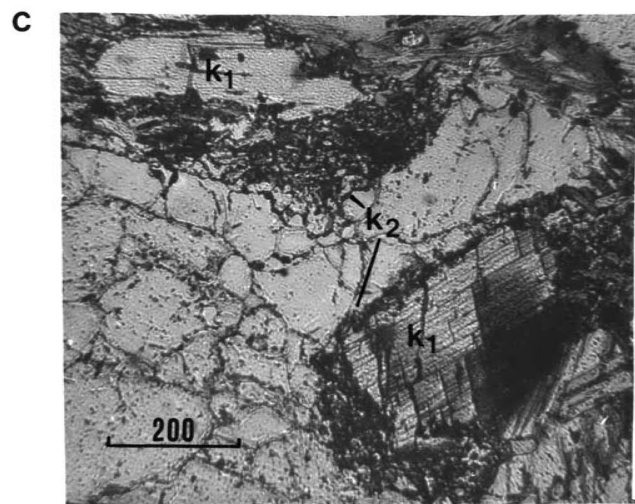
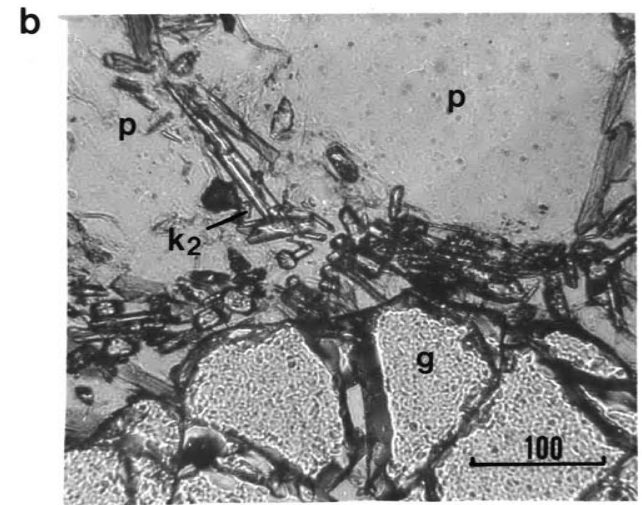
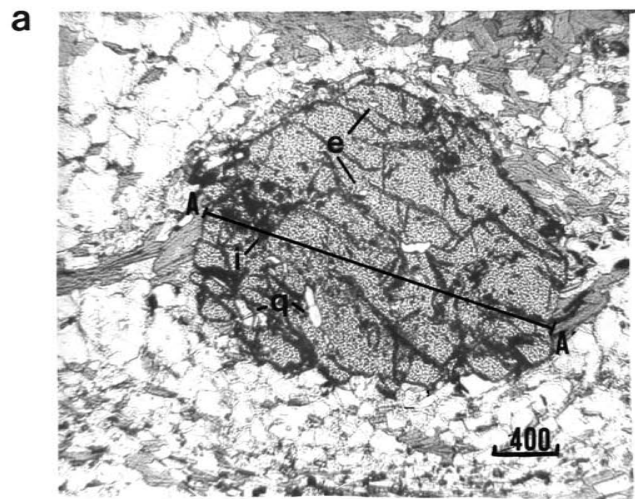
Note: K_1 assumes ideal Fe-Mg solution in biotite and garnet. The correction factor of 2.5 for non-ideal solution behavior in K_2 is after Ghent et al. (1979). Formulation for K_3 is after Ghent and Stout (1981).

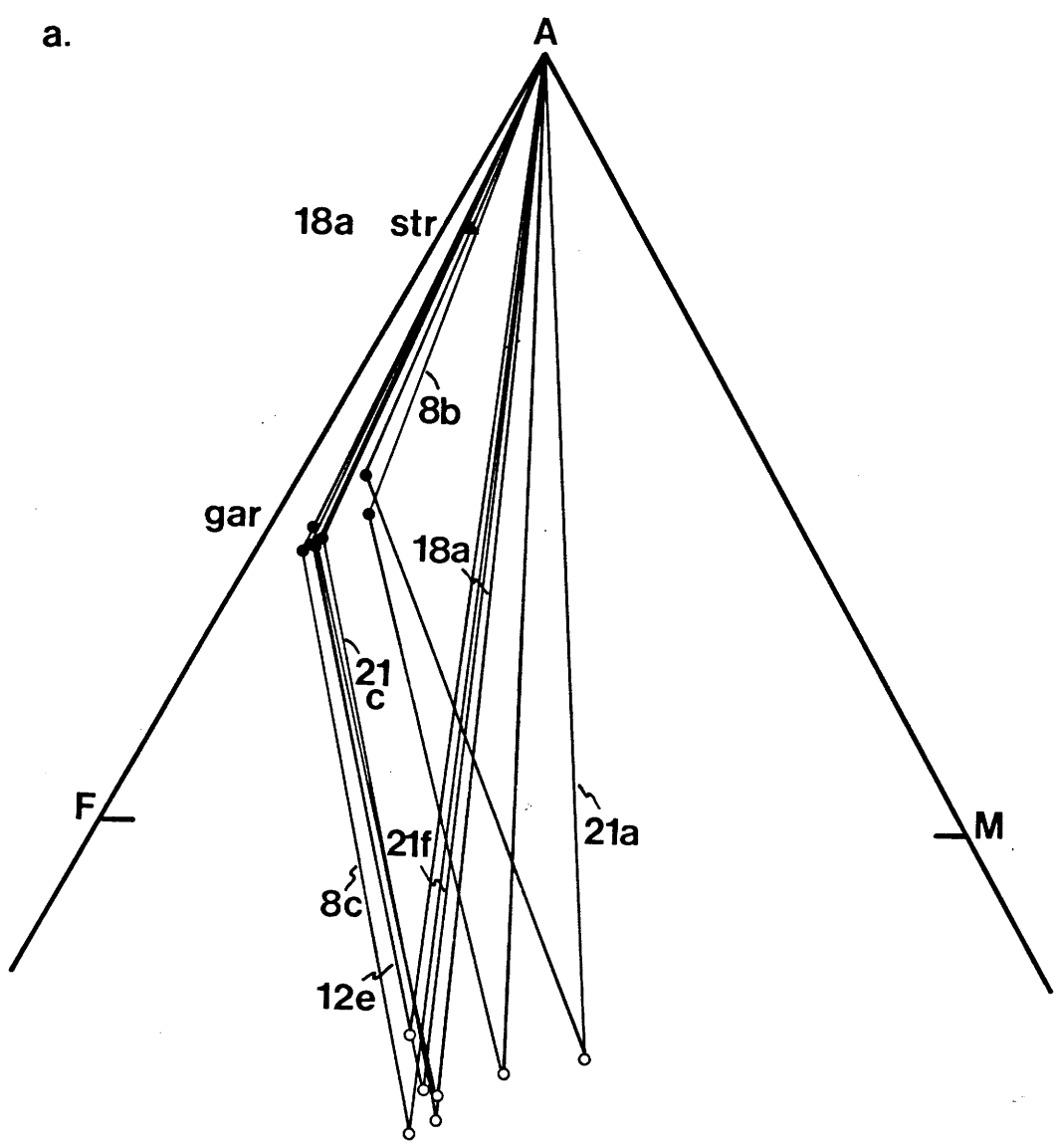
Figure Captions

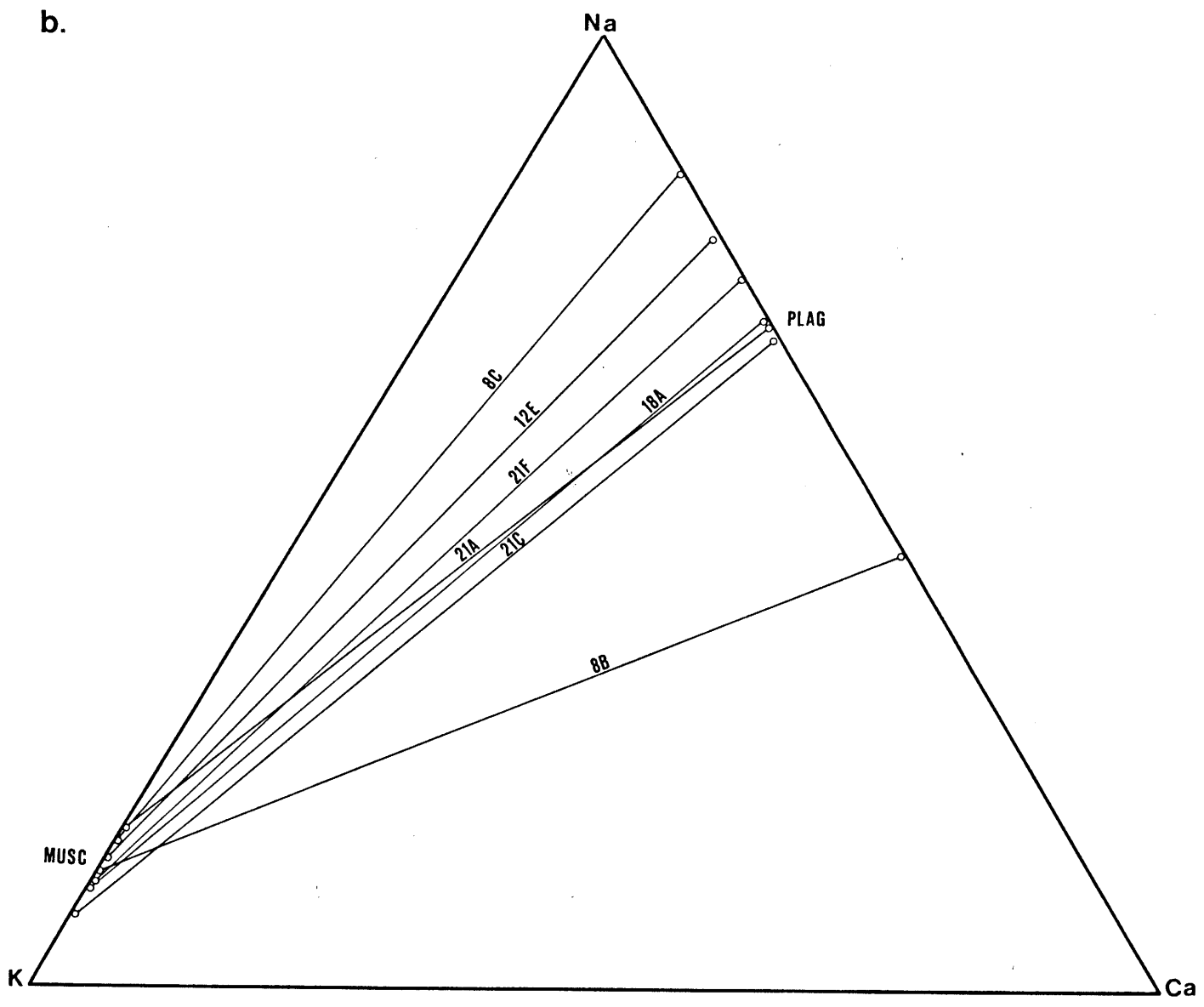
- Figure 1. Tectonic map of the Aefjord area ($68^{\circ}15'N$, $16^{\circ}45'E$), northern Norway, showing sample localities. Prefix of 79- for sample numbers has been deleted for clarity.
- Figure 2. Retrograde textures in pelitic schists from the Aefjord area. a. Garnet from sample 79-18A showing rotated core, with abundant quartz (q) + ilmenite (i) inclusions, surrounded by a static overgrowth with epidote (e) + quartz + ilmenite inclusions. Solid line indicates path of garnet transect shown in Figure 6d. b. second stage kyanite (k_2) + quartz growing along a garnet(g) - plagioclase (p) interface in sample 79-21C. c. Epitaxial overgrowth of (k_2) on first stage kyanite (k_1) in sample 79-21C. d. Overgrowth of muscovite (m) on (k_1) from sample 79-21C. Scales shown on photomicrographs are in microns.
- Figure 3. Ternary phase diagrams. a. Al-Fe-Mg projection from quartz, muscovite and H₂O of garnet-biotite-kyanite assemblages from the Aefjord area. Composition of staurolite from 79-18A is indicated by triangle. b. K-Na-Ca projection from kyanite, quartz and H₂O of plagioclase-muscovite assemblages.
- Figure 4. Stereoscopic projections of phase diagrams. a. Mg-Al-Fe-H₂O projection from muscovite and quartz of garnet-kyanite-muscovite assemblages. Kyanite plots at Al apex, biotite plots outside of tetrahedron due to muscovite projection. Assemblages in order of increasing H₂O content in biotite are: 79-18A, 79-21C, 79-21F, 79-8C, 79-8B, and 79-21A. b. Fe-Mg-Ca-Na projection from quartz, muscovite, kyanite and H₂O of garnet (plotting nearest Fe apex), biotite (plotting along Fe-Mg join), and plagioclase (plotting along Ca-Na join). Assemblages in order of increasing Ca content in plagioclase are: 79-8C, 79-12E, 79-21F, 79-18A, 79-21A, 79-21C, and 79-8B.
- Figure 5. Distribution coefficient plots for equilibria (1; a) and (2; b). Limiting K_d 's are shown for reference.

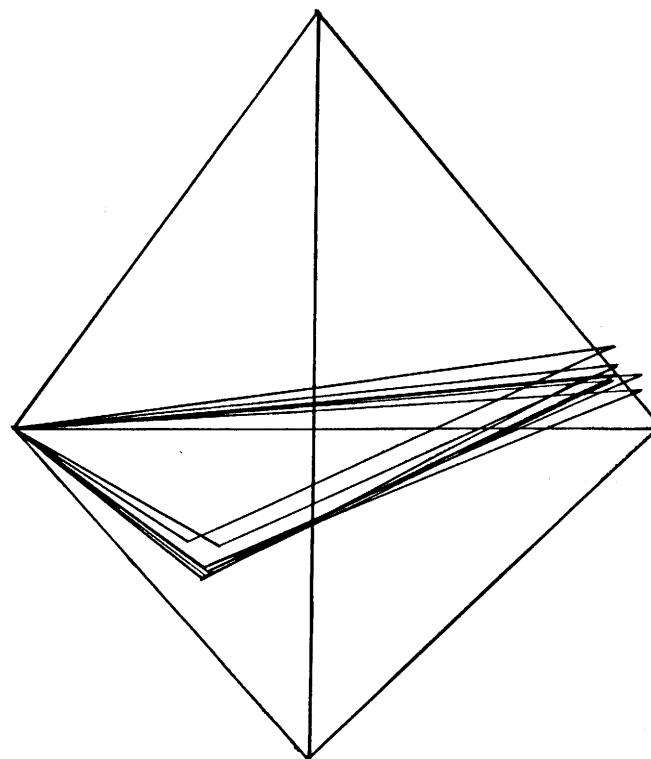
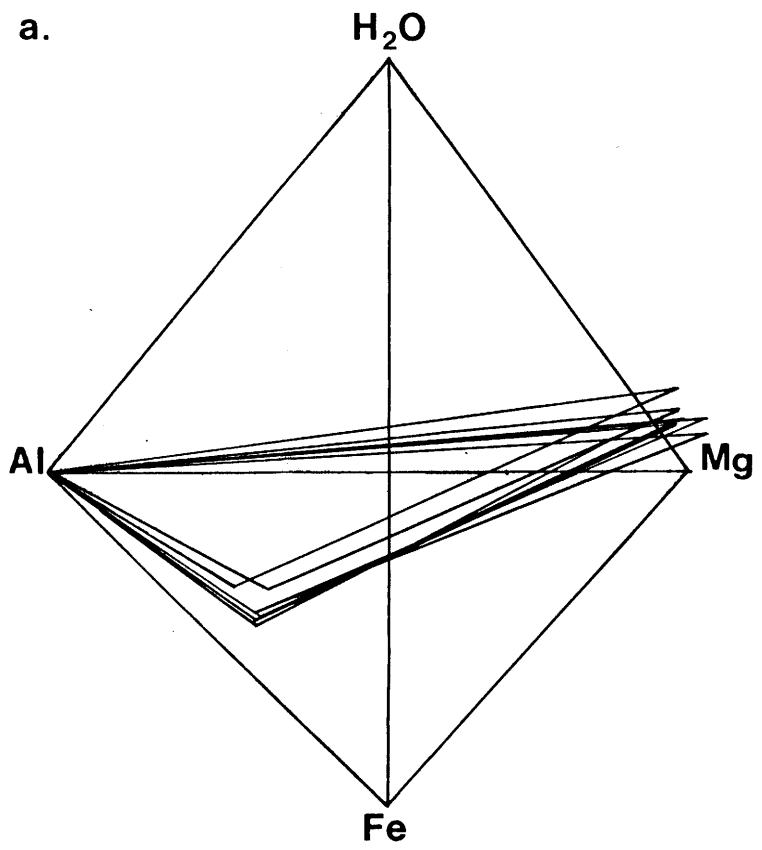
- Figure 6. Compositional profiles for the largest garnet in each sample. Adjacent phases at profile termini are indicated. Scale is the same in each.
- Figure 7. P-T plots of equilibria (1) -(3) for the Aefjord samples. Short-long dashed curves = equilibrium (1), solid curves = equilibrium (2), and dashed curves = equilibrium (3). Each pair of curves represents $\pm 1\sigma$ for calculated equilibrium constants.
- Figure 8. Synoptic P-T diagram showing simultaneous solutions of equilibria (1) and (2) (shaded) and of equilibria (1) and (3) (unpatterned) for the Aefjord samples. Aluminosilicate stability fields after Holdaway (1971). Note that all samples fall within the kyanite stability field, consistent with a retrograde P-T trajectory involving growth of k₂ kyanite.
- Figure 9. Plot of temperatures ($^{\circ}\text{C}$), calculated using simultaneous solution of equilibria (1) and (2), vs. mole fraction grossular (a) and mole fraction spessartine (b) in garnets from each sample.

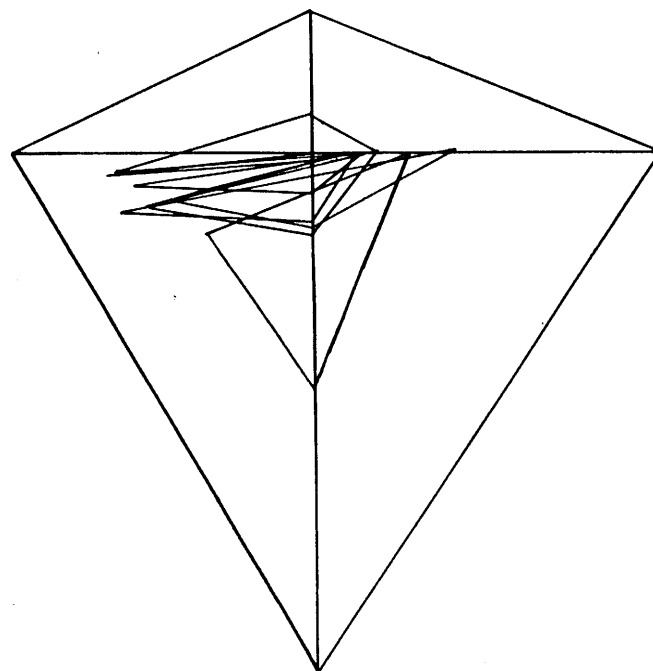
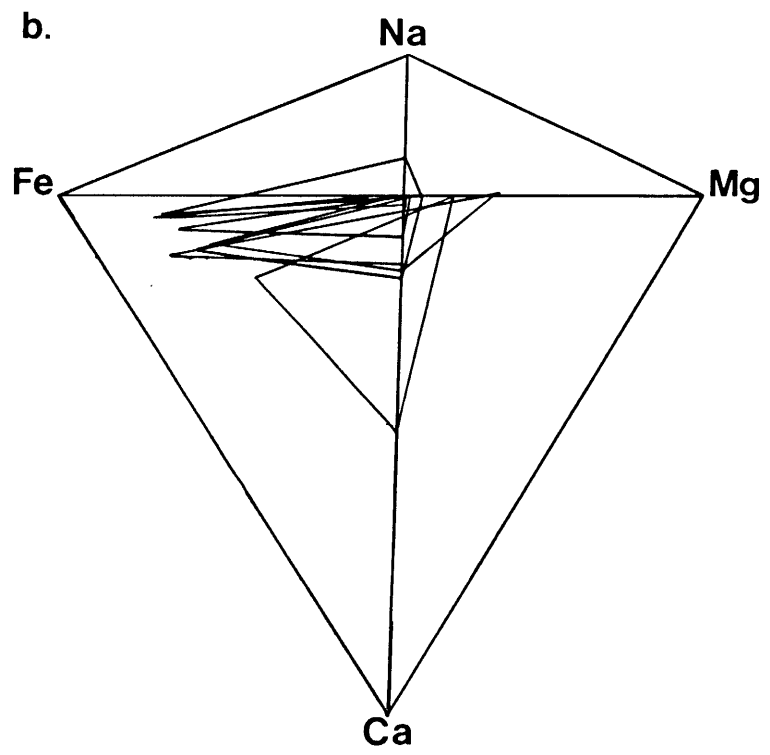


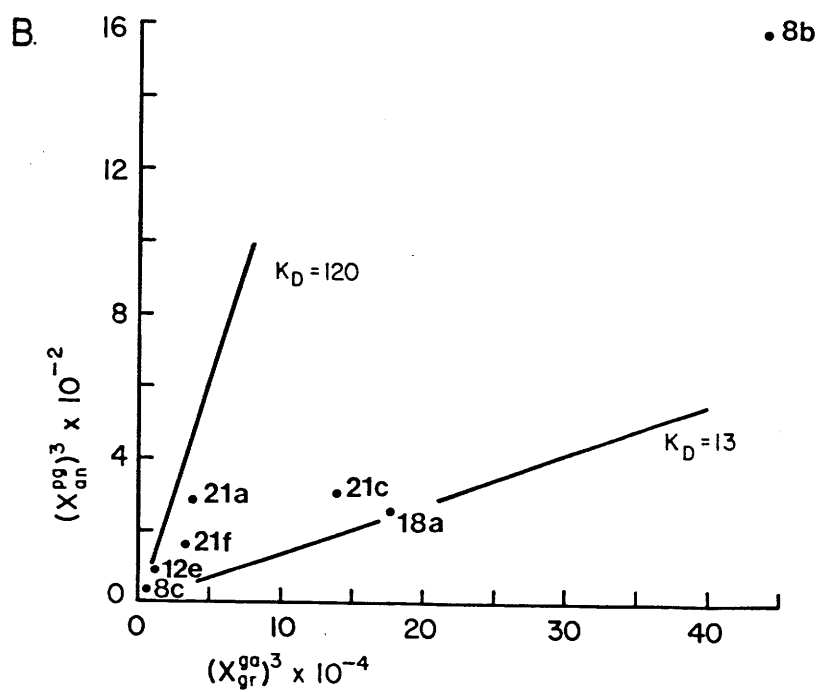
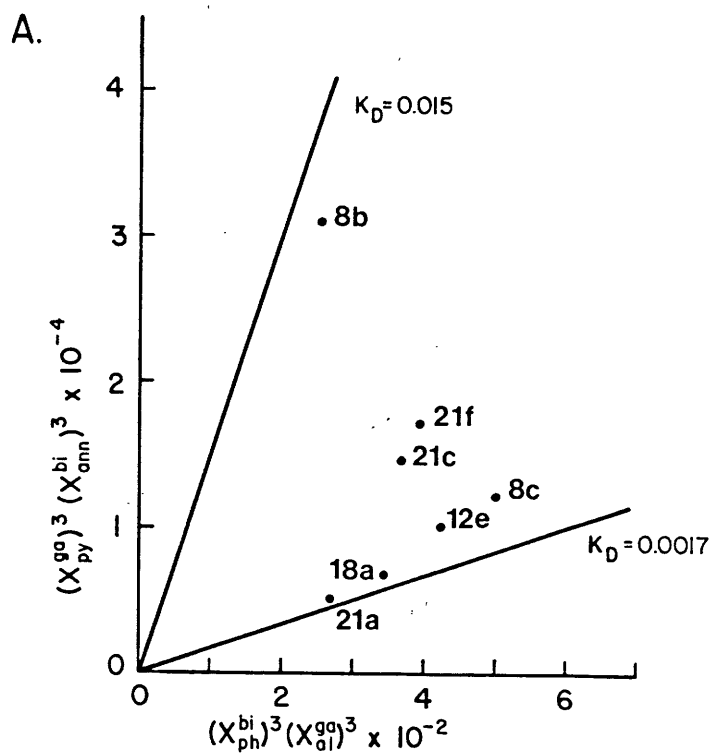




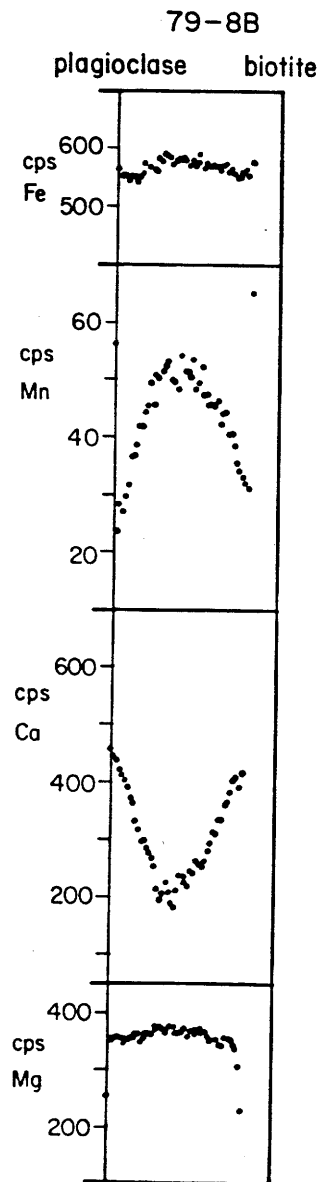




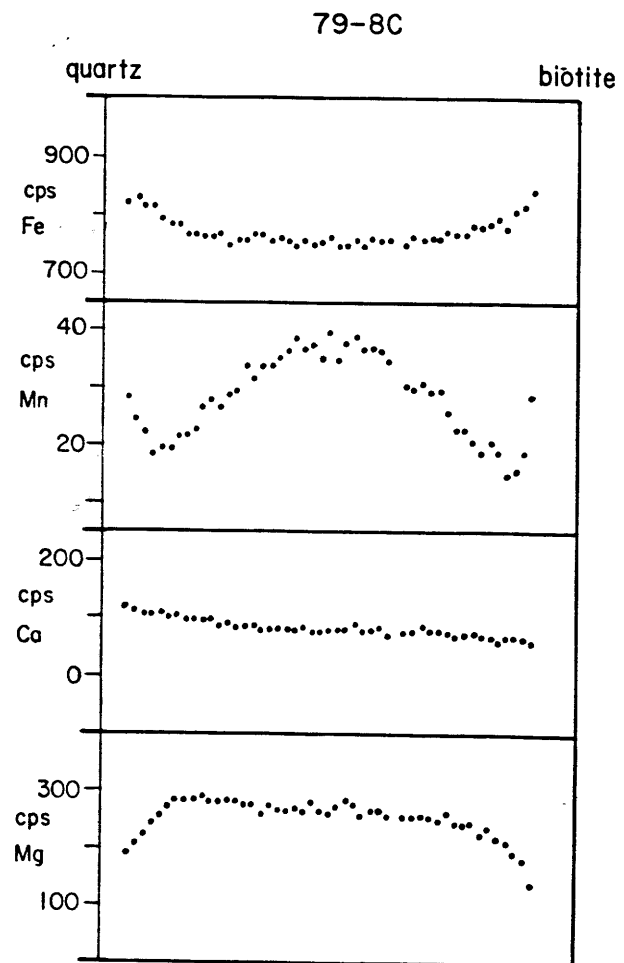




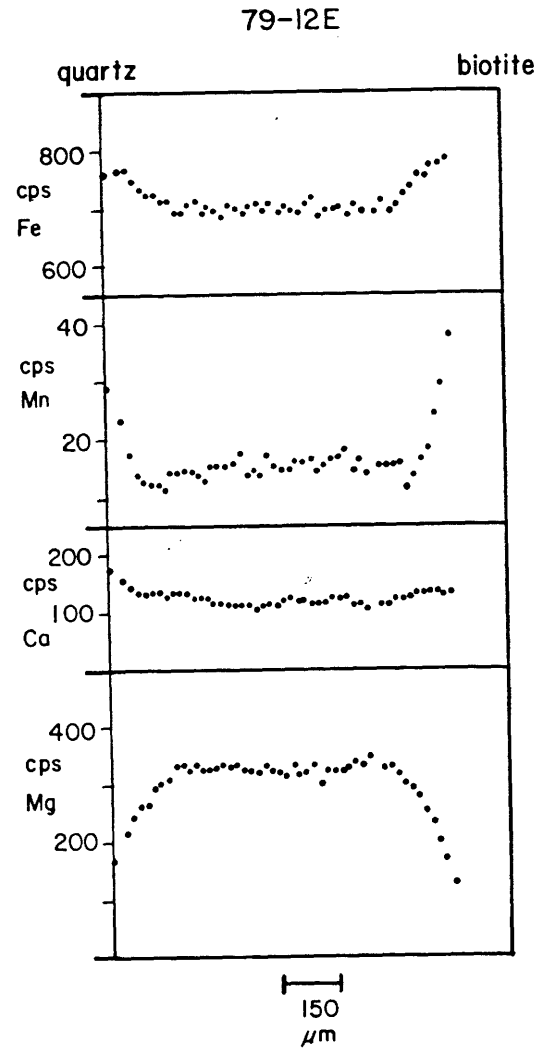
a.



b.

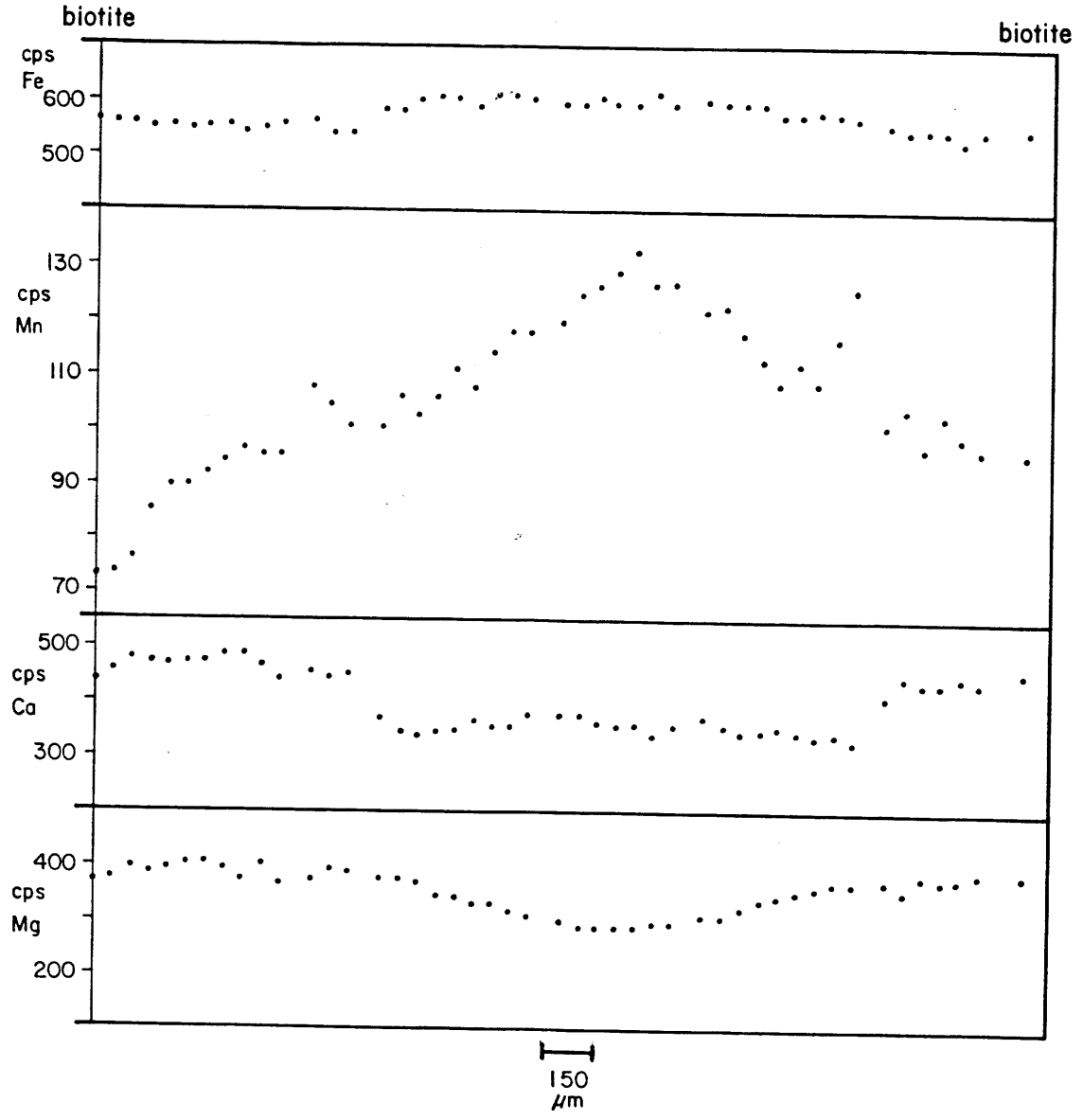


C.

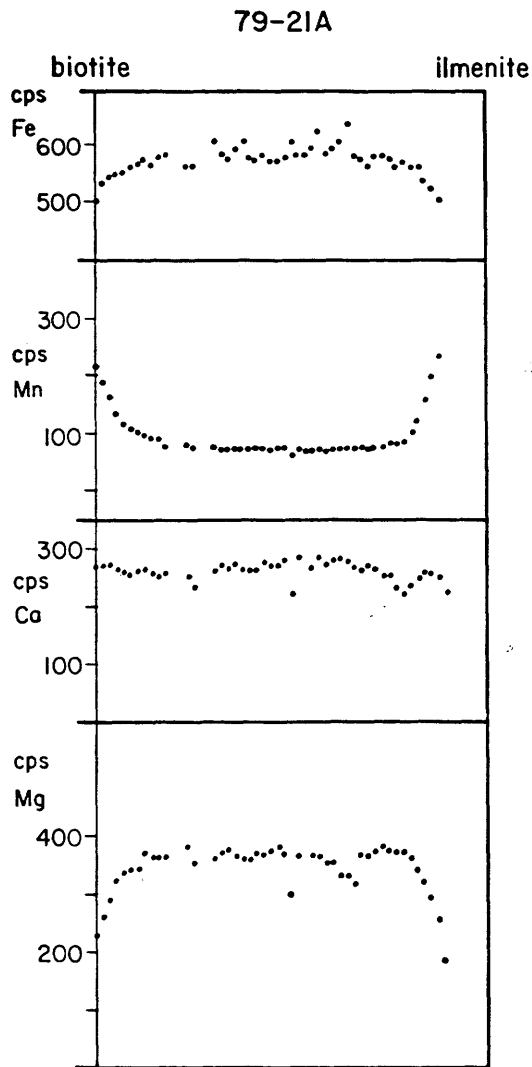


d.

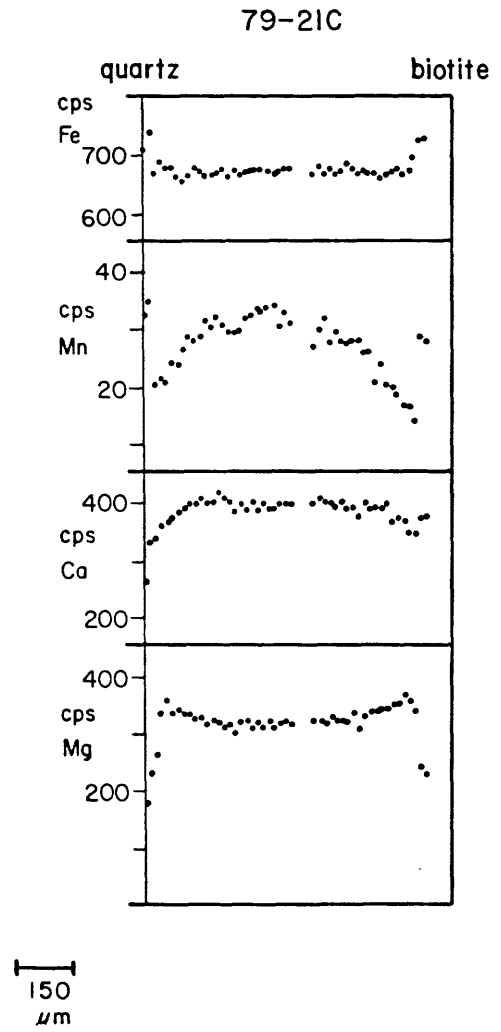
79-18A



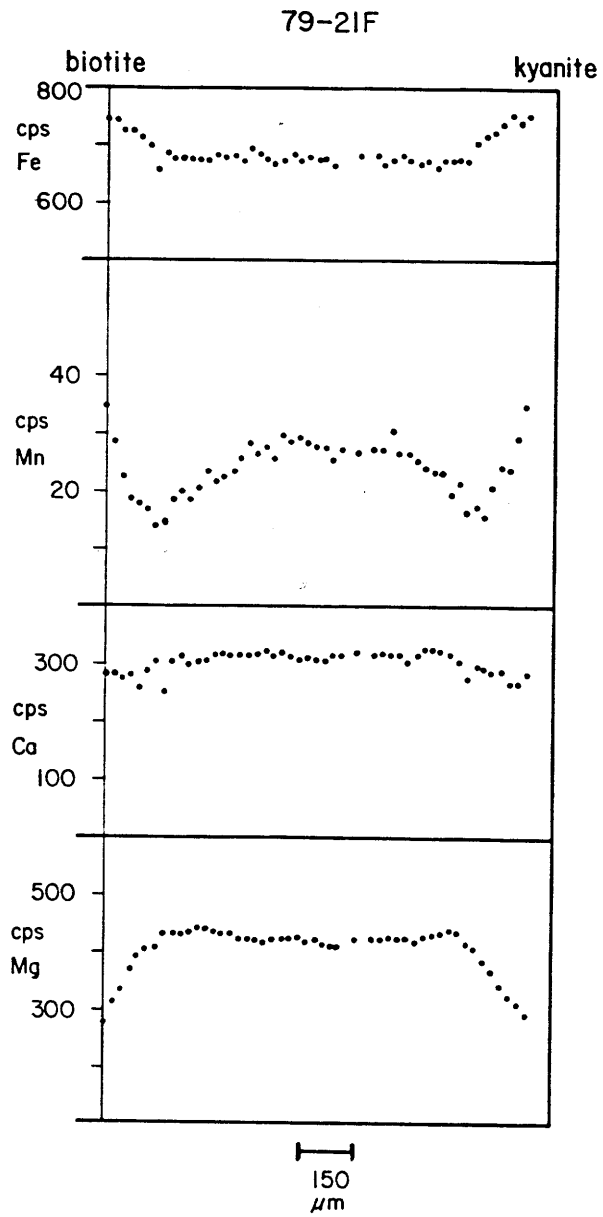
e.



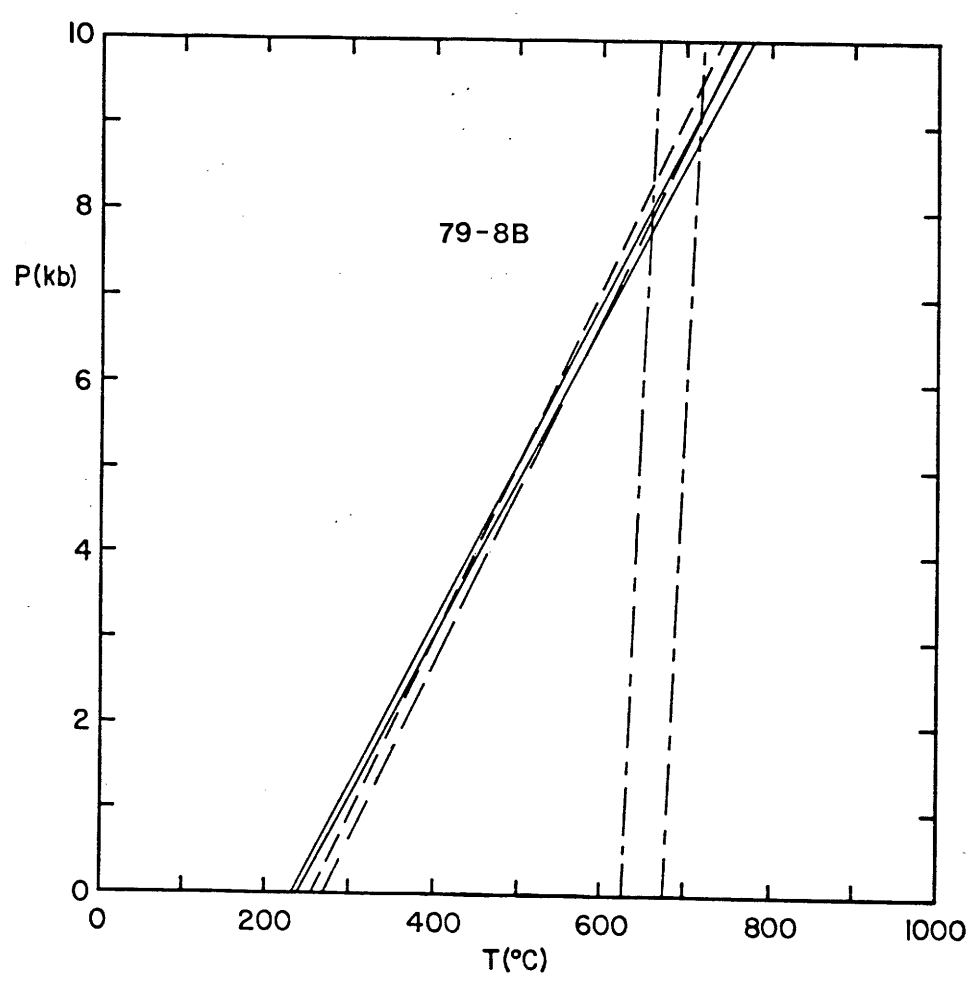
f.



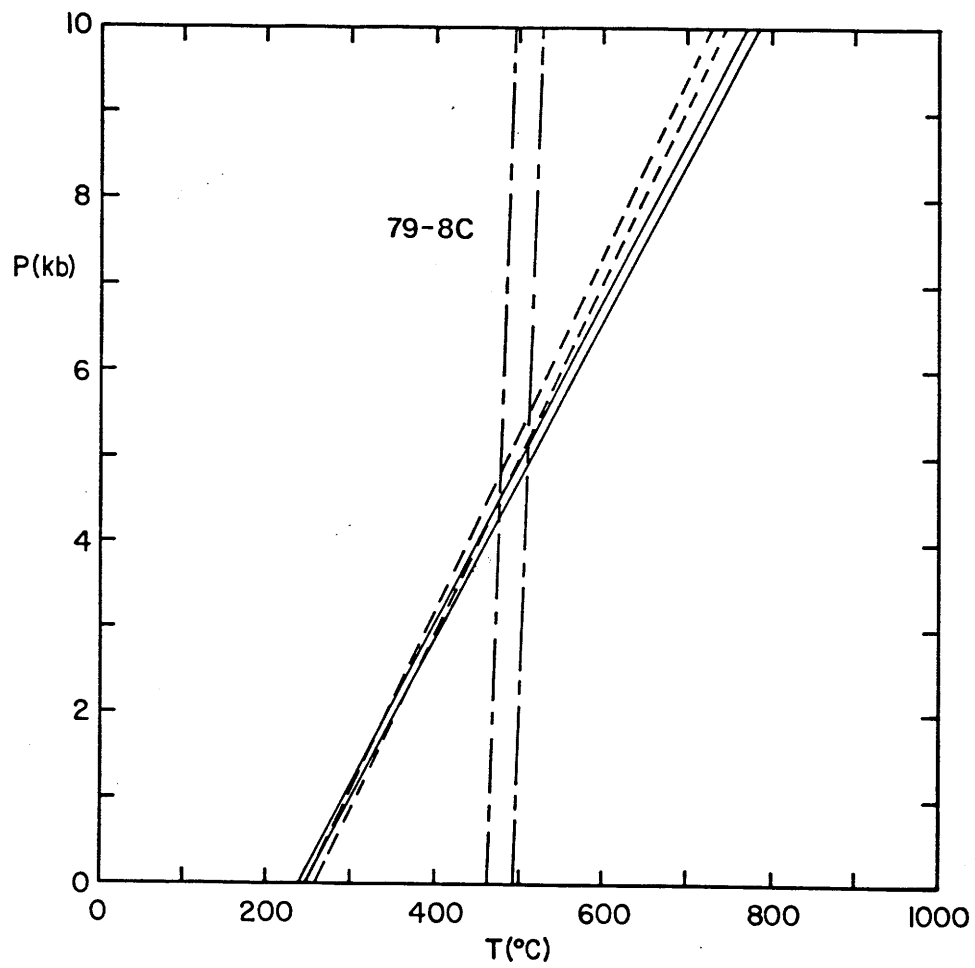
g.



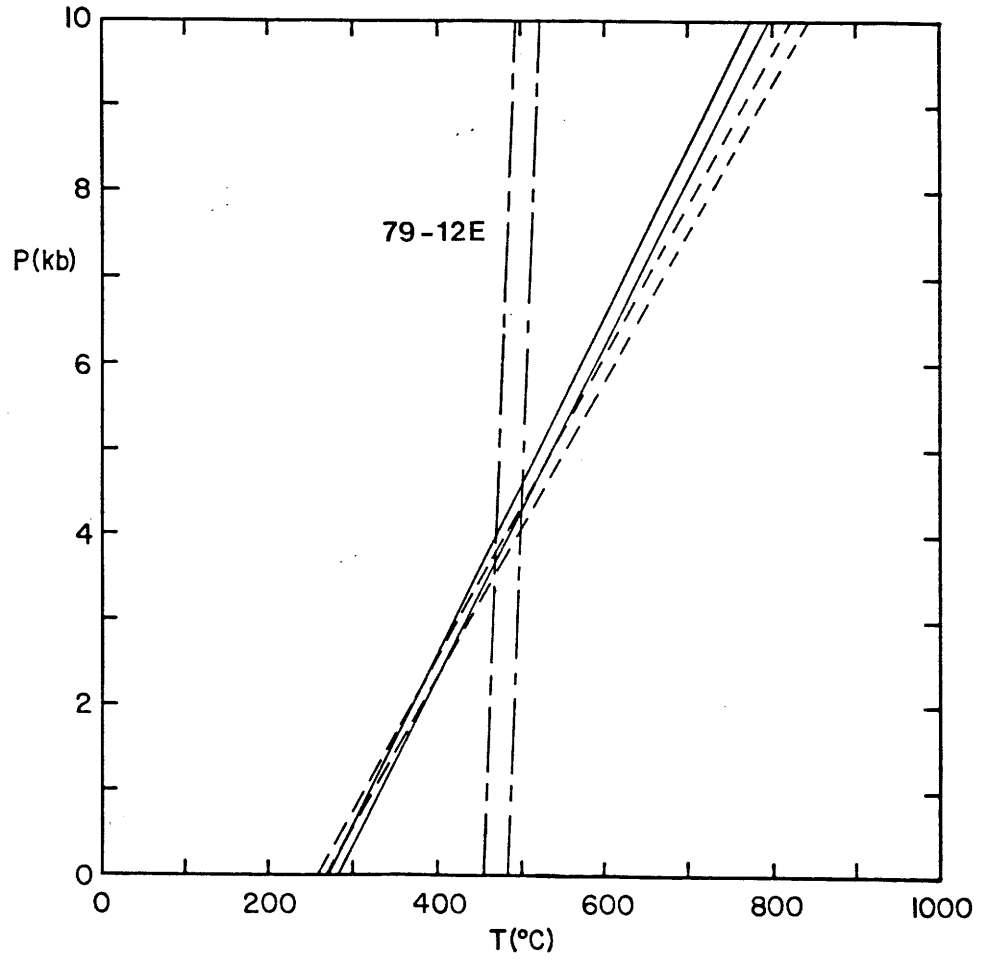
a.



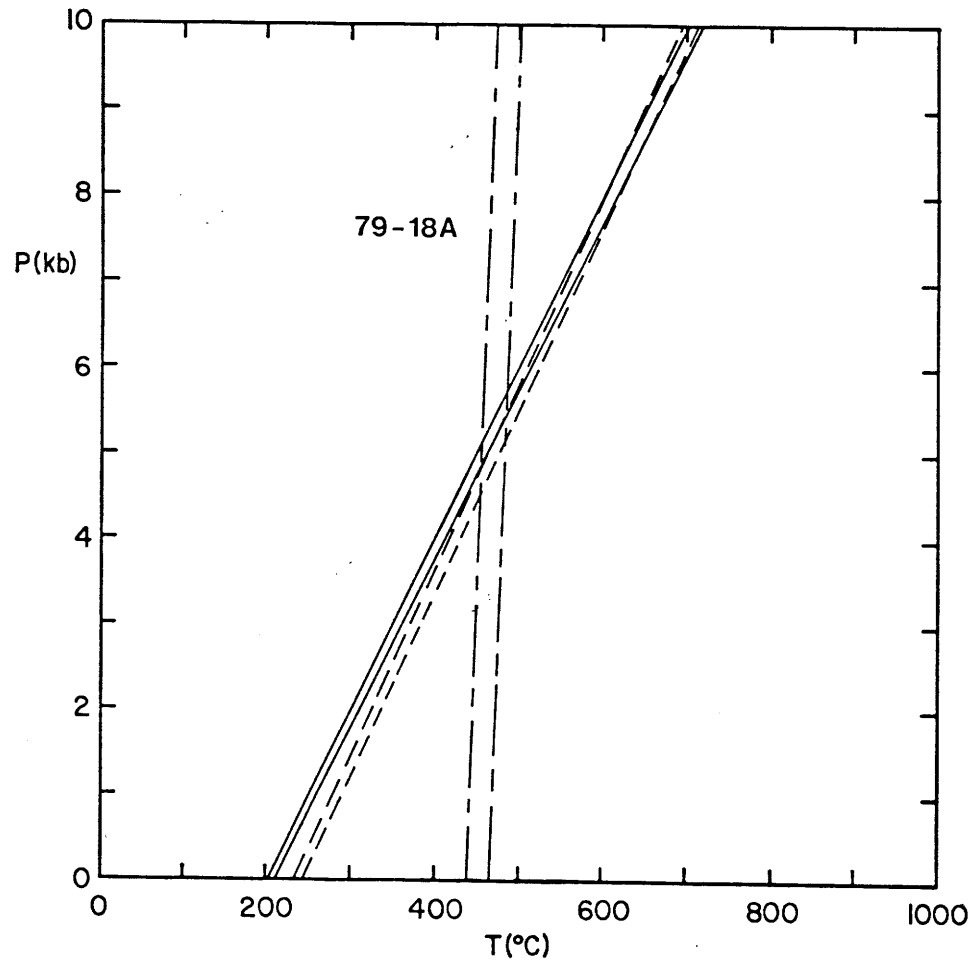
b.



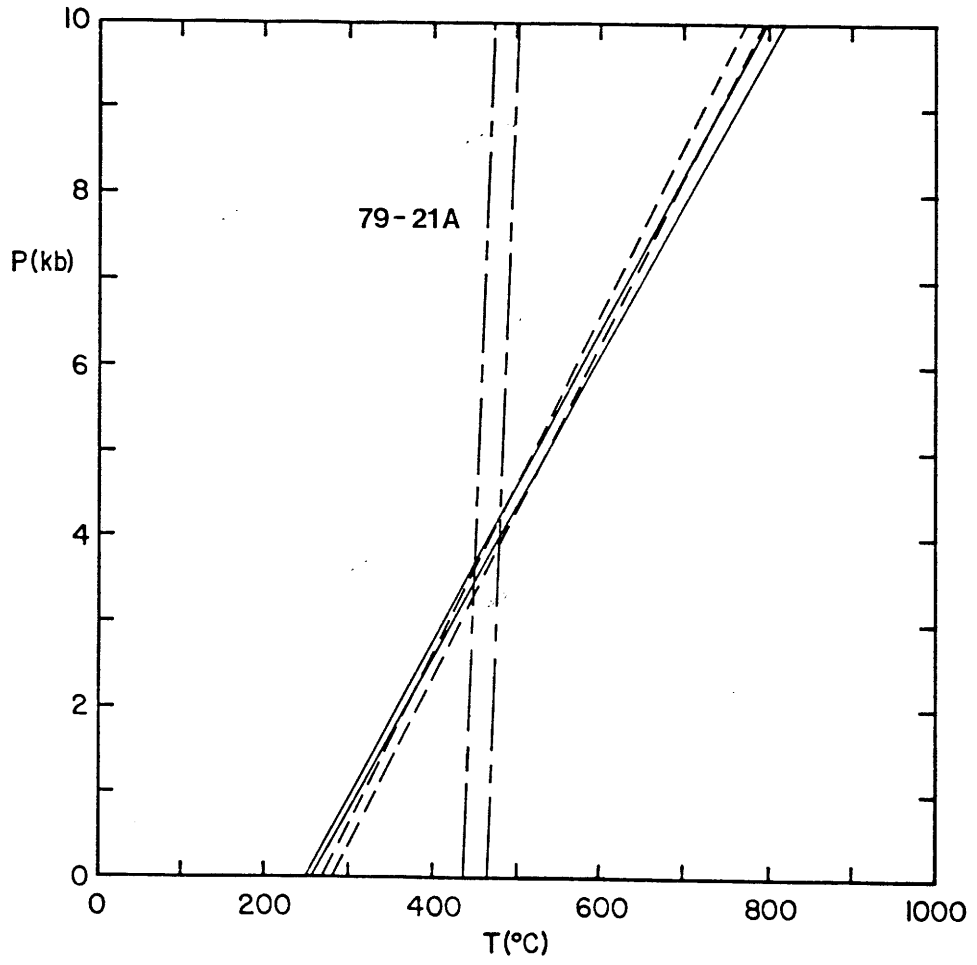
c.



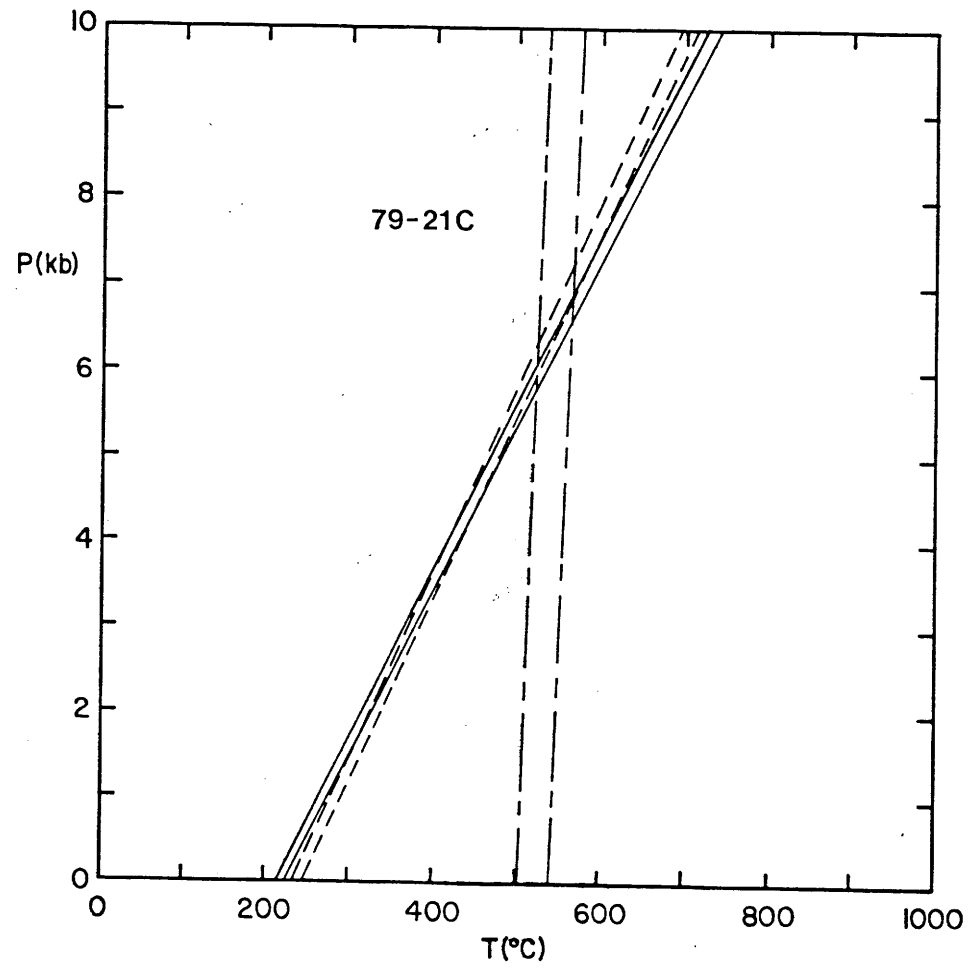
d.



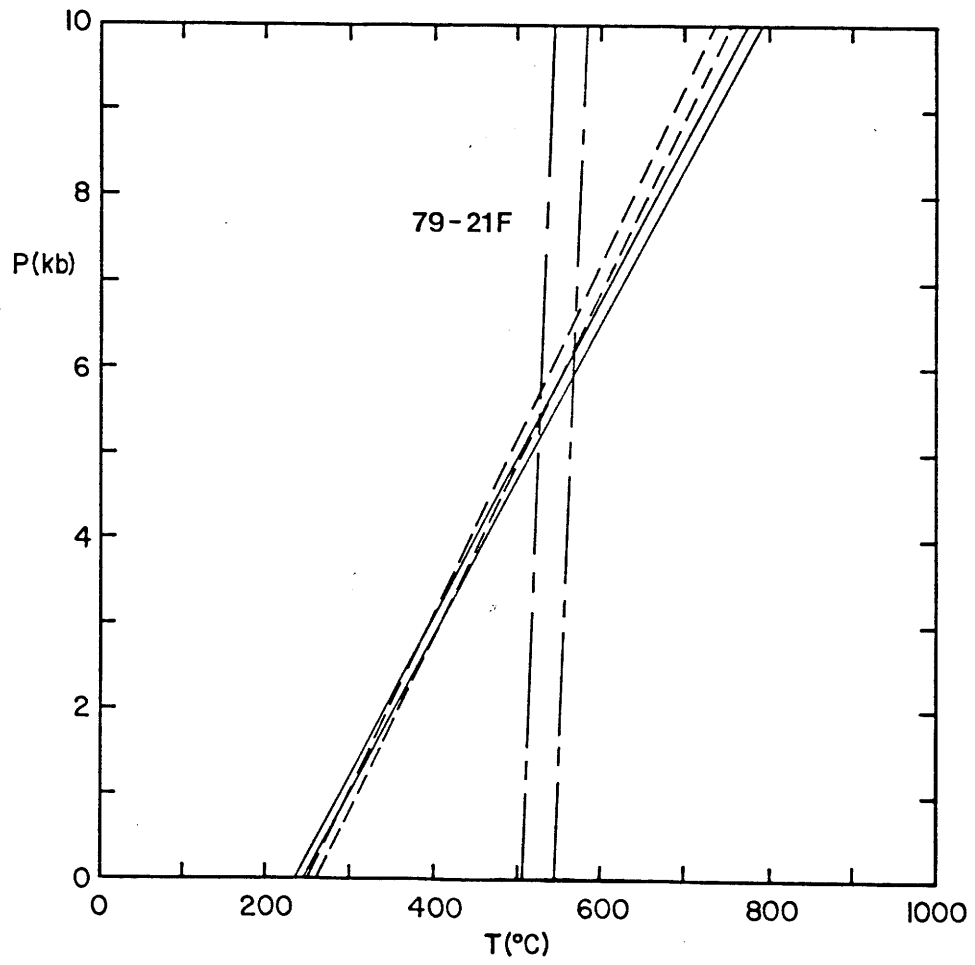
e.

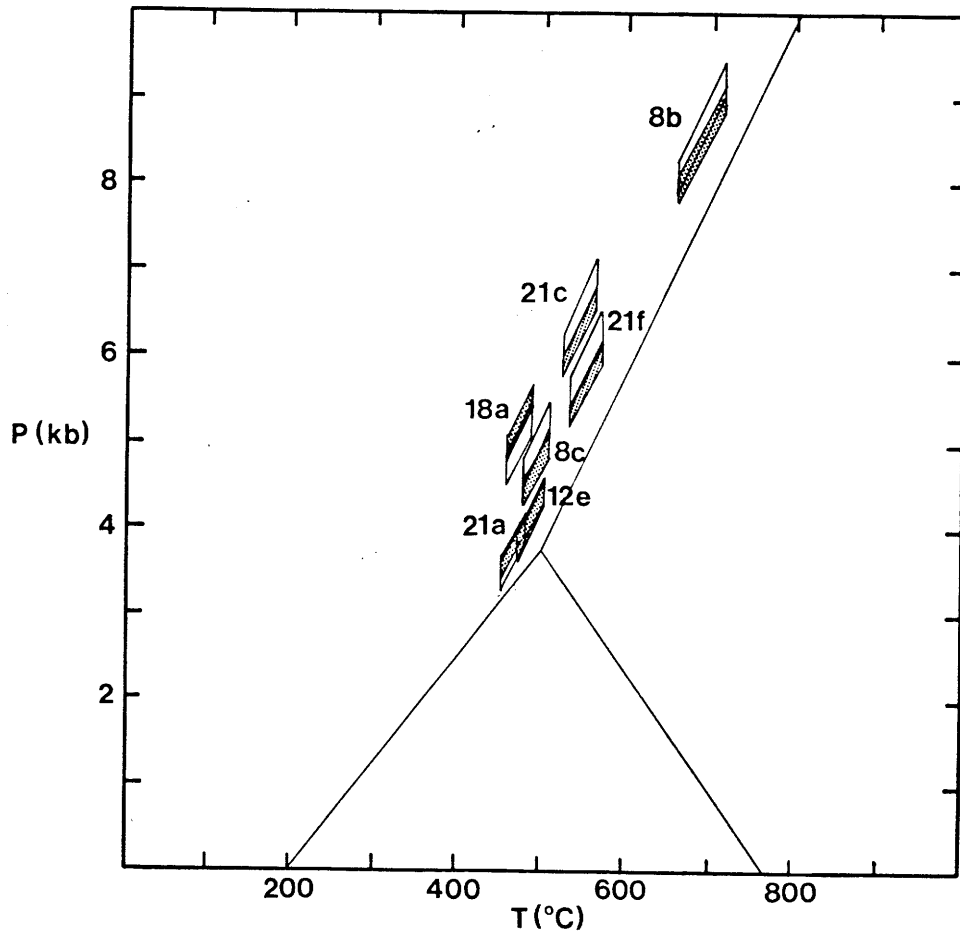


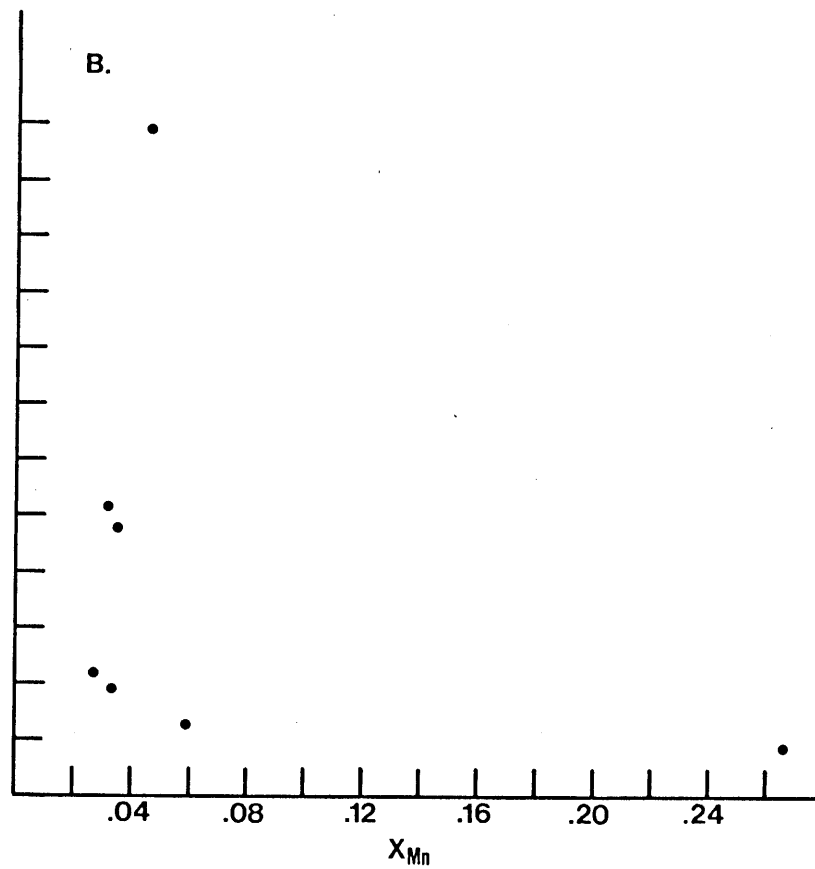
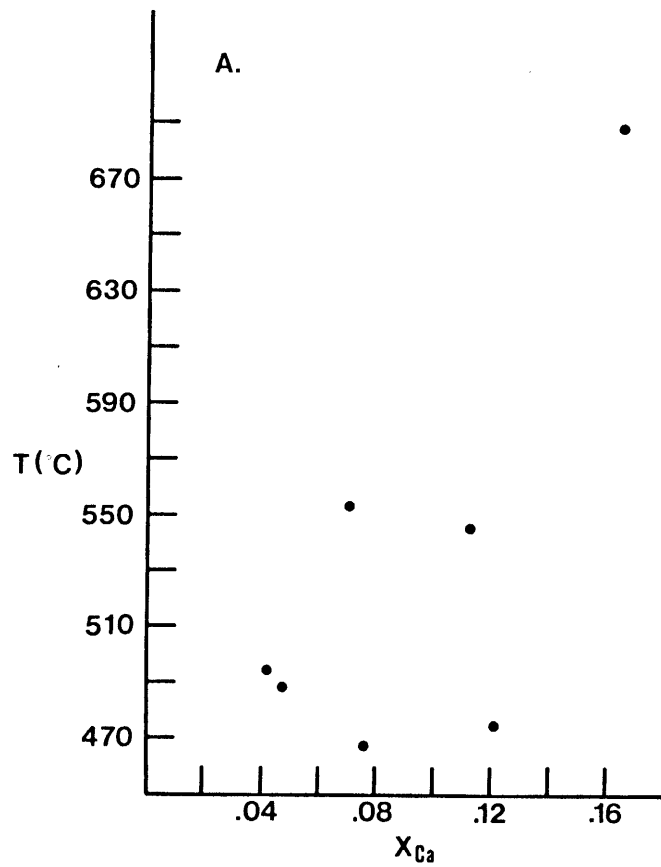
f.



g.







PART IV

STRUCTURAL EVOLUTION OF AN A-TYPE SUBDUCTION ZONE, LOFOTEN-ROMBAK AREA,
NORTHERN SCANDINAVIAN CALEDONIDES

STRUCTURAL EVOLUTION OF AN A-TYPE SUBDUCTION ZONE, LOFOTEN-ROMBAK AREA,
NORTHERN SCANDINAVIAN CALEDONIDES

ABSTRACT

The climactic phase of the Caledonian orogeny in Scandinavia involved collision of the Baltic and Greenland cratons in late Ordovician (?) to Silurian time. We infer that the collision resulted in large-scale subduction of the leading edge of the Baltic craton beneath an "Andean-type" Greenland continental margin. Deep erosional levels in the Lofoten-Rombak area, Norway-Sweden (~ 69°N) permit direct examination and evaluation of the structural evolution of a continental or A-type subduction zone. The early stages of collision involved en bloc underthrusting of the continental margin to depths of at least 30 km. During this process, deformational effects in the lower plate were restricted to its upper few hundred meters. Ultimately, en bloc A-type subduction should be limited by buoyancy effects. As convergence continued, the lower plate became involved in a series of imbricate thrusts with the same vergence as the initial subduction zone. The temporal and spatial relationships between these basement-involved thrusts are similar to those observed in foreland fold and thrust terrains. Field and geophysical data bearing on lower plate behavior elsewhere in the Caledonides and in other collisional orogens suggest that the structural features observed in the Lofoten-Rombak area may be generally characteristic of A-type subduction in continent-continent collisional settings.

INTRODUCTION

Foreland fold and thrust belts are undoubtedly the best structurally understood portions of the world's orogens. This is largely a consequence of the hydrocarbon potential of these terrains, and the integration of surface mapping with drillhole and seismic data has yielded extremely detailed, three-dimensional structural information. Armed with such data and a few critical geometric assumptions (Dahlstrom, 1969) it is possible to construct rigorously balanced cross sections which, in turn, allow palinspastic restorations of the external parts of orogenic belts to their pre-deformational configurations (Bally et al., 1966; Gwinn, 1970; Royse et al., 1975). As noted by Bally (1981), essentially all such quantitative reconstructions lead to the conclusion that the amount of original stratigraphic basement required for the sedimentary rocks involved in foreland deformation exceeds presently exposed structural basement. In other words, while the upper crust is involved in thin-skinned foreland deformation, considerable amounts of middle and lower crustal "basement" must be disposed of in some fashion.

The earliest published recognition of this problem appears to have been made by Otto Ampferer (1906; Ampferer and Hammer, 1911), who proposed, based on his work in the Eastern Alps, that large amounts of crustal material must have been underthrust to great depths, a process he termed "verschluckung." Ampferer's concept evolved into "subduction" through Andre Amstutz (1955; see White et al., 1970), and with the advent of plate tectonics it became worthwhile for Bally (1975) to differentiate between geologic situations where continental lithosphere was being

subducted (A-type or Ampferer subduction) and those where oceanic lithosphere was being subducted (B-type or Benioff subduction). The term "A-type subduction" (as we will use it) refers only to the removal of crustal material implied by the apparently inadequate amount of exposed stratigraphic basement for deformed cover sequences. It does not necessarily imply that the subducted continental crust ends up in the mantle, as is apparently the fate of oceanic crust in B-type subduction. We do not, however, exclude that possibility.

If we accept the apparent necessity for A-type subduction in many orogenic terrains, a number of basic questions arise. What becomes of the middle and lower crust after it has been "swallowed up", as Ampferer would have said? How much of this material can be subducted, and to what depths? What is its deformational response to orogenesis? In order to bring field evidence to bear on these problems, we have been mapping a transect across the northern Scandinavian Caledonides at approximately 69°N latitude where a deep erosional level and excellent exposures combine to provide an ideal setting for the study of collisional orogenesis at intermediate crustal levels. Our project is ongoing, and in a sense this is a progress report. We feel, however, that many of our observations thus far, and our conclusions based on them, have important implications concerning the internal zones of collisional orogens.

GEOLOGIC SETTING OF THE LOFOTEN-ROMBAKEN TRANSECT

The Scandinavian and East Greenland Caledonides formed as a result of the early-to-mid-Paleozoic closing of the late Proterozoic(?)—early Paleozoic Iapetus Ocean which separated the Greenland and Baltic cratons (Dewey, 1969; Harland and Gayer, 1971; Gee, 1975). The climactic phase involved continent-continent collision between the two cratonic terrains and resulted in predominately east-verging structures in Scandinavia and predominately west-verging structures in eastern Greenland. Thus, the Scandinavian Caledonides represent the eastern portion of a two-sided orogenic belt (in the sense of Burchfiel and Davis, 1968) which was split as a result of the Cenozoic opening of the present-day North Atlantic (Talwani and Eldholm, 1977).

Archean and Proterozoic crystalline basement rocks occur in three distinct settings in the Scandinavian Caledonides (Fig.1). These are: (1) the stable Baltic foreland east of the orogen; 2) a belt of windows through the Caledonian nappe terrain which run roughly N-S along the Norway-Sweden international boundary; and 3) a discontinuously exposed Western Gneiss Terrain along the Norwegian coast. Autochthonous, pre-Caledonian stratigraphic cover sequences in the Baltic foreland and the fenster belt are strikingly similar, an observation which has led most workers to propose that the fenster belt represents a western continuation of the Baltic foreland beneath the Caledonian nappe terrain (see, for example, Hogbom, 1909; Gee, 1975). In similar fashion, stratigraphic cover in the Western Gneiss Terrain has been correlated with Baltic foreland sequences (e.g., Kautsky, 1953; Gee, 1975; Bartley, 1981b). It appears, then, that all three principal basement terrains in the

Scandinavian Caledonides are of Baltic Shield affinity and form a more or less continuous substratum for the Caledonian allochthon. This observation, coupled with predominantly eastward structural vergence in the Scandinavian Caledonides, has led to minimum estimates of several hundred kilometers for the amount of shortening recorded in the orogen (Tornebohm, 1896; Høgbom, 1909; Gee, 1978).

Our research in the Scandinavian Caledonides has centered on an area at approximately 69°N latitude (Fig. 2). Two distinct basement terrains occur in the area: the Lofoten-Vesterålen islands in the west, and the Rombak window in the east. A narrow band of complexly deformed, metasedimentary and metaigneous rocks lies between the two basement terrains, and it represents the main Caledonian allochthon at this latitude.

Basement lithologies exposed in the Lofoten-Vesterålen islands include: 1) Archean (~2700 my) migmatitic gneisses and early Proterozoic (~2100-1800 my) supracrustal rocks, both of which were affected by an ~1800 my granulite-upper amphibolite facies metamorphic event; 2) Svecofennian (~1800-1700 my) intrusions, predominantly the Raftsund mangerite; and 3) the ~1380 my Lodingen granite (Griffin et al., 1978). Two late Proterozoic cover sequences occur on the archipelago: the Austerfjord Group of Hakkinen (1977), exposed in central Hinnoy, and the Leknes Group of Tull (1978), exposed on the islands of Vestvågøy and Vaerøy. Mica schists, amphibolites, quartzites, and marbles of the Austerfjord Group were apparently deposited subsequent to the ~1800 my high-grade metamorphic event and were intruded by the Lodingen granite (Hakkinen, 1977). The Leknes Group is lithologically similar to the Austerfjord Group, but has been assigned an age of 1140 ± 135 my based on

Rb-Sr whole-rock analyses (Griffin et al., 1978). The Leknes Group may have been subjected to kyanite-grade metamorphism during the interval 900-1200my based on ^{40}Ar - ^{39}Ar , K-Ar, and Rb-Sr biotite ages (Tull, 1978; Griffin et al., 1978), although complexities in the isotopic systematics make interpretation of these ages uncertain.

On eastern Hinnoy, the Lofoten-Vesteralen basement terrain is unconformably overlain by a transgressive quartzite, schist and marble sequence which was described and named the Storvann Group by Bartley (1981b). Similarities between this sequence and basal transgressive sequences on the Baltic foreland at this latitude (Vogt, 1967) have led Bartley (1981b) to propose that the Storvann Group represents the westward extension of the late Precambrian-early Paleozoic stratigraphic sequence developed on the stable Baltic platform prior to the Caledonian orogeny.

The Lofoten-Vesteralen terrain continues onto the Norwegian mainland in the form of large, monotonous tracts of the Tysfjord granite gneiss of Foslie (1941) and other subordinate rock types. There have been no isotopic age determinations for any of these rocks. Autochthonous and parautochthonous Storvann Group lithologies can be traced discontinuously from their type area on eastern Hinnoy onto the mainland at least as far southeast as the Indre Tysfjord (Figure 2; Tull et al., in press ; Bartley, in preparation).

Basement lithologies within the Rombak window include an older sequence of intermediate metavolcanics and metasedimentary rocks intruded by various gabbroic, syenitic and granitic plutons (Vogt, 1942; Gustavson, 1974). The predominant lithology along the western margin of the window is the Rombak granite gneiss which has yielded the only isotopic age obtained

to date for a Rombak window lithology: 1707 ± 40 my (Rb-Sr whole-rock isochron; Heier and Compston, 1969). Erosional remnants of the Caledonian stratigraphic cover of these basement rocks occur at places within the window (Vogt, 1942; Kulling, 1964; Tull et al., in press). This sequence includes basal conglomerates and quartzites which have been correlated with autochthonous Cambrian "Hyalolithus Zone" sediments in the Baltic foreland (Vogt, 1918; Kulling, 1964).

The main Caledonian allochthon at this latitude is composed of an assortment of middle amphibolite facies metasedimentary and metaigneous rocks. The lithologic character and structural complexity of this terrain has been described in detail elsewhere (Bartley, 1981a, in press; Hodges, in preparation; Tull et al., in press). Of particular interest here is that rocks of probable oceanic affinity occur in this allochthon. These include: the Stangnes Group of Bartley (1981a) on eastern Hinnoy, which consists of banded amphibolites and isotopically primitive, tonalitic to trondhjemitic gneisses; and the Rauvatn complex (Hodges, in preparation) occurring between Aefjord and Sitasjaure, which is a tectonic melange involving amphibolites, trondhjemites, marbles and serpentized peridotites.

The band of Caledonian allochthonous rocks is narrowest immediately east of Aefjord, where only 15-20 km separates exposures of Tysfjord granite gneiss in the Aefjord culmination from exposures of Rombak granite gneiss along the western margin of the Rombak window (Figure 2). Vogt (1942) and Gustavson (1966) remarked on the striking similarity between the Rombak and Tysfjord granite gneisses in hand specimen and thin section; even relatively unusual accessory minerals such as fluorite are common to both lithologies. Moreover, the basal portions of the

autochthonous Storvann Group in the Lofoten-Vesteralen-Aefjord terrain closely resemble the tectonic remnants of the stratigraphic cover sequence in the Rombak window. We conclude, therefore, that the basement terrains include correlative lithologies, although we will argue in the next section that a thrust fault of probable major proportions separates the two.

BASEMENT-COVER RELATIONSHIPS

We have studied the structural relationships between the main Caledonian allochthon and the Lofoten-Vesteralen-Aefjord-Rombak basement terrain in three areas: in eastern Hinnoy, in the Aefjord culmination, and along the western margin of the Rombak window near Sitasjaure.

Eastern Hinnoy

Two generations of Caledonian thrusting are apparent on eastern Hinnoy. The Stangnes and Tjeldsund thrusts (shown on Figure 3a) are of the first generation, while the Austerfjord and Vikeland thrusts are of the second.

The Stangnes thrust, emplacing Stanges Group lithologies on the autochthonous Storvann assemblage, is concordant on outcrop scale but discordant on a regional scale as lower plate Storvann Group members are truncated along strike. A zone of tectonic slivers of calcareous and pelitic schist, marble and amphibolite often occurs immediately subjacent to the thrust. The affinity of these lithologies is not always clear, although components of both the main Caledonian allochthon and the Storvann Group appear to be present. Stangnes Group amphibolites immediately above the thrust exhibit a well-defined, blastomylonitic texture which becomes progressively protomylonitic to granoblastic

structurally upward. This mylonitic cleavage is parallel to non-mylonitic S_2 penetrative schistosity away from the thrust, and, in the absence of evidence for transposition of either of the two cleavages by the other, the Stanges thrust has been assigned a D_2 age.* This conclusion is further supported by the apparent lack of metamorphic discontinuity across the thrust, since textural relationships indicate that staurolite-kyanite grade regional metamorphism was at least partly synkinematic with respect to S_2 cleavage development in the area.

The Tjeldsund thrust forms the upper boundary of the Stanges Group and carries calcite marbles, pelitic schists and conglomerates of the Salangen Group (a structurally higher unit within the Caledonian allochthon) in its upper plate. This thrust appears to cut structurally downward passing from north to south on eastern Hinnoy until Salangen Group lithologies are juxtaposed directly onto Storvann Group lithologies. Structural relationships along the Tjeldsund thrust are similar to those described above for the Stanges thrust, and the two thrusts are considered to have developed approximately synchronously.

* In this paper, we will use the convention that the number assigned to a cleavage or fold phase corresponds to the deformational event during which it was formed. In mapping the Aefjord-Sitas area, Hodges (in preparation) recognized deformational phases which are not manifested on eastern Hinnoy (Bartley, 1981a; in press). Thus, D_1 in the Aefjord-Sitas area does not correspond to D_1 on eastern Hinnoy. In order to avoid confusion, we will adopt the sequential designation used by Hodges (in preparation) throughout this paper.

Where initially described by Hakkinen (1977), the Austerfjord thrust places Archean gneisses upon Austerfjord Group lithologies and the Lodingen granite which intrudes them. The Austerfjord thrust is generally characterized by this juxtaposition on eastern Hinnoy, although the Austerfjord Group is occasionally cut out altogether and the thrust places Precambrian gneisses on Precambrian gneisses. Estimates of the age and amount of displacement for the thrust hinge on the structural relationships observed near Fjelldal (Fig. 3a). Here the Austerfjord thrust places Precambrian granite gneiss and remnants of its autochthonous-parautochthonous Storvann Group cover onto overturned Austerfjord Group lithologies. Salangen Group lithologies in the upper plate of the Tjeldsund thrust occur beneath the Austerfjord Group at this locality, the immediate lower plate of the Austerfjord thrust here forming the overturned limb of a recumbant F_3 isocline cored by Salangen Group lithologies (Fig. 3b). A few kilometers to the south, the Storvann Group and its subjacent stratigraphic basement appear beneath the Salangen Group in the upright lower limb of the fold. Thus, Storvann Group lithologies appear in both the upper and lower plates of the Austerfjord thrust, suggesting considerably less displacement for this thrust than for the Stangnes or Tjeldsund thrusts which juxtapose rocks of drastically different tectonic provenance (oceanic vs. continental). The involvement of Salangen Group lithologies in the Austerfjord thrust also suggests that its development postdated the D_2 Tjeldsund thrust which emplaced the Salangen Group upon the Lofoten-Vesteraleen terrain. Bartley (1981, in press) presents arguments that the Austerfjord thrust is of D_3 age, and was intimately associated with large, southeast-vergent, F_3 recumbent folds which involve basement rocks.

The Vikeland thrust places Precambrian basement gneiss on basement gneiss and on Storvann Group lithologies and has also been assigned a D₃ age by Bartley (1981a). No metamorphic discontinuity is associated with either the Austerfjord or Vikeland thrusts, and the relationships between D₃ tectonite fabrics and metamorphic mineral growth (e.g., inclusion trails in garnet porphyroblasts curve into S₃ in the surrounding matrix) developed synmetamorphically. Both structures are characterized by zones of mild to very intense, high-temperature mylonitization from a few meters to several hundreds of meters thick; in general, mylonitic fabrics extend much further away from the thrust surface in the upper plate than in the lower. The mylonite zone along the Vikeland thrust sometimes shows a prominent stretching lineation bearing S64E, corroborating evidence based on separation angle analysis of small-scale F₃ folds and on the vergence of large-scale F₃ folds that D₃ transport directions were southeasterly (Bartley, in press).

Both Hakkinen (1977) and Bartley (1982) have noted that Caledonian fabrics decrease rapidly in intensity passing structurally downward into the Lofoten-Vesteralen basement. Below a few hundred meters structurally beneath basement-cover contacts on eastern Hinnoy, essentially no structural vestiges of the Caledonian orogeny are present. This is most strikingly illustrated on Middagstind (Fig. 3a) where a contact metamorphic hornfels texture developed around the ~1720 my Middagstind quartz syenite was scarcely affected by Caledonian deformation (Bartley, 1981c). The preserved Precambrian contact aureole lies no more than 500m structurally below the base of the Caledonian allochthon. Bartley (in press) suggests that the involvement of the uppermost levels of the Lofoten-Vesteralen terrain in Caledonian structures was catalyzed by

volatiles released through dehydration reactions in the adjacent stratigraphic and tectonic cover. Thus, the lack of involvement of deeper portions of the basement may be a consequence of the limited availability of fluids at these levels.

The Aefjord Culmination

The Aefjord culmination (Fig. 2) is an elongate dome produced by interference between ~E-W trending F_4 and ~N-S trending F_6 folds (Hodges, in preparation). As a result of this doming, the basement-cover contact in this area is continuously exposed over a distance of 20-30 km around the edges of the culmination. Our research to date has focused on the northern and eastern segments of this contact.

The basement-cover contact in this area is a thrust fault which we call the Forsa thrust after a small village on the eastern shore of Aefjord (Fig. 4). The Forsa thrust emplaces metasedimentary and metaigneous rocks of the main Caledonian allochthon (the Narvik Group of Vogt, 1942, and Gustavson, 1966) upon the Aefjord basement terrain. Along most of its mapped length, the lower plate of the Forsa thrust is composed of monotonous Tysfjord granite gneiss. Near Forsa, however, an incomplete, parautochthonous section of Storvann Group is preserved between the Tysfjord granite gneiss and the Narvik Group rocks of the main Caledonian allochthon.

During the course of mapping in the Aefjord area, Hodges (in preparation) subdivided the Narvik Group into five tectono-stratigraphic units. A variety of these units form the hanging wall of the

thrust along its extent. This evidence for regional discordance is extremely important because the basement-cover contact is invariably concordant on a local scale. The thrust is absolutely knife-sharp and subparallel to a penetrative S_2 schistosity in upper plate lithologies, and this cleavage greatly intensifies over a distance of 10m approaching the thrust. This same phenomenon is observed in the lower plate near Forsa where it is composed of Storvann Group metasedimentary rocks. Where Tysfjord granite gneiss forms the lower plate, a prominent blastomylonitic cleavage is developed immediately beneath the thrust. Textures become more protomylonitic passing structurally downward, and only a penetrative cleavage, essentially non-mylonitic, remains 30m below the thrust.

There is no evidence for a metamorphic discontinuity across the Forsa thrust. Hornblende mineral separates from metabasites within the Narvik Group and an amphibolite dike cutting the Tysfjord granite gneiss near Forsa yield statistically identical K-Ar ages (449 ± 19 m.y.; Hodges et al., in preparation), suggesting that both the upper and lower plates of the Forsa thrust experienced similar, late-metamorphic cooling histories. Since the Forsa thrust is everywhere parallel to the S_2 cleavage in the main Caledonian allochthon and textural evidence suggests that major porphyroblast growth was approximately synchronous to S_2 cleavage development, Hodges (in preparation) interprets the Forsa thrust to be a synmetamorphic D_2 structure.

Western Edge of the Rombak Window

Along the western edge of the Rombak window, a zone of tectonic slices is interposed between Narvik Group lithologies and basement

lithologies of the Rombak window (Fig. 4). This schuppenzone has been termed the Storriten Complex by Hodges (in preparation) for excellent exposures on the mountain Storriten along the Swedish-Norwegian border. The lower boundary fault of the Storriten Complex was named the Frostisen thrust for a large glacier near Skjomen; whereas the upper boundary fault was named the Mereftasfjell thrust for a mountain immediately west of Storriten (Hodges, in preparation).

The Storriten Complex consists of large plates or slabs of granitic gneisses in a phyllonitic matrix. The gneissic schuppen invariably exhibit a protomylonitic to blastomylonitic cleavage which is generally strongest near their margins. Often a well-developed stretching lineation bearing $\sim N58^{\circ}W$ is associated with the mylonitic cleavage. Many of the gneissic schuppen contain accessory fluorite and strongly resemble the Rombak and Tysfjord granitic gneisses of the basement terrain, although other schuppen mapped by P.C Crowley (personal communication, 1981) along the southern rim of the window bear little resemblance to the Tysfjord-Rombak gneisses and are of uncertain provenance. Because of the granitic character of the schuppen and the observation that many of them are probably Rombak or Tysfjord granite gneiss, we believe that these are tectonic slivers of Baltic cratonal basement.

The matrix for the basement schuppen in the Storriten Complex is predominately a graphitic, phyllitic schist. Occasionally, irregularly shaped stringers of light to dark gray, fine-grained orthoquartzite occur in the schistose matrix. Three penetrative fabrics occur in the Storriten Complex matrix: 1) an axial planar, S_2 cleavage that is preserved only as intrafolial folds in S_3 ; 2) an axial planar, S_3 cleavage which strongly transposes S_2 ; and 3) a slightly anastomosing phyllonitic cleavage that

cross-cuts and in places transposes both S_3 and S_2 . The acute angle between the phyllonitic cleavage sets is seldom as great as 30° , and the bisectrix of this angle is subparallel to the gently westward dipping mylonitic cleavage in the basement schuppen. Similarity in the orientations of the mylonitic and phyllonitic cleavage suggests that the two formed roughly synchronously.

The above description of the Storriten Complex is strikingly similar to that given by Kautsky (1953) for the Akkajaure complex in its type area south of the Rombak window. Both the Storriten and Akkajaure complexes are probably also correlative with the "middle and lower thrust rocks" of Kulling (1964). Kautsky (1953) and Kulling (1964) pointed out the strong similarities between metasedimentary rocks in the schuppenzone and those of the Hyolithus zone in the Baltic foreland. This observation is supported by an occurrence of Lower Cambrian faunal assemblages in the "lower thrust rocks" near Tornetrask reported by Kulling (1964). It is tempting to correlate the graphitic matrix of the Storriten Complex with the Middle (?) Cambrian organic-rich alum shales described by Kulling (1964) from the upper part of the Hyolithus zone. If valid, this correlation may have important tectonic implications, since Cambrian black shales often form the frontal decollement along the easternmost edge of the Scandinavian Caledonides (Gee, 1980).

The Frostisen thrust places the Storriten Complex onto Rombak granite gneiss in the Sitasjaure area. Reconnaissance mapping near Frostisen reveals that a five to ten meter thick remnant of autochthonous Dividal Group basal quartzite forms the foot wall of the Frostisen thrust in that area. Other than the observation that the thrust must cut down section between Frostisen and Sitasjaure in order to eliminate the

Dividal Group quartzite, discordance is difficult to prove. The Frostisen thrust is everywhere subparallel to the schuppenzone phyllonitic cleavage, which becomes slightly more intense near the thrust. Where quartzite forms the lower plate of the thrust it is a protomylonite. Where Rombak granite gneiss forms the lower plate, it exhibits a conspicuous augen texture and a moderately well-developed protomylonitic cleavage. The augen texture dies out within less than 10m passing structurally downward. Beneath this level, a penetrative cleavage is often difficult to distinguish. Ductile shear zones, two to ten centimeters wide, are common in the Rombak granite gneiss basement away from the thrust. The strike of these shear zones is roughly parallel to that of the Frostisen thrust, although their dip is generally much steeper ($>60^{\circ}W$) than that of the thrust ($<30^{\circ}W$). The significance of these features or their age with respect to the Frostisen thrust are as yet unclear. J. Tull and A. Andresen (in Tull et al., in press) have described similar shear zones from the basement on the north side of the Rombak window, which are truncated by the apparent continuation of the Frostisen thrust. Locally, along the western edge of the Rombak window, the shear zones dip more shallowly near the Frostisen thrust. If this reflects rotation of pre-existing structures during thrusting, a general SE direction of movement is indicated for the Frostisen thrust plate.

The Mereftasfjell thrust carries Narvik Group lithologies onto the Storriten Complex. Exposures of this thrust are relatively poor in the Sitasjaure area, and although the lower plate phyllonitic cleavage generally intensifies approaching the thrust, outcrops of the Narvik Group lithologies immediately above the thrust are insufficient to say anything

definitive about tectonite fabric development in these rocks. The thrust is subparallel to the phyllonitic cleavage in the Storriten Complex but noticeably discordant to the predominant S_2 cleavage in the upper plate.

The Mereftasfjell thrust marks an important metamorphic discontinuity: upper plate lithologies were metamorphosed to middle amphibolite facies (kyanite grade), whereas rocks of the Storriten Complex were metamorphosed to lower amphibolite facies (garnet grade). Conversely, there is no evidence for a metamorphic break across the Frostisen thrust, although lithologies with mineral assemblages which might be diagnostic of metamorphic grade are absent in the immediate lower plate.

Parallelism between the Frostisen and Mereftasfjell thrusts and mylonitic and phyllonitic cleavages in the Storriten Complex suggest that all were developed more or less synchronously. As previously mentioned, the phyllonitic cleavage in the Storriten Complex crosscuts and transposes the S_3 axial planar cleavage. There is no evidence for folding of the phyllonitic cleavage by -E-W-trending, F_4 cross folds, although it is commonly folded by later, -N-S-trending folds. Thus, movement along the Mereftasfjell and Frostisen thrusts and development of related fabrics occurred either synchronously with F_4 crossfolding or between development of the E-W and N-S fold sets. The first possibility requires that F_4 axes trend at low angles to the southeasterly transport direction of the Mereftasfjell and Frostisen thrusts inferred from the orientations of stretching lineations in Storriten Complex basement schuppen. This geometric relationship has been reported elsewhere in the Scandinavian Caledonides (e.g., Hansen, 1971), although it is generally

associated with structures formed early in the deformational sequence. We tentatively assign the Mereftasfjell and Frostisen thrusts and the development of the schuppenzone to a unique event (D₅) while recognizing the possibility of a D₄ age.

Relationships Between the Rombak and Aefjord Basement-Cover Contacts

Previous interpretations of the region between the Lofoten-Vesteralen islands and the Rombak window have held that the main Caledonian allochthon occupies a broad synclorium between the two basement terrains which are structurally continuous at depth (e.g., Gustavson, 1974). In this older model, basement-cover thrusts along either side of the allochthon are correlative. The results of detailed mapping in the Aefjord-Sitasjaure area require more complicated structural relationships.

The Forsa thrust is a D₂ structure; it is everywhere concordant with the S₂ penetrative cleavage and does not represent a metamorphic discontinuity. The Mereftasfjell and Frostisen thrusts are interpreted as D₄ structures, but are certainly post-D₃; both are parallel to the phyllonitic cleavage in the Storriten Complex which crosscuts and transposes S₃, and the Mereftasfjell thrust is a significant metamorphic break. It is inescapable that the basement-cover relationships along the western edge of the Rombak window developed after those in the Aefjord culmination.

The Mereftasfjell and Frostisen thrusts dip generally less than 45° to the west where exposed. Mapping by Hodges (in preparation) between Aefjord and Sitasjaure shows that neither these thrusts nor the Storriten Complex resurface between the Rombak window and the Norwegian coastline.

This strongly suggests that both the Frostisen and Mereftasfjell thrusts root into the Tysfjord-Rombak basement terrain beneath the main Caledonian allochthon. The alternative explanation, that the Mereftasfjell-Frostisen thrust complex is simply a post-metamorphic reactivation of the Forsa thrust, seems difficult to reconcile with the total lack of evidence for post-metamorphic movement or lower plate imbrication along the Forsa thrust.

The easterly dip of the Forsa thrust beneath the main Caledonian allochthon suggests that it must interact at depth with the Mereftasfjell and Frostisen thrusts. The simplified geologic cross section in Figure 5 illustrates our current conception of basement-cover relationships beneath the Aefjord-Sitasjaure area. Note that this cross section is only semi-quantitative; non-cylindrical folding in plastically deformed terrains renders large-scale downplunge projections or attempts at rigorous balancing of cross sections virtually worthless. Undulations in the Forsa, Mereftasfjell and Frostisen thrusts shown in Figure 5 are the results of constraining the Forsa thrust to be subparallel to S_2 everywhere beneath the allochthon, and the Frostisen and Mereftasfjell thrusts to be subparallel to the phyllonitic cleavage in the Storriten Complex. These assumptions are clearly open to debate, but the gross geometry shown in Figure 5, with the Mereftasfjell-Frostisen thrust complex truncating the Forsa thrust, must be correct.

POSITION OF THE LOFOTEN-ROMBAK AREA WITHIN THE OROGEN

Table 1 summarizes the characteristics of and temporal relationships between major thrust faults in the region. At this point, it is useful to ask: what was the structural position of the Lofoten-Rombak area within the Caledonian orogen?

The Scandinavian Caledonides record the early to middle Paleozoic closing of the Iapetus Ocean and subsequent continent-continent collision between the Baltic and Greenland cratons. The tectonic evolution of the orogen was long and complicated (see Gee, 1975; Sturt *et al.*, 1978; and Stephens and Gee, 1981, for examples), but two general statements can be made that are of great importance to our interpretation of the Lofoten-Rombak area.

The first is that the Baltic continental margin was the site of passive platformal to miogeosynclinal sedimentation from Cambrian to Silurian time (e.g., Bassett, 1981; Bruton and Lindstrom, 1981; Gee, 1981). Evidence for this at the latitudes of our transect include the Storvann and Dividal Groups in the Lofoten-Rombak area and the Hyolithus zone sequences on the Baltic foreland.

The second point is that the climactic, continent-continent collisional event was accomplished through underthrusting of the passive, "Atlantic-type" Baltic continental margin beneath an active, "Andean-type" Greenland continental margin. The argument for a continental arc in eastern Greenland rests on the widespread occurrence of Caledonian calc-alkaline plutons in the East Greenland Caledonides which clearly intrude pre-Caledonian basement lithologies (Coe, 1975; Steiger *et al.*, 1979; Henkixsen, 1981). Direct evidence for large-scale subduction of

Baltic craton is provided by the occurrence of eclogite facies metamorphic assemblages of apparent Caledonian age (based on Sm-Nd, garnet--clinopyroxene mineral isochrons) occurring within Western Gneiss Terrain crystalline basement in southern Norway (Brueckner and Griffin, 1980). Geothermometry and geobarometry based on eclogite mineral equilibria suggests progressively higher equilibration pressures and temperatures from east to west in the Western Gneiss Terrain of southern Norway, consistent with west-dipping subduction of the terrain beneath eastern Greenland (Griffin *et al.*, 1981).

This general tectonic scheme is not seriously modified by recent paleomagnetic evidence for as much as 2000km of left-lateral strike-slip movement between the North American - Greenland and Baltic cratons after the collision (Kent and Oppdyke, 1978; Van der Voo and Scotese, 1981). The belt of middle Paleozoic plutons along the eastern margin of the North American -Greenland craton extends from Greenland down the entire length of the Appalachians. We are not alone in suggesting that these plutons represent an ancient Andean-type margin (Rodgers, 1981), or at least a magmatic arc built on North American - Greenland continental crust (Cooke *et al.*, 1979).

Our mapping in the Lofoten-Rombak area shows that primary emplacement of the nappe complexes of the main Caledonian allochthon onto the Baltic craton was synmetamorphic. Caledonian metamorphic assemblages on eastern Hinnoy and the Norwegian mainland are indicative of relatively high pressures and temperatures of metamorphism; garnet-kyanite-biotite assemblages are common in rocks of pelitic composition. Garnet-biotite

geothermometry and garnet-plagioclase-kyanite-quartz geobarometry constrain peak metamorphic conditions in the Aefjord area to have been at least 650°C and 8kb. (Hodges and Royden, in preparation). Assuming reasonable rock densities and lithostatic pressures, these data indicate that nappe emplacement in the area occurred at depths in excess of 30 kilometers.

The presence of tectonic remnants of autochthonous, early Paleozoic stratigraphic cover sequences beneath the main Caledonian allochthon suggests that the present erosional level in the Lofoten-Rombak area exposes the basal portions of the Caledonian nappe complex and the uppermost Baltic continental crust. We conclude that the relationships observed in this area between structural basement and cover were developed during underthrusting of the passive, Baltic continental margin beneath the Greenland "Andean-type" margin, and that the resulting structures reflect how upper continental crust responds to A-type subduction to intermediate crustal depths (>30km).

STRUCTURAL EVOLUTION OF AN A-TYPE SUBDUCTION ZONE - AN INTERPRETIVE MODEL

Based on our interpretation of the structural position of the Lofoten-Rombak area within the Caledonian orogen and our structural data, we can make the following observations.

The earliest structures clearly attributable to A-type subduction in this area are the Stangnes, Tjeldsund, and Forsa thrusts which record en bloc underthrusting of the Baltic craton beneath a complexly deformed composite of metasedimentary and metaigneous units of variable provenance: the main Caledonian allochthon. Mapping in the nappe complex between

Aefjord and Sitasjaure suggests that principal stacking of the nappe sequence within the main Caledonian allochthon occurred prior to underthrusting of the Baltic structural basement. This early stacking may be the result of intra-Iapetus plate margin interactions, for which there is direct evidence in the central Scandinavian Caledonides in the form of probable ensimatic island arc components in the Koli nappe sequence (e.g., Stephens, 1981), or may have developed along the "Andean-type" margin of Greenland during the final closure of Iapetus. In the latter scenario the nappe complex might be considered an A-type analog of an accretionary wedge in a B-type subduction zone.

Tectonic overlap requires at least 250 km of continental subduction, and metamorphic phase equilibria suggest that Baltic Shield lithologies were taken to depths of at least 30km as a result. Tectonic transport of this magnitude is not a new concept in Scandinavian tectonics, and it is a tribute to the unique structural level of exposure in the Scandinavian Caledonides that Tornebohm (1896) suggested similar thrust transport distances nearly a hundred years ago. It is perhaps more surprising to find that Caledonian structures and fabrics extend only a few hundred meters structurally downward into the underthrust plate. It appears that the leading edge of the Baltic craton behaved as a more or less rigid, structurally continuous block during the early stages of A-type subduction. Only the uppermost portions of the block actively participated in Caledonian folding and thrusting, a process which may have been triggered by an influx of volatiles produced by prograde Caledonian metamorphism of adjacent stratigraphic and structural cover (Bartley, 1982).

During subduction of the Baltic plate, much of its pre-Caledonian stratigraphic cover was stripped away, leaving only scattered tectonic remnants beneath the nappe complex. Portions of the detached material may have been subducted along with the Baltic craton, becoming part of the high-grade nappe complex. The remainder may have remained at higher levels in the orogen to form "Helvetic-style" sedimentary nappes or "Jura-style" foreland folds and thrusts.

Theoretically, the amount of continental crust that can be subducted is limited by its buoyancy (Molnar and Gray, 1979). As en bloc subduction effectively ceased, convergence was accommodated in part by basement-involved thrusts and recumbent folds in the downgoing plate. The earliest structures of this type in the Lofoten-Rombak region are the Austerfjord and Vikeland thrusts and related D₃ structures on eastern Hinnoy. With continued convergence, basement-involved structures stepped progressively eastward, as evidenced by the D₅ age of the Frostisen-Mereftasfjell thrust complex.

Our conceptual model of the development of an A-type subduction zone, based on structural relationships in the Lofoten-Rombak area, is illustrated by a series of cartoons in Figure 6. Most of the convergence is accommodated by en bloc underthrusting of the lower plate. Further convergence results in intraplate deformation of the downgoing slab which steps progressively further into the interior of the plate with time. The temporal and spatial relationships between the basement-involved structures are strikingly similar to those deduced from detailed studies in foreland fold and thrust belts (e.g., Royse et al., 1975). In particular, faults become younger in the direction of tectonic transport

of the upper plates relative to the lower plates, and the Frostisen-Mereftasfjell thrust complex clearly ramps from lower to higher tectonic levels in the direction of transport. We might extend the foreland fold and thrust analogy to suggest that many of the coastal gneiss domes in Norway, which have classically been attributed to basement diapirism (e.g., Ramberg, 1981), might be basement-cored ramp anticlines developed during imbrication of the downgoing Baltic plate. For example, this is a viable mechanism for producing the Aefjord culmination.

GENERAL APPLICABILITY OF THE MODEL

The conceptual model for A-type subduction which we have presented is based on a relatively small-scale study in one collisional orogen. Its applicability to similar tectonic environments elsewhere is an open question, although structural relationships consistent with our model have been widely reported in the geologic literature.

Our model is generally consistent with an increasing body of excellent field data from the central Scandinavian Caledonides (Gee, 1975, 1978; Dyrelus et al., 1980). In fact, Figure 6 of this paper has many features in common with Figures 9-11 in Gee (1975). Elsewhere in the Caledonides, Coward (1980) notes the propagation of basement-involved thrusts in the direction of tectonic transport in the Moine thrust zone of N.W. Scotland, and follows Elliot and Johnson (1978) and Barton (1978) in drawing analogies between this process and the development of foreland fold and thrust belts. COCORP deep seismic reflection profiling in Georgia, North Carolina and Tennessee reveal a series of subhorizontal reflectors extending beneath much of the crystalline southern Appalachians (Cook, et al., 1979). If the prevalent interpretation of these reflectors

as autochthonous, Cambrian-Ordovician platformal sequences is correct, then the COCORP data can be taken as evidence for large-scale, en bloc A-type subduction of the North American cratonal margin and portions of its pre-Caledonian stratigraphic cover.

Matte and Burg (1981) interpret the Variscan arc of western Europe as the result of continent-continent collision, and argue for a transition from en bloc continental subduction to lower plate imbrication with continued convergence. In the Western and Central Alps, where large-scale A-type subduction is a geologic necessity (Trumpy, 1963), available data points to a northward-progressing imbrication of the downgoing European plate (sensu lato) beginning with Eocene-Oligocene thrusting of the Pennine zone beneath the Austroalpine nappe complex (Trumpy, 1975), and culminating in Miocene subduction of the stratigraphic basement of the cover sequences involved in the Helvetic nappes (Trumpy, 1969; Milnes, 1978).

In the Dinarides and Hellenides of the Eastern European alpine system, late Cretaceous (?) - Paleocene collision between the Apulian and Rhodopian continental fragments resulted in A-type subduction of the Apulian plate, and imbrication of the downgoing plate proceeded from the internal (eastern) to the external (western) portions of the belt during Eocene and Miocene time (Burchfiel, 1980). The Himalaya provide one of the few opportunities to observe a presently active collisional orogen in the latter stages of its development. The Himalayan orogen apparently records the closing of Tethys along a north-dipping B-type subduction zone beneath a Transhimalayan "Andean-type" continental margin, and subsequent

continent-continent collision between India and Asia beginning approximately 45 m.y. ago (Dewey and Bird, 1970; Le Fort, 1975). The collision resulted in A-type subduction of the Indian plate beneath Asia along what is now the Indus-Tsangpo Suture Zone (Gansser, 1964). The amount of continental crust subducted along this boundary is completely unknown. The three-dimensional velocity structure of the Pamir-Hindu Kush region as deduced from inversion of P and S wave arrival times reveals a low velocity region which envelopes the Pamir-Hindu Kush seismic zone at depths of ~70-150 km (Roecker, 1982). Roecker suggests that this low velocity region represents continental crust, implying that the leading edge of the Indian plate was subducted to depths of at least 150 km beneath Asia during continent-continent collision.

After the initial collision between India and Asia, continued convergence appears to have been accommodated in part by southward-stepping, basement-involved thrusts within the Indian plate (Le Fort, 1975). The northernmost of these is the Main Central Thrust, along which the Lesser Himalaya sequences underthrust those of the Greater Himalaya (Gansser, 1964). Le Fort (1975) argues for synchronicity between development of the Main Central Thrust and Miocene regional metamorphism in the area. Further south, the Main Boundary Thrust represents underthrusting of the Siwalik molasse and its stratigraphic basement beneath the Lesser Himalaya. Translation along the Main Boundary and associated thrusts must post-date Miocene-Pleistocene deposition of the Siwaliks, and these thrusts appear to be seismically active (Fitch, 1970; Le Fort, 1975).

Consideration of available geologic and geophysical data leads us to

conclude that large-scale, A-type subduction is a common (if not universal) process in the construction of continent-continent collisional orogens. In many examples, initial subduction along a zone transitional from B-type to A-type is followed by progressive imbrication of the lower plate along subsidiary A-type thrusts.

A-TYPE SUBDUCTION AND THE NATURE OF THE LOWER LITHOSPHERE

Recognition of the importance of A-type subduction in continental tectonics leads to an important caveat concerning geochemical and geophysical studies of the lower lithosphere. The so-called "metamorphic cores" of many orogens may be partly or entirely allochthonous, overlying a lower crustal structural element which may be largely unaffected by the orogenic events recorded in the upper crustal nappes. The original lower crust and mantle lithosphere which formed the stratigraphic basement for these nappes may have been detached and largely or wholly subducted. Thus, the present-day structural basement for these nappes may bear little resemblance to their stratigraphic basement. It is clear, in these cases, that the trace element and isotope geochemistry of igneous rocks in the upper crustal nappes which are older than the A-type subduction event tell us nothing concerning the nature of the lower lithosphere currently beneath the nappes. However, geochemical studies can provide a wealth of information about the subducted lithosphere which would be otherwise unattainable. While geophysical studies can characterize the present-day lower crust and mantle lithosphere in these terrains, such data cannot be used to constrain the structural history of the overlying upper crustal nappes, nor their initial lithospheric basement.

CONCLUSIONS

We interpret major Caledonian structures in the Lofoten-Rombak transect as the results of A-type subduction of the Baltic craton beneath the Greenland craton in late Ordovician-Silurian time. Temporal and spatial relations between Caledonian structures suggest that the earliest stages of continent-continent collision involved underthrusting of a relatively coherent Baltic continental margin to depths of at least thirty kilometers, while the later stages involved imbrication of the Baltic craton along thrusts with the same sense of vergence as the original subduction zone. The intraplate thrusts appear to become younger and ramp upsection in the direction of tectonic transport (relative to the Baltic plate). These relationships are similar to those observed in upper crustal foreland fold and thrust belts. By analogy to those terrains, we suggest that many of the late-stage gneiss domes and basement windows in the Scandinavian Caledonides may be large-scale, basement-cored ramp anticlines developed as a result of the Baltic plate imbrications.

The developmental sequence of A-type thrusting deduced from the Lofoten-Rombak area may have applicability to other collisional orogens. Plate tectonic interpretations of the Appalachian, Variscan and Alpine-Himalayan chains often involve a sequence of thrust development similar to that required by field data in the Lofoten-Rombak transect. Oversimplifications in our model will no doubt become increasingly apparent as more data becomes available, but we feel that this same data will reinforce the tectonic importance of the process envisioned by Otto Ampferer so long ago.

REFERENCES

- Ampferer, O., Über das Bewegungsbild von Faltengebirgen, Austria, Jahrb. geol. Bundesant, 56, 539-622, 1906.
- Ampferer, O., and W. Hammer, Geologisches Querschnitt durch die Ostalper vom Allgau zum Gardasee, Jahrb. geol. Reichsanst., 61, 531-710, 1911.
- Amstutz, A., Structures Alpines: subductions successive dans l'Ossola, Acad. Sci. Paris Comptes Rendus, 241, 967-969, 1955.
- Bally, A.W., Ageodynamic scenario for hydrocarbon occurrences, Proc. Ninth World Petrol. Congr. Tokyo, 2, 33-44, 1975.
- Bally, A.W., Thoughts on the tectonics of folded belts, in Thrust and Nappe Tectonics, edited by K.R. McClay and N.J. Price, pp.13-32, Blackwell, Oxford, 1981.
- Bally, A.W., P.L. Gordy, and G.A. Stewart, Structure, seismic data, and orogenic evolution of Southern Canadian Rocky Mountains, Bull. Can. Pet. Geol., 14, 337-381, 1966.
- Bartley, J.M., Structural Geology, Metamorphism and Rb/Sr Geochronology of East Hinnoy, North Norway, Ph.D. Thesis, 263p., Massachusetts Institute of Technology, Cambridge, Massachusetts, 1981a.

- Bartley, J.M., Lithostratigraphy of the Storvann Group, east Hinnoy, north Norway, and its regional implications, *Norges geol. Unders.*, 370, 11-24, 1981b.
- Bartley, J.M., Field relations, metamorphism and age of the Middagstind Quartz Syenite, Hinnoy, north Norway, *Norsk geol. Tidsskr.*, 61, 237-248, 1981c.
- Bartley, J.M., Limited basement involvement in Caledonian deformation, Hinnoy, north Norway, and tectonic implications, *Tectonophysics*, 83, 185-203, 1982.
- Barton, C.M., An Appalachian view of the Moine thrust, *Scott. J. Geol.*, 14, 247-257, 1978.
- Bassett, M.G., Silurian stratigraphy and facies development in Scandinavia, *Terra Cognita*, 1, 34, 1981.
- Brueckner, H.K., and W.L. Griffin, Caledonian Sm/Nd ages of Norwegian eclogites, *Trans. Amer. Geophys. Union (EOS)*, 61, 389, 1980.
- Bruton, D.L., and M. Lindstrom, The Ordovician of Scandinavia, *Terra Cognita*, 1, 37, 1981.

- Burchfiel, B.C., Eastern European alpine system and the Carpathian orocline as an example of collision tectonics, Tectonophysics, 63, 31-61, 1980.
- Burchfiel, B.C., and G.A. Davis, Two-sided nature of the Cordilleran orogen and its tectonic implications, Internat. Geol. Congr, 23rd, Prague, Proc., 175-184, 1968.
- Coe, K., The Hurry Inlet granite and related rocks of Liverpool Land, East Greenland, Gron. Geol. Unders., 115, 1-34, 1975.
- Cook, F.A., D.S. Albaugh, L.D. Brown, S. Kauffman, J. Oliver, and R.D. Hatcher, Thin-skinned tectonics in the crystalline southern Appalachians, COCORP seismic reflection profiling of the Blue Ridge and Piedmont, Geology, 7, 563-567, 1979.
- Coward, M.P., The Caledonian thrust and shear zones of N.W. Scotland, Jour. Struct. Geol., 2, 11-17, 1980.
- Dahlstrom, C.D.A., Balanced cross sections, Can. J. Earth Sci., 6, 743-758, 1969.
- Dewey, J.F., Evolution of the Appalachian/Caledonide orogen, Nature, 222, 124-129, 1969.

Dewey, J.F., and J.M. Bird, Mountain belts and the new global tectonics, Jour. Geophys. Res., 75, 2625-2647, 1970.

Dyrelius, D., D.G. Gee, R. Gorbatshev, H. Ramberg, and E. Zachrisson, A profile through the central Scandinavian Caledonides, Tectonophysics, 69, 247-284, 1980.

Elliot, D., and M.R.W. Johnson, Discussion on structures found in thrust belts, J. geol. Soc. Lond., 135, 250-260, 1978.

Fitch, T.J., Earthquake mechanisms in the Himalayan, Burmese, and Andaman regions and continental tectonics in central Asia, Jour. Geophys. Res., 75, 2699-2709, 1970.

Foslie, S., Tysfjords Geologi, Norges geol. Unders., 149, 1-298, 1941.

Gansser, A., Geology of the Himalayas, Interscience, London, 289p., 1964.

Gee, D.G., A tectonic model for the central part of the Scandinavian Caledonides, Am. J. Sci., 275A, 468-515.

Gee, D.G., Nappe displacement in the Scandinavian Caledonides, Tectonophysics, 47, 393-419, 1978.

Gee, D.G., Basement-cover relationships in the central Scandinavian Caledonides, Geol. For. Stockh. Forh., 102, 455-474, 1980.

- Gee, D.G., Cambrian successions in the Caledonian allochthon of Scandinavia, *Terra Cognita*, 1, 44, 1981.
- Griffin, W.L., P.N. Taylor, J.W. Hakkinen, K.S. Heier, I.K. Iden, E.J. Krogh, O. Malm, K.I. Olsen, D.E. Ormaasen, and E. Tveten, Archean and Proterozoic crustal evolution in Lofoten-Vesteraalen, North Norway, *J. geol. Soc. Lond.*, 135, 629-647, 1978.
- Griffin, W.L., H. Austrheim, K. Brastad, I. Bryhni, A. Krill, E. Krogh, M.B.E. Mork, H. Qvale, and B. Torudbakken, High-pressure metamorphism in the Scandinavian Caledonides, *Terra Cognita*, 1, 48, 1981.
- Gustavson, M., The Caledonian mountain chain of southern Troms and Ofoten areas, Part I: Basement rocks and Caledonian metasediments, *Norges geol. Unders.*, 239, 1-162, 1966.
- Gustavson, M., Narvik, Beskrivelse til det berggrunnsgeologiske gradteigskart 1:100,000, *Norges geol. Unders.*, 308, 1-34, 1974.
- Gwinn, V.E., Kinematic patterns and estimates of lateral shortening, Valley and Ridge and Great Valley provinces, in *Studies of Appalachian Geology, Central and Southern*, edited by G.W. Fisher et al., Wiley, New York, 1970.

Hakkinen, J.W., Structural geology and metamorphic history of western Hinnoy and adjacent parts of eastern Hinnoy, North Norway, Ph.D. thesis, 161p., Rice University, Houston, 1977.

Hansen, E., Strain Facies, Springer-Verlag, Berlin, 1-207, 1971.

Harland, W.B., and R.A. Gayer, The Arctic Caledonides and earlier oceans, Geol. Mag., 109, 289-314, 1971.

Heier, K.S., and W. Compston, Interpretation of Rb-Sr age patterns in high-grade metamorphic rocks, North Norway, Norsk geol. Tidsskr., 49, 257-283, 1969.

Henriksen, N., The Caledonides of central East Greenland, Terra Cognita, 1, 51, 1981.

Hogbom, A.G., Studies in the post-Silurian thrust region of Jamtland, Geol. For. Stockh. Forh., 31, 1-57, 1909.

Kautsky, G., Der Geologische bau des Sulitelma-Salojauregebietes in den Nordscandinavischen Kaledoniden, Sverges geol. Unders., 528, 1-228, 1953.

Kent, D.V., and N.D. Oppdyke, Paleomagnetism of the Devonian Catskill redbeds: evidence for motion of the coastal New England - Canadian maritime region relative to cratonic North America, Jour. Geophys. Res., 83, 4441-4450, 1978.

Kulling, O., Oversikt over norra Norrbottensfjällens kaledonberggrund, Sverges geol. Unders., 19, 1-166, 1964.

LeFort, P., Himalayas: the collided range. Present knowledge of the continental arc, Am. J. Sci., 275A, 1-44, 1975.

Matte, P., and J.P. Burg, Sutures, thrusts and nappes in the Variscan Arc of western Europe: plate tectonic implications, in Thrust and Nappe Tectonics, edited by K.R. McClay and N.J. Price, pp.353-358, Blackwell, Oxford, 1981.

Milnes, A.G., Structural zones and continental collision, central Alps, Tectonophysics, 47, 369-392, 1978.

Molnar, P., and D. Gray, Subduction of continental lithosphere: some constraints of certainties, Geology, 7, 58-62, 1979.

Ramberg, H., The role of gravity in orogenic belts, in Thrust and Nappe Tectonics, edited by K.R. McClay and N.J. Price, pp.125-140, Blackwell, Oxford, 1981.

Rodgers, J., The Merrimack synclinorium in northeastern Connecticut, Am. J. Sci., 278, 176-186, 1981.

- Roecker, S.W., Velocity structure of the Pamir-Hindu Kush region: Possible evidence of subducted crust, J. Geophys. Res., 87, 945-960, 1982.
- Royse, F., M.A. Warner, D.C. Reese, Thrust belt structural geometry and related stratigraphic problems, Wyoming-Idaho-northern Utah, Rocky Mtn. Ass. Geol. Symp., Deep Drilling Frontiers in Central Rocky Mountains, 41-54, 1975.
- Steiger, R.H., B.T. Hansen, C. Schuler, M.T. Bar, and N. Henriksen, Polyorogenic nature of the southern Caledonian fold belt in East Greenland: an isotopic study, J. Geol., 87, 475-495, 1979.
- Stephens, M.B., Evidence for Ordovician arc build-up and arc splitting in the upper allochthon of Central Scandinavia, Terra Cognita, 1, 75, 1981.
- Stephens, M.B., and D.G. Gee, A plate tectonic model for Caledonian orogenesis in the central Scandinavian Caledonides, Terra Cognita, 1, 76, 1981.
- Sturt, B.A., I.R. Pringle, and D.M. Ramsay, The Finnmarkian phase of the Caledonian orogeny, J. geol Soc. Lond., 135, 597-610, 1978.
- Talwani, M., and O. Eldholm, Evolution of the Norwegian-Greenland Sea, Geol. Soc. Amer. Bull., 88, 969-999, 1977.

Tornebohm, A.E., Grunddragen af det centrala Skandinaviens bergbyggnad, Kongliga Svenska Vetenskaps Akademiens Handlingar, 28, 1-210, 1896.

Trumpy, R., Sur les racines des nappes helvetiques, in Livre a la Memoire du Professeur Paul Fallot, edited by M.D. Delga, pp.419-430, Societe Geologique de France, Paris, 1963.

Trumpy, R., Die helvetischen Decken der Ostschweiz. Versuch einer palinspatischen korrelation und ansatze zu einer kinetischen analyse, Ecolg. Geol. Helv., 62, 105-142, 1969.

Trumpy, R., Penninic-Austroalpine boundary in the Swiss Alps: a presumed former continental margin and its problems, Am. J. Sci., 275A, 209-238, 1975.

Tull, J.F., Geology and structure of Vestvagoy, Lofoten, North Norway, Norges geol. Unders., 333, 1-59, 1978.

Van der Voo, R., and C.R. Scotese, Paleomagnetic evidence for a large (~2000km) sinistral offset along the Great Glen Fault during Carboniferous time, Geology, 9, 583-589, 1981.

Vogt, T., Geologiske studier langs den ostlige del av fjellkjeden i Tromso amt, Norsk geol. Tidsskr., 4, 1-260, 1918.

Vogt, T., Trekk av Narvik-Ofoten traktens geologi, Norges geol. Unders.,
21, 198-213, 1942.

Vogt, T., Fjellkjedestudier i den østlige del av Troms, Norges geol.
Unders., 248, 1-59, 1967.

White, D.A., D.H. Roeder, T.H. Nelson, and J.C. Crowell, Subduction, Geol.
Soc. Amer. Bull., 81, 3431-3432, 1970.

Table 1. Sequence of Thrust Development in the Lofoten-Rombak Area

	<u>Deformational Phase</u>	<u>Age</u>	<u>Inferred Transport Direction</u>	<u>Effect</u>
Stangnes, Tjeldsund, and Forsa thrusts	D ₂ (D ₁ of Bartley, in press)	~450 my	~WNW-ESE (?)	Emplace main Caledonian allochthon onto Lofoten - Tysfjord basement gneisses and their autochthonous sedimentary cover.
Austerfjord and Vikeland thrusts	D ₃ (D ₂ of Bartley, in press)	?	~ N60°W - S60°E	Imbricate Lofoten basement gneisses, their Storvann Group stratigraphic cover, and lithologies of the main Caledonian allochthon.
Frostisen and Mereftasfjell thrusts	D ₅ (?)	?	~ N70°W - S70°E	Imbricate Rombak - Tysfjord basement gneisses, their Dividal Group stratigraphic cover, and lithologies of the main Caledonian allochthon.

FIGURE CAPTIONS

Figure 1: Generalized tectonic map of the Scandinavian Caledonides showing the distribution of structural basement (unpatterned) and structural cover (shaded).

Figure 2: Generalized tectonic map of the Lofoten-Rombak region showing structural basement (unpatterned) and structural cover (shaded). Areas shown in Figures 3 and 4 are outlined. VA -Vaeroy; VE -Vestvagoy; H -Hinnoy; F -Fjelldal; AC -Aefjord Culmination; SK -Skjomen; SI -Sitasjaure; and RW -Rombak window.

Figure 3: a. Generalized tectonic map of eastern Hinnoy and the adjacent mainland. b. Structural cross section across northern Fjelldal. Line of section is indicated in 3a. Patterns used to distinguish tectonic units are the same as those in 3a. No vertical exaggeration.

Figure 4: Generalized tectonic map of the Aefjord-Sitas area. Line of section shown in Figure 5 is indicated by B-B'.

Figure 5: Structural cross section across the Aefjord-Sitas area. Patterns used to distinguish tectonic units are the same as those in Figure 4. No vertical exaggeration.

FIGURE CAPTIONS (continued)

Figure 6: Cartoon drawings of the evolution of an A-type subduction zone. Although these sketches were not drawn to a particular scale, vertical exaggeration has been kept to a minimum. a. Initial subduction of continental crust occurs along a former B-type subduction boundary. An accretionary wedge (shaded) forms as remnants of the former ocean basin as well as much of the sedimentary cover of the downgoing plate "piles up" in the subduction zone. The lower plate behaves as a generally rigid, structurally coherent block. Dotted lines indicate incipient thrusts which will become active in frames b and c. The downgoing slab is subdivided by these thrusts into three domains which are labeled 1, 2, and 3 for reference in frames b and c. b. As en bloc subduction ceases due to buoyancy effects, continued convergence leads to the development of a basement-involved thrust in the downgoing plate which verges in the same direction as the original subduction boundary. With further convergence, these secondary basement--involved thrusts step progressively further into the downgoing plate (c).

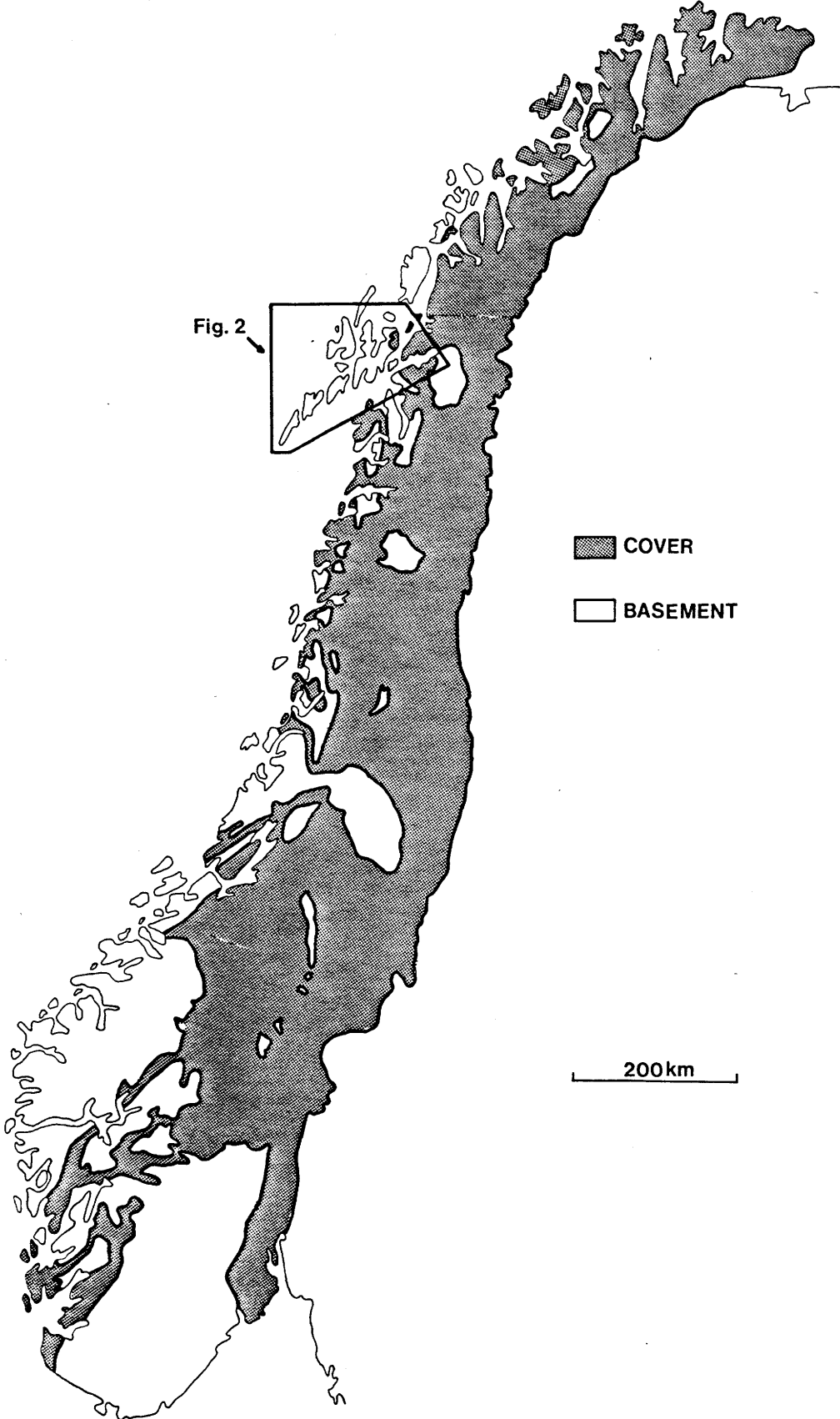
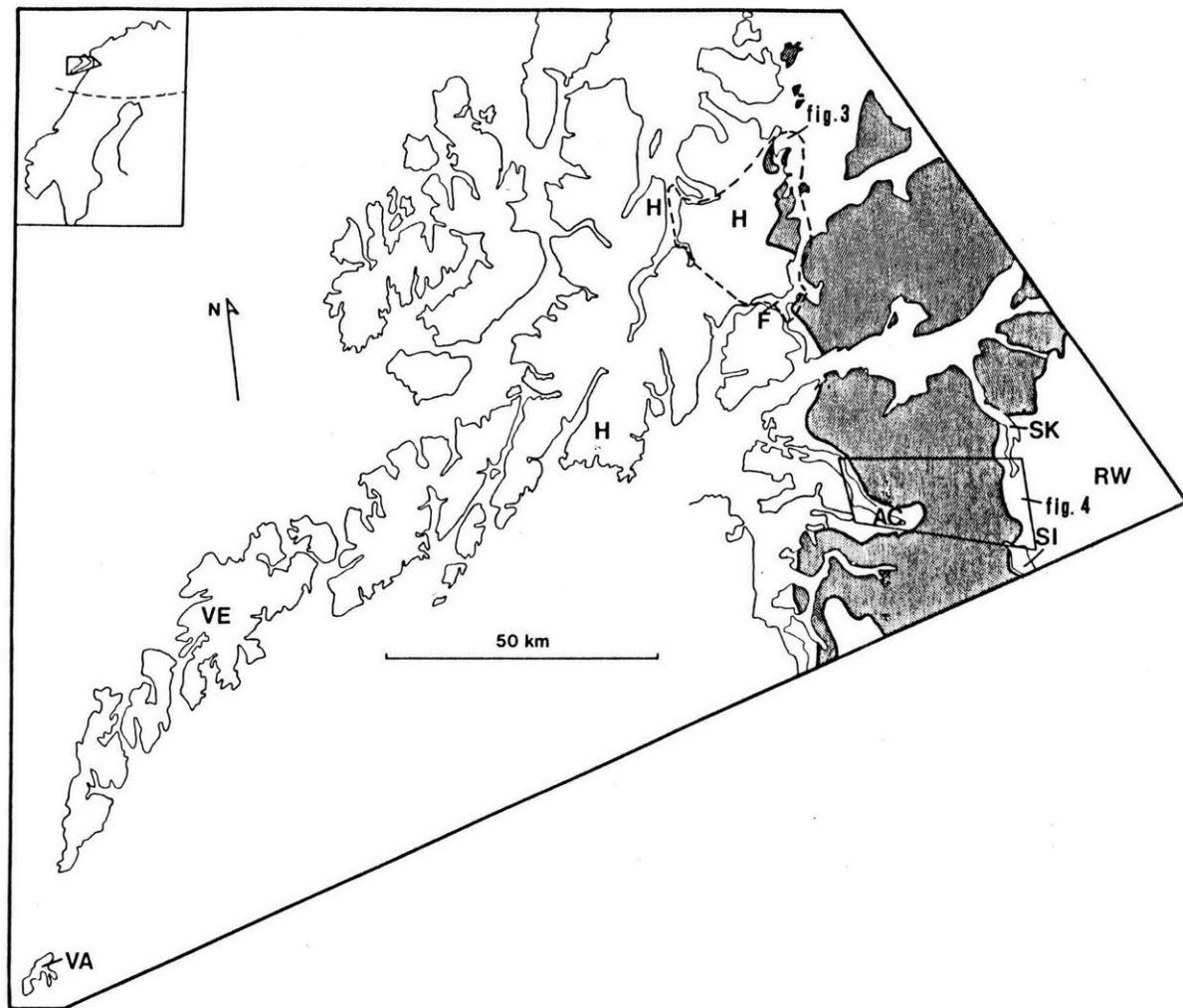


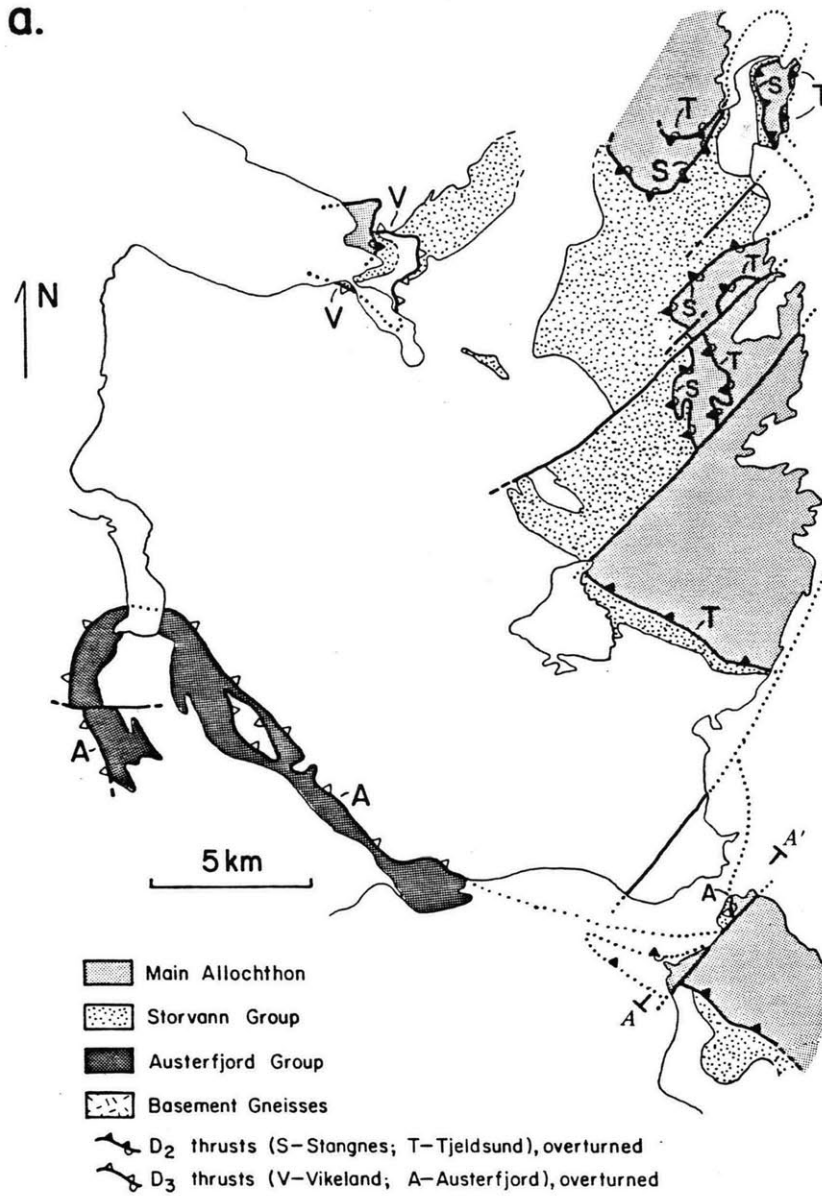
Fig. 2

COVER
BASEMENT

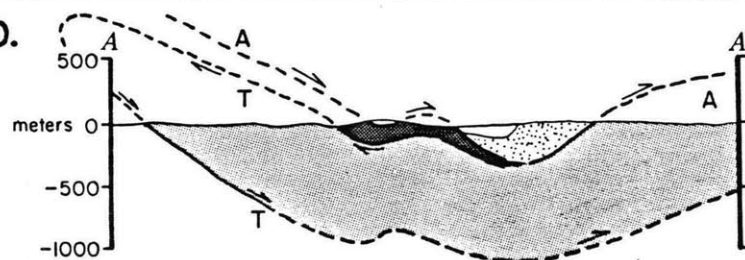
200 km

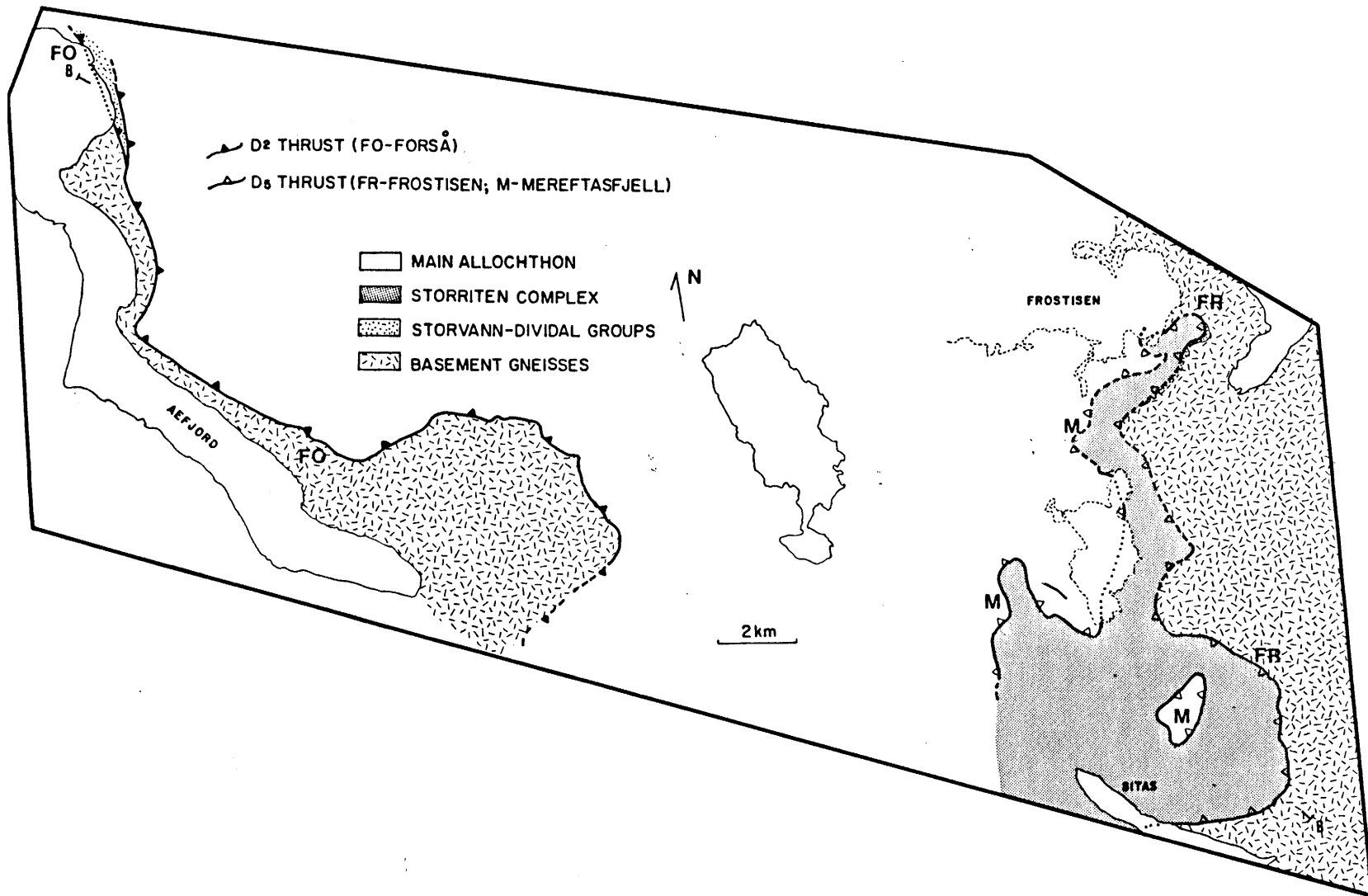


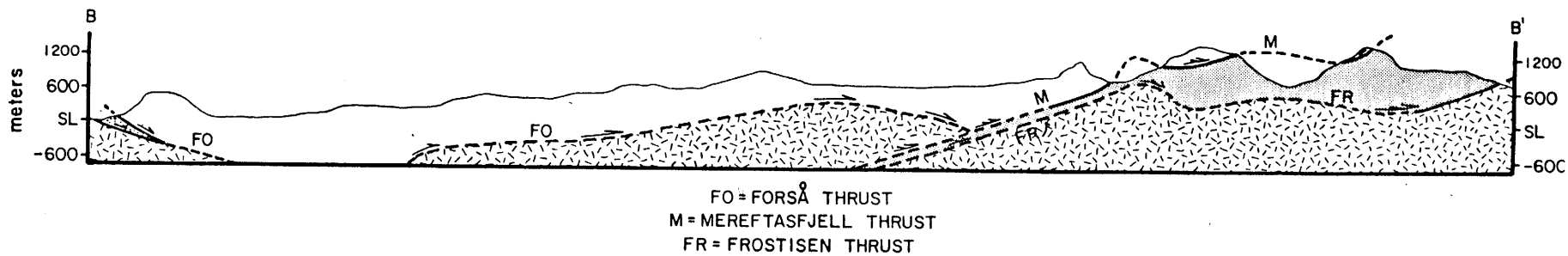
a.



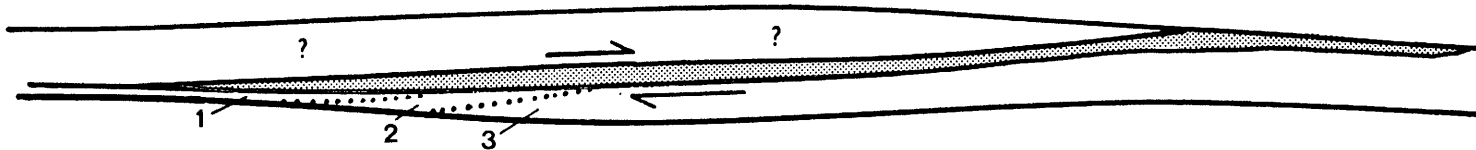
b.



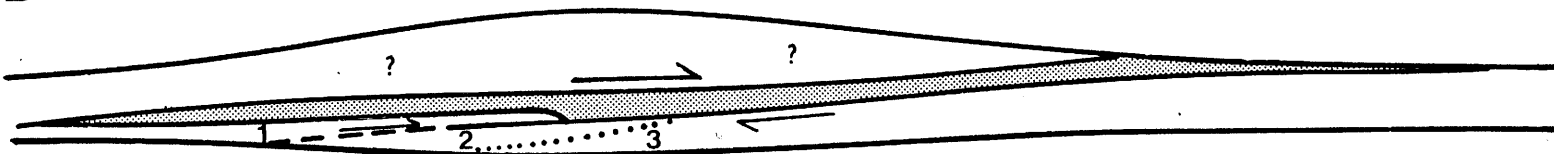




A



B



C

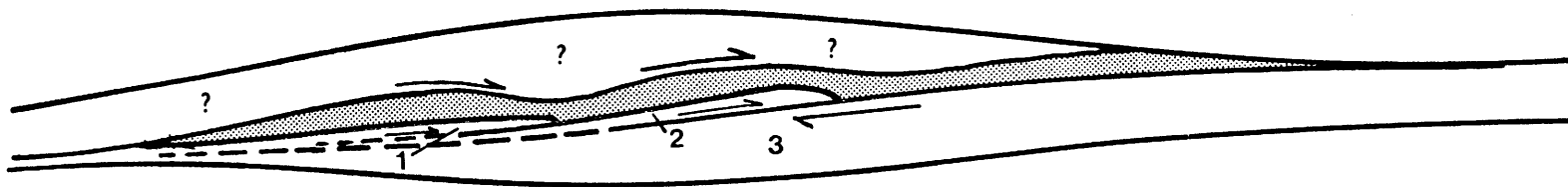
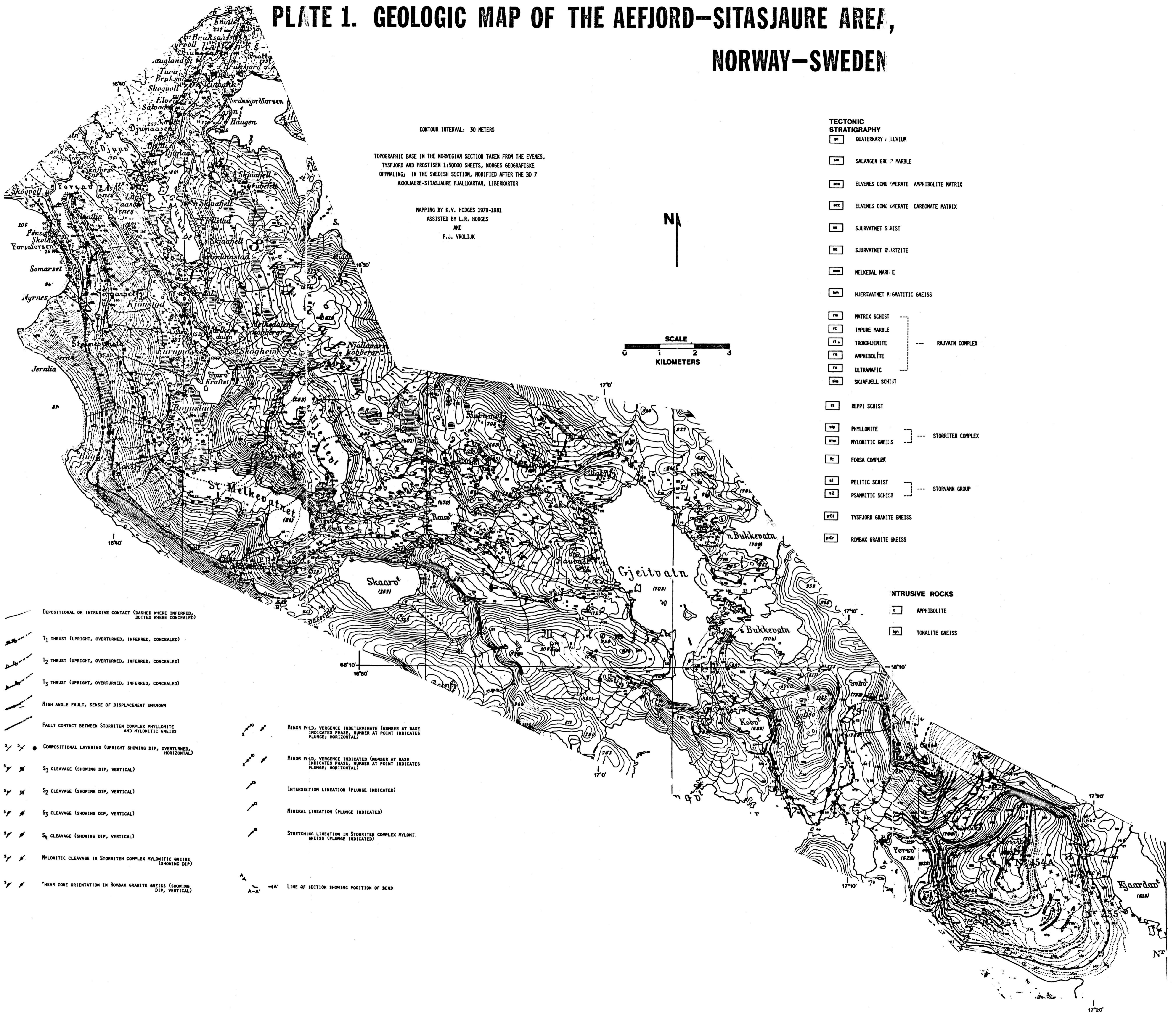


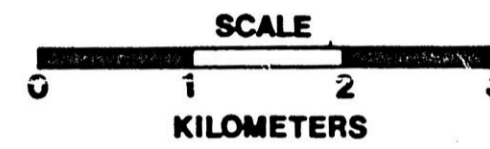
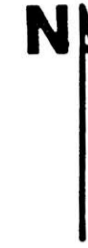
PLATE 1. GEOLOGIC MAP OF THE AEFJORD-SITASJAURE AREA, NORWAY-SWEDEN



CONTOUR INTERVAL: 30 METERS

TOPOGRAPHIC BASE IN THE NORWEGIAN SECTION TAKEN FROM THE EVENES, TYSFJORD AND FROSTISEN 1:50000 SHEETS, NORGES GEOGRAFISKE OPPMALING; IN THE SWEDISH SECTION, MODIFIED AFTER THE BD 7 AKKAJAURE-SITASJAURE FJALLKARTAN, LIBERKARTOR

MAPPING BY K.V. HODGES 1979-1981
ASSISTED BY L.R. HODGES
AND
P.J. VROLTIJK



TECTONIC STRATIGRAPHY

- Q QUATERNARY / LUVIUM
 - S SALANGEN GROUP MARBLE
 - E ELVENES CONGLOMERATE AMPHIBOLITE MATRIX
 - EC ELVENES CONGLOMERATE CARBONATE MATRIX
 - SJ SURVATNET SCHIST
 - QZ SURVATNET QUARTZITE
 - M MELKEDAL MARBLE
 - H HJERTVATNET GNEISS
 - M MATRIX SCHIST
 - IC IMPURE MARBLE
 - T TRONDHEMITE
 - AM AMPHIBOLITE
 - UL ULTRAMAFIC
 - SK SKJAFJELL SCHIST
 - RE REPPI SCHIST
 - PH PHYLLONITE
 - MY MYLONITIC GNEISS
 - FO FORSA COMPLEX
 - PE PELITIC SCHIST
 - PS PSAMMITIC SCHIST
 - TYS TYSFJORD GRANITE GNEISS
 - RO ROMBAK GRANITE GNEISS
- RAVVATH COMPLEX
- STORRITEN COMPLEX
- STORVANN GROUP

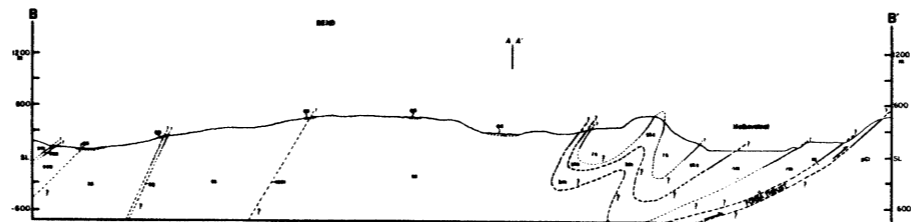
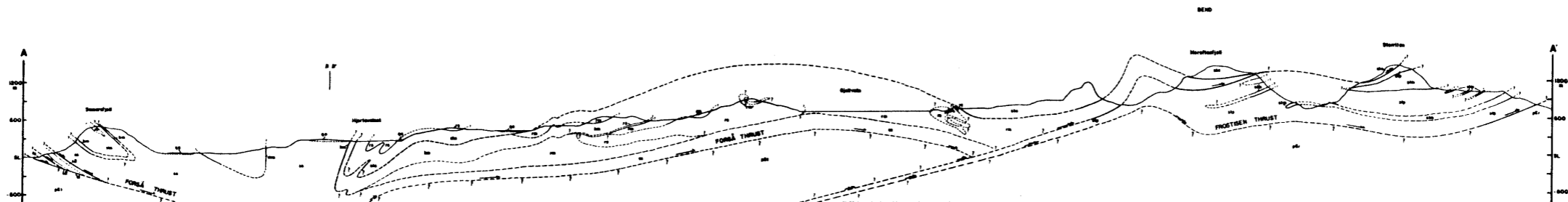
INTRUSIVE ROCKS

- AM AMPHIBOLITE
- TO TONALITE GNEISS

- DEPOSITIONAL OR INTRUSIVE CONTACT (DASHED WHERE INFERRED, DOTTED WHERE CONCEALED)
- T₁ THRUST (UPRIGHT, OVERTURNED, INFERRED, CONCEALED)
- T₂ THRUST (UPRIGHT, OVERTURNED, INFERRED, CONCEALED)
- T₃ THRUST (UPRIGHT, OVERTURNED, INFERRED, CONCEALED)
- HIGH ANGLE FAULT, SENSE OF DISPLACEMENT UNKNOWN
- FAULT CONTACT BETWEEN STORRITEN COMPLEX PHYLLONITE AND MYLONITIC GNEISS
- COMPOSITIONAL LAYERING (UPRIGHT SHOWING DIP, OVERTURNED, HORIZONTAL)
- S₁ CLEAVAGE (SHOWING DIP, VERTICAL)
- S₂ CLEAVAGE (SHOWING DIP, VERTICAL)
- S₃ CLEAVAGE (SHOWING DIP, VERTICAL)
- S₄ CLEAVAGE (SHOWING DIP, VERTICAL)
- MYLONITIC CLEAVAGE IN STORRITEN COMPLEX MYLONITIC GNEISS (SHOWING DIP)
- "HEAR ZONE ORIENTATION IN ROMBAK GRANITE GNEISS (SHOWING DIP, VERTICAL)

- MINOR FOLD, VERGENCE INDETERMINATE (NUMBER AT BASE INDICATES PHASE, NUMBER AT POINT INDICATES PLUNGE; HORIZONTAL)
- MINOR FOLD, VERGENCE INDICATED (NUMBER AT BASE INDICATES PHASE, NUMBER AT POINT INDICATES PLUNGE; HORIZONTAL)
- INTERSECTION LINEATION (PLUNGE INDICATED)
- MINERAL LINEATION (PLUNGE INDICATED)
- STRETCHING LINEATION IN STORRITEN COMPLEX MYLONITIC GNEISS (PLUNGE INDICATED)
- A-A' LINE OF SECTION SHOWING POSITION OF BEND

PLATE 2: GEOLOGIC CROSS SECTIONS, AEFJORD-SITAS AREA, NORWAY & SWEDEN



NO VERTICAL EXAGGERATION

- T₁ THRUST
- T₂ THRUST
- T₃ THRUST